

Copyright  
by  
Wendy Marie Robertson  
2014

**The Dissertation Committee for Wendy Marie Robertson certifies that this is the approved version of the following dissertation:**

**ANTHROPOGENIC IMPACTS ON RECHARGE PROCESSES AND WATER  
QUALITY IN BASIN AQUIFERS OF THE DESERT SOUTHWEST: A  
COUPLED FIELD OBSERVATION AND MODELING STUDY**

**Committee:**

---

**John M. Sharp Jr., Supervisor**

---

**M. Bayani Cardenas**

---

**Bridget R. Scanlon**

---

**Daniel O. Brecker**

---

**John Karl Böhlke**

**ANTHROPOGENIC IMPACTS ON RECHARGE PROCESSES AND WATER  
QUALITY IN BASIN AQUIFERS OF THE DESERT SOUTHWEST: A  
COUPLED FIELD OBSERVATION AND MODELING STUDY**

by

**Wendy Marie Robertson, B.S. Geo. Sci.; M.S.**

**Dissertation**

Presented to the Faculty of the Graduate School of

The University of Texas at Austin

in Partial Fulfillment

of the Requirements

for the Degree of

**Doctor of Philosophy**

The University of Texas at Austin

May 2014

## **Acknowledgements**

I would like to thank my supervisor, Jack Sharp, for the opportunity to pursue this research under his guidance here at UT. Thank you to my committee members, Drs. Bayani Cardenas, Bridget Scanlon, Dan Breecker, and J.K. Böhlke for your mentorship and time. Also, a big thank you to Philip Guerrero, the graduate program coordinator for the Jackson School, for your advice, excellent listening skills, and FFF. I am grateful to my family and friends for their support through the graduate school journey. Thank you especially to my parents, my friends Brigette F., Joe B., Leslie T.M., and Sarah E., and to my wonderful fiancé (soon to be husband!), Jason. Y'all are the best.

Funding sources: This research would not have been possible without financial support from the following:

The Jackson School of Geosciences

Geological Society of America Graduate Research Grants

Sigma Xi Graduate Research Grant

Ozarka Earth Sciences Scholarship

Copyright information: Chapters 2 and 3 of this dissertation are published works in Environmental Earth Sciences Journal

(<http://www.springer.com/earth+sciences+and+geography/geology/journal/12665>) and

Hydrogeology Journal

(<http://www.springer.com/earth+sciences+and+geography/hydrogeology/journal/10040>)

respectively. The original publications are available at [www.springerlink.com](http://www.springerlink.com).

**ANTHROPOGENIC IMPACTS ON RECHARGE PROCESSES AND WATER  
QUALITY IN BASIN AQUIFERS OF THE DESERT SOUTHWEST: A  
COUPLED FIELD OBSERVATION AND MODELING STUDY**

Wendy Marie Robertson, Ph.D.  
The University of Texas at Austin, 2014

Supervisor: John M. Sharp Jr.

The development of natural grass/scrubland for agricultural use within the Trans-Pecos basins has altered recharge mechanisms and raised questions about groundwater sustainability. Past efforts focused on recharge in arid basin systems used three main assumptions: there is minimal modern recharge, no widespread recharge on basin floors, and no recharge from anthropogenic sources. However, in the Trans-Pecos, nitrate ( $\text{NO}_3^-$ ) concentrations have increased in basin groundwater (up by 3-4 mg/l as  $\text{NO}_3^-$  in 40 yrs), refuting the “classic” model and posing water quality risks. Grazing and irrigated agriculture have impacted basin hydrology by altering vegetation regime and the magnitude and spatial distribution of infiltration. This has increased recharge,  $\text{Cl}^-$ , and mobile N flux to basin groundwater. A series of spatially-distributed net infiltration models were used to estimate potential recharge from natural and anthropogenic sources. Between 7-20% of potential recharge results from widespread recharge on the basin floors. Additionally, from 1960-2000, irrigation return flow may have contributed  $3.0 \times 10^7$  -  $6.3 \times 10^7$   $\text{m}^3$  of recharge. These results are supported by field observations. Cores collected beneath agricultural land document changes in water content and pore water chemistry that imply increased downward flux of moisture and solute, and  $\text{NO}_3^-$  and  $\text{Cl}^-$  inventories beneath irrigated land are distinct in amount and profile from those in natural areas. There are significant implications for sustainability based upon the trends in groundwater  $\text{NO}_3^-$  concentrations, core results, and net infiltration models: more recharge may enter the basins than previously estimated and there is a potential long-term concern

for water quality. Due to thick unsaturated zones in the basins, long travel times are anticipated. It is unknown if  $\text{NO}_3^-$  and  $\text{Cl}^-$  flux has peaked or if effects will continue for years to come. Further study should be undertaken to examine anthropogenic impacts on basin water quality. Additionally, these impacts may occur in similar systems globally and there is considerable evidence for the re-evaluation of the validity of the “classic” model of recharge in arid basin systems. Future studies and management plans should incorporate potential impacts of changes in vegetation and land use on recharge processes and water budgets in arid basins.

## Table of Contents

List of Figures.....	viii
List of Tables.....	xii
Chapter 1: Introduction.....	1
Chapter 2: Variability of groundwater nitrate concentrations over time in arid basin aquifers: sources, mechanisms of transport, and implications for conceptual models.....	6
Chapter 3: Estimates of recharge in two arid basin aquifers: a model of spatially variable net infiltration and its implications (Red Light Draw and Eagle Flats, Texas, USA).....	29
Chapter 4: Estimates of potential recharge in arid basins and impacts on infiltration processes and solute flux due to land use and vegetation change.....	55
Chapter 5: Impacts of land-use change on vadose zone and groundwater nitrate concentrations in desert basin aquifers in the Southwestern U.S.....	91
Chapter 6: Summary.....	125
Appendix A: Additional figures on groundwater NO <sub>3</sub> <sup>-</sup> concentrations and land use in the Trans-Pecos region not included in chapters 2-5.....	128
Appendix B: Raw CFC data and modeled CFC values.....	133
Appendix C: Estimates of labile N (from soil N, atmospheric deposition, and synthetic fertilizer application) and the resultant groundwater NO <sub>3</sub> <sup>-</sup> concentrations based on 130 years (1880-2010) of INFIL modeled potential recharge in Wild Horse/Michigan Flats and Lobo/Ryan Flats basins.....	135
References.....	139

## List of Figures

Fig. 2.1	Location of the four study basins.....	8
Fig. 2.2	Map of the 2011 NO <sub>3</sub> <sup>-</sup> concentrations.....	15
Fig. 2.3	Map of trends in NO <sub>3</sub> <sup>-</sup> concentrations from the 1940's to present.....	17
Fig. 2.4	Scatter plot of NO <sub>3</sub> <sup>-</sup> concentrations over time for all wells with available water quality data.....	18
Fig. 2.5	Box and whisker plots of NO <sub>3</sub> <sup>-</sup> concentration by decade.....	19
Fig. 3.1	(a) Map of the area of interest within the Trans-Pecos Region of Texas, USA. b) Location of the modeled area; Red Light Draw and Eagle Flats basins and their contributing watersheds.....	32
Fig. 3.2	Map of precipitation distribution modeled by PRISM for the area of interest...	43
Fig. 3.3	Distribution of precipitation using the quadratic regression method in the INFIL model.....	44
Fig. 3.4	Plot of PRISM modeled precipitation values versus INFIL modeled precipitation values for the 148 control points across the model extent.....	45
Fig. 3.5	Crossplot of Thornthwaite estimated PET versus INFIL estimated PET.....	46
Fig. 3.6	Daily PET for the Thornthwaite and calibrated INFIL models.....	47
Fig. 3.7	Average values of annual net infiltration estimated using the INFIL model.....	50
Fig. 3.8	Bar graph of recharge estimates for Red Light Draw and Eagle Flats.....	53
Fig. 4.1	Map of the area of interest within the Trans-Pecos Region of Texas, USA with outlines of the basins, their contributing watersheds and model extent(s)...	58
Fig. 4.2	Plot of PET estimates and precipitation from 1937 to 2010 in Valentine, TX (located in the Lobo/Ryan Flats basin).....	65
Fig. 4.3	Plot of daily and cumulative precipitation and PET for the month of July 1972 in Valentine, TX (located in LRF Flats basin)....	66
Fig. 4.4	Map of precipitation distributions using PRSIM and INFIL models.....	72



Fig. 4.5 Plot of PRISM modeled precipitation values versus INFIL modeled precipitation values for the 600 control points across the model extent.....	73
Fig. 4.6 Map of the distribution of false weather stations in the Antelope Valley irrigation district model.....	76
Fig. 4.7 Crossplot of Thornthwaite estimated PET versus INFIL estimated $PET^i_d$ at Van Horn, TX (grid cell ID: 11928).....	78
Fig. 4.8 Daily PET for the Thornthwaite and calibrated INFIL models at Van Horn, TX (grid cell ID: 11928).....	78
Fig. 4.9 Average values of annual net infiltration estimated using the INFIL model.....	81
Fig. 4.10 Comparison of net infiltration in the Wild Horse/Michigan Flats and Lobo/Ryan Flats INFIL model (large model) with 3 separate vegetation regime scenarios.....	83
Fig. 4.11 Diagram displaying precipitation distribution and net infiltration with (right center and far right) and without (far left and left center) added irrigation water for the three smaller models of irrigation districts.....	85
Fig. 5.1 Map of the study site in the Trans-Pecos region of west Texas including basin names, locations of core samples, and outlines of irrigation districts within the basins.....	95
Fig. 5.2 Map of the spatial distribution of potential recharge within the Trans-Pecos basins resulting from both natural (i.e., precipitation) and anthropogenic (i.e., irrigation return flow) sources.....	97
Fig. 5.3 Distribution of groundwater $NO_3^-$ trends in the Trans-Pecos basins by overlying land-use type.....	98
Fig. 5.4 Profiles of water content, $Cl^-$ , and $NO_3^-$ concentration beneath representative core samples from grazed land (GR), land with historic irrigated row crops and current grazing (IRC $\rightarrow$ GR), land with historic irrigated row crops and current irrigated orchard (IRC $\rightarrow$ IO), an irrigated orchard (IO), and irrigated row crops (IRC).....	102
Fig. 5.5 Vadose zone $NO_3^-$ and $Cl^-$ inventories from this study (black dots) and literature values.....	107

Fig. 5.6 Plots of isotopic composition of $^{15}\text{N}$ and $^{18}\text{O}$ of $\text{NO}_3^-$ in groundwater (top) and pore water extracts (bottom), with ranges of literature values from labile N sources and $^{15}\text{N}$ from bulk soil/sediment in the Trans-Pecos cores.....	110
Fig. 5.7 Plots of isotopic composition of $^{15}\text{N}$ and $^{18}\text{O}$ of $\text{NO}_3^-$ in groundwater identified by land use.....	112
Fig. 5.8 Plots of (a) Cl concentration vs Cl/Br ratio in Trans-Pecos groundwater samples with ranges of precipitation values from the Trans-Pecos region and ranges of values from underlying aquifer systems, (b) Cl concentration vs Cl/Br ratio in vadose zone pore water extracts with ranges of precipitation and Trans-Pecos groundwater values, and (c) profiles of Cl/Br ratio in vadose zone pore water extracts with depth.....	115
Fig. 5.9 Plots of (a) Cl vs $\text{NO}_3^-$ in pore water extracts with the ratio in modern atmospheric deposition, Trans-Pecos groundwater (red), and irrigation water with added fertilizer based on USDA agricultural census data of fertilizer application rates for cotton and pecans in Texas (green), (b) $\text{NO}_3^-$ concentrations vs $^{15}\text{N}$ in pore water extracts (dots) and Trans-Pecos groundwater (red), and (c) $\text{NO}_3^-/\text{Cl}^-$ ratios vs $^{15}\text{N}$ in pore water extracts (dots) and Trans-Pecos groundwater (red).....	118
Fig. 5.10 Profiles of $\text{NO}_3^-$ concentration and isotopic composition ( $^{15}\text{N}$ and $^{18}\text{O}$ ) of pore water $\text{NO}_3^-$ beneath representative core samples from grazed land (GR), land with historic irrigated row crops and current grazing (MU (IRC + GR)), land with historic irrigated row crops and current irrigated orchard (MU(IRC + IO)), an irrigated orchard (IO), and irrigated row crops (IRC).....	119
Fig. 5.11 Comparison of net infiltration in the Wild Horse/Michigan Flats and Lobo/Ryan Flats basins with 2 vegetation regime scenarios.....	122
Fig. A.1 Locations of TWDB wells with historical water quality data (including $\text{NO}_3^-$ ) in the four basins of interest, Trans-Pecos, Texas, U.S.A.....	128
Fig. A.2 Wells in the Trans-Pecos basin aquifers with ‘elevated’ (>140 $\mu\text{mol/l}$ ) $\text{NO}_3^-$ concentrations in red .....	128
Fig. A.3 Wells in the Trans-Pecos basin aquifers that demonstrated a trend in $\text{NO}_3^-$ concentration over time in purple.....	129

Fig. A.4 Patterns of land use change from 1980-2000 (based on the International Satellite Land Surface Climatology (ISLSCP) Initiative (1980's) and the National Land Cover Dataset (2001)) and trends in groundwater  $\text{NO}_3^-$  concentration (1965-2011) in wells of the Red Light Draw and Eagle Flats basins.....130

Fig. A.5 Patterns of land use change from 1980-2000 (based on the International Satellite Land Surface Climatology (ISLSCP) Initiative (1980's) and the National Land Cover Dataset (2001)) and trends in groundwater  $\text{NO}_3^-$  concentration (1965-2011) in wells of Lobo and Ryan Flats.....131

Fig. A.6 Patterns of land use change from 1980-2000 (based on the International Satellite Land Surface Climatology (ISLSCP) Initiative (1980's) and the National Land Cover Dataset (2001)) and trends in groundwater  $\text{NO}_3^-$  concentration (1965-2011) in wells of Wild Horse and Michigan Flats.....132

## List of Tables

Table 2.1 Range of concentrations of $\text{NO}_3^-$ and their relative abundance measured in the 80 wells sampled in 2011.....	14
Table 2.2 CFC results for groundwater collected during 2011.....	20
Table 3.1 Previous estimates of annual recharge volume in the Red Light Draw and Eagle Flats basins, Trans-Pecos, Texas, USA.....	49
Table 3.2 Estimates of annual recharge volume on the basin floors and for the watersheds of Red Light Draw and Eagle Flats basins using the INFIL model...	53
Table 4.1 Range of storm event magnitudes at Valentine, TX, and the number of days required (at two estimates of average daily PET) for total water loss via evapotranspiration.....	64
Table 4.2 List of datasets and input values (and their sources) used in INFIL model simulations.....	69
Table 4.3 Values for run-on, run-off, and % difference in net infiltration used to determine that the smaller models of irrigation districts can be evaluated independent of the influence from adjacent cells (in large model).....	76
Table 4.4 Results of one-at-a-time sensitivity analyses.....	79
Table 4.5 Estimates of net infiltration from the INFIL model simulations.....	82
Table 4.6 Comparison of net infiltration in the Wild Horse/Michigan Flats and Lobo/Ryan Flats INFIL model (large model) with 3 separate vegetation regime scenarios.....	84
Table 5.1 Summary of vadose zone core samples collected in fall 2012 from the Trans-Pecos basins.....	105
Table B.1 Well information, raw CFC concentrations (in water), modeled atmospheric CFC concentrations, and apparent groundwater ages based on CFC data.....	133
Table C.1 Three major sources of labile N in the Trans-Pecos basins.....	135
Table C.2 Mass of labile N (from the sources outlined in Table C.1) within Wild Horse/Michigan Flats and Lobo/Ryan Flats basins.....	136

Table C.3 Total mass of labile N in Wild Horse/Michigan Flats and Lobo/Ryan Flats basins (sum of labile N from Table C.2).....	136
Table C.4 Estimates of total volume of recharge to Lobo/Ryan Flats and Wild Horse/Michigan Flats basins from 1880-2010 under different modeled vegetation regimes.....	137
Table C.5 Estimates for basin groundwater NO <sub>3</sub> <sup>-</sup> concentrations (assuming no loss/assimilation) based on labile N sources listed in Table C.1 and recharge rates based on INFIL model simulations (Table C.4).....	138

## **Chapter 1: Introduction**

This dissertation details the results of a coupled field observation and modeling study of modern recharge processes, solute flux, and nitrogen (N) dynamics in a series of arid basin aquifers in the Trans-Pecos region of west Texas. The intent is to improve understanding of arid basin hydrology and examine the effects that anthropogenic processes have on these systems. Because of thick vadose zones, high potential evapotranspiration (PET) rates, and minimal rainfall, groundwater in these systems is generally assumed to be ‘detached’ from surface processes. This implies that changes in land cover, vegetation regime, and addition of irrigation water/fertilizers/ treatments to the basin floors have no effect on the underlying groundwater systems. The only impact (and source of concern for sustainability) is that of groundwater extraction rates exceeding recharge resulting in decreasing water tables and projections for long-term water shortfalls. This research calls into question these fundamental assumptions and examines how combining field observations with computational models can improve our understanding of arid basin hydrology and our predictions of how these systems will respond to change. By using long-term groundwater quality, isotopic composition of  $\text{NO}_3^-$  (in ground and pore water), vadose zone characteristics, and spatially distributed models of net infiltration, impacts of anthropogenically driven land use and vegetation change on recharge and solute flux are quantified.

The project arose from a conflict between the assumptions of the previous research into Trans-Pecos basin recharge dynamics (i.e., minimal modern recharge, no widespread recharge on basin floors, and no recharge from anthropogenic sources) and an observation in both the amount of  $\text{NO}_3^-$  in basin groundwater and in its variability in concentration over time as documented in the Texas Water Development Board’s (TWDB) historical water quality data. Questions arise when examining these data: 1) where is the  $\text{NO}_3^-$  coming from, and 2) how is it entering the basin groundwater? To address these questions, field studies and computational modeling simulations were undertaken to link observed changes in groundwater quality to surface processes, identify source(s) of labile nitrogen (N) within the basins, and explain the mechanisms for

recharge and  $\text{NO}_3^-$  flux to basin groundwater. The following paragraphs provide a brief outline of the work, its results, and their implications.

Chapter 2 documents the temporal variability (and general upward trend) of  $\text{NO}_3^-$  concentration in basin groundwater, proposes likely sources of labile N in the basins, and puts forth a revised conceptual model of recharge processes that accounts for the addition of  $\text{NO}_3^-$  to groundwater during the past 60-70 years. Combining historical water quality data from the TWDB with results from a synoptic survey of ~100 wells in the four basins and age-dating results from five wells, this work establishes that the trends observed in the historical data of increasing  $\text{NO}_3^-$  concentrations in the basin groundwater continue to present (the time of the survey, summer 2011) and that young (<70 year old) water is present at depth within the basins. Possible sources of  $\text{NO}_3^-$  to the system are considered in the context of land use, known rates of atmospheric deposition, and documented conditions in these and similar systems from previous research and likely sources of  $\text{NO}_3^-$  to the groundwater were hypothesized to be: 1) mobilization of soil N previously sequestered in and beneath the root zones of grassy vegetation; 2) concentrations of  $\text{NO}_3^-$  salts documented at depth in these and similar systems; and 3) anthropogenic fertilizers (both synthetic and natural). The paper also addresses the conflict between the ‘classical’ model of recharge dynamics in arid basin systems and the observed trends; because the likely sources of  $\text{NO}_3^-$  to the basin groundwater are all located on the floors of the basins (and not the adjacent mountains), there must be some component of modern recharge occurring through the basin floor sediments, and, it must be widespread because increases in  $\text{NO}_3^-$  concentrations were observed in 1) wells within all four basins, and 2) the majority (64.5%) of wells with multiple data points. Additionally, because CFCs were found in groundwater of all of the tested wells (n=5), this indicates that modern recharge may be occurring in the basins.

Two sources of modern recharge are proposed: 1) anthropogenically induced recharge from irrigation return flow, and 2) natural recharge (resulting from changes in vegetation cover and land use since the 1950’s and due to flushing during major storm events). The resulting revised conceptual model combines mountain-front and mountain-

block recharge sources (source of modern recharge in the ‘classical’ model) with anthropogenic and natural recharge processes on the basin floors. It acknowledges that recharge is likely both spatially and temporally variable and proposes further research to quantify the source(s) of  $\text{NO}_3^-$  and modern recharge to the basin groundwater as well as to examine the implications for water quality and sustainability based upon the findings of this research.

Chapters 3 and 4 detail the results of modeling simulations undertaken to estimate the magnitude and spatial distribution of net infiltration (and thus potential recharge) in the basins. The INFIL 3.0.1 model, a USGS model of spatially distributed net infiltration, was implemented in three studies. Chapter 3 presents simulations of net infiltration for Red Light Draw and Eagle Flats basins (based solely on natural precipitation inputs) and a comparison of modeling techniques for recharge estimations. The INFIL simulations predict that: 1) recharge occurs through mountain-front zones and through basin floor sediments; 2) there is significant potential for recharge (up to 15% of total potential recharge) on the basin floors; 3) basin floor recharge is spatially variable; and 4) there is potential for recharge due to both runoff and through direct precipitation on the basin floors. There are important implications for these results; they support the revised conceptual model of flow (outlined in Chapter 2) which includes basin floor recharge from direct precipitation, they delineate a potential mechanism by which  $\text{NO}_3^-$  (and other solutes such as  $\text{Cl}^-$ ) may be transported to basin groundwater, and they raise questions about long-term sustainability of basin groundwater resources both from a quantity (how much recharge) and quality (risk for contamination and degraded water quality) standpoint.

Chapter 4 focuses on INFIL simulations in the Wild Horse/Michigan Flats and Lobo/Ryan Flats basins. In this set of studies, net infiltration was modeled for both natural (rain and snowfall) and anthropogenic (irrigation return flow) sources of water as well as for a range of vegetation regimes reflecting pre-western settlement (thick, dense grasslands interspersed with occasional woody vegetation and succulents) and current vegetation cover (sparse grasses, increased bare ground cover, and encroachment of



woody vegetation onto the basin floors). The simulations were separated into a large (basin scale) model of infiltration and three smaller scale (covering the three main irrigation districts) models to quantify net infiltration resulting from irrigation return flow.

The large model using a vegetation scenario consistent with the current vegetation regime produced results consistent with those from the Red Light Draw and Eagle Flats basin model (Chapter 3), with the same predictions (i.e., recharge occurring on basin floors, recharge is spatially variable, etc.). When compared to simulations of net infiltration in scenarios with pre-disturbance vegetation (one with higher vegetation density in the grasslands, one with both higher vegetation density in the grasslands and replacement of scrubland (zones of encroachment) with dense grasses) it was observed that simulated infiltration in the model with the current vegetation regime is up to 48% higher than the pre-settlement/pre-disturbance regimes. The smaller models highlight the potential for enhanced net infiltration in irrigated areas. This added source of recharge, while not contributing to the overall water budget (irrigation in this region uses groundwater) does provide evidence for anthropogenic impacts on recharge processes and identifies a mechanism by which additional labile N (and potentially other solutes/contaminants) could be transported to basin groundwater.

Chapter 5 details the impacts of land use and vegetation change on the vadose zone and groundwater in the Wild Horse/Michigan Flats and Lobo/Ryan Flats basins through analyses of core samples collected in fall of 2012 and groundwater from the 2011 synoptic survey. From analyzing the variations in physical properties (e.g., water content), chemistry (e.g., pore water  $\text{Cl}^-$  and  $\text{NO}_3^-$  concentrations, salt inventories), and isotopic composition ( $\delta^{15}\text{N}$  of sediment N and  $\delta^{15}\text{N}/\delta^{18}\text{O}$  of  $\text{NO}_3^-$ ) of cores collected beneath different land uses and comparing them to the chemical (major constituents including  $\text{Cl}^-$  and  $\text{NO}_3^-$ ) and isotopic composition ( $\delta^{15}\text{N}/\delta^{18}\text{O}$  of  $\text{NO}_3^-$ ,  $\delta^{18}\text{O}$  of  $\text{H}_2\text{O}$  [previous studies]) of groundwater it was established that: 1) vegetation type (i.e., grass/shrub-land vs. pecan trees vs. cotton/hay) influences water content and salt inventory in the vadose zone; 2) irrigation practices generally enhance (even in this arid

environment) downward flux of both water and solute; 3) the isotopic composition of pore water  $\text{NO}_3^-$  is consistent with a soil N source; and 4) the isotopic composition of groundwater  $\text{NO}_3^-$  is consistent with the isotopic composition of the pore water.

Additionally, it appears that grazing practices *may* have an influence on water and solute flux; in comparison to cores collected from grass/scrub-land in these basins in previous studies, the salt inventories of cores beneath grazed land are slightly lower than those beneath undisturbed land. These results provide a link between the trends in  $\text{NO}_3^-$  concentration of groundwater and basin floor sources of mobile N and show results consistent with the predictions of the INFIL modeling simulations and with the revised conceptual model of flow outlined in chapter 2.

This dissertation demonstrates that the simplified approach to modeling recharge processes (i.e., no recharge from direct precipitation on the basin floors and no impact on recharge resulting from anthropogenic activities) in arid basin systems overlooks potentially significant contributions. Anthropogenic processes (land-use and vegetation changes) alter both recharge and solute flux in these systems. The dissertation also documents changes in water quality, presence of CFCs in groundwater, and alterations to the physical and chemical properties of the vadose zone in response to modern downward moisture flux and recharge processes (both natural and anthropogenic). Furthermore, it utilizes computational modeling simulations to predict potential recharge natural and anthropogenic and inform the processes by which solute flux from basin floor sources may enter groundwater. It combines field observations and modeling techniques to explain previously overlooked phenomena (i.e., increasing trends in  $\text{NO}_3^-$  concentration) and provides concrete evidence for the need to revise how these basins and similar systems worldwide are treated in scientific investigations and in management plans. The following chapters detail these results and their implications.

## **Chapter 2:** Variability of groundwater nitrate concentrations over time in arid basin aquifers: sources, mechanisms of transport, and implications for conceptual models

### **Abstract**

In groundwater of the Trans-Pecos region of West Texas, unexpectedly high levels of nitrate ( $\text{NO}_3^-$ ) are documented in four basins: Red Light Draw, Eagle Flats, Wild Horse and Michigan Flats, and Lobo and Ryan Flats.  $\text{NO}_3^-$  concentrations are changing over time in the majority (82.8%) of wells and are increasing in most (69.8%). The temporal change raises questions about the potential sources of  $\text{NO}_3^-$  and about flow dynamics in these basins. Presence of  $\text{NO}_3^-$  and temporal variability in concentration has implications beyond contamination risk because it indicates relatively rapid recharge (<60 years) to the basin groundwaters which was not expected based on previous estimates from chloride mass balance models and groundwater age dating techniques. This research combines existing data ranging back to the 1940s with data collected in 2011 to document a multi-decadal trend of overall increasing  $\text{NO}_3^-$  concentration in deep basin groundwaters. CFC (chlorofluorocarbon) analyses of groundwater collected during 2011 indicate the presence of young (<70 years old) water in the basins. The authors infer from these data that there are mechanism(s) by which relatively more rapid and widespread recharge occurs on the basin floors; that recharge is spatially and temporally variable and it results from both anthropogenic (irrigated agriculture) and natural (precipitation) sources. In light of these observations, fundamental conceptual models of flow in these basins should be re-evaluated.

### **2.1 Introduction**

Models of recharge in arid mountain-basin systems commonly disregard the potential contribution of direct recharge through basin floor sediments (e.g. Scanlon 1991; Darling et al. 1998; Wilson and Guan 2004; Beach et al. 2004, 2008). Basin floor recharge is assumed to have no impact on water budget analyses and water quality of basin groundwater. This assumption is at odds with observed decadal trends in water quality in the Trans-Pecos region of West Texas, USA. Water quality (specifically  $\text{NO}_3^-$  concentration) in basin groundwater has been changing throughout the basins and on

relatively rapid (decadal) time scales, which indicates that some amount of water and solute flux must be occurring on the basin floors. By examining apparent groundwater ages in selected wells and  $\text{NO}_3^-$  concentration trends over time throughout the basin aquifers, this paper proposes possible mechanisms of recharge and sources of  $\text{NO}_3^-$  to basin groundwater and looks to revise the conceptual model of recharge in these systems.

## **2.2 Site Description**

The Trans-Pecos region of West Texas is the easternmost extent of the Basin and Range Province of the Western United States. High topographic relief separates the basin floors and adjacent mountain blocks (Fig. 2.1). Soil horizons in the region are generally thin ( $<0.5$  m) and rocky in the mountain areas and thicker ( $\sim 1$  m) in the valleys with little organic matter present (Soil Survey Staff, accessed 2011). Underlying bedrock is largely composed of Cretaceous and Permian carbonates and both intrusive and extrusive igneous volcanic rocks (related to the Late Cretaceous Laramide orogeny and Tertiary rifting). Basin infill is thick late Tertiary and Quaternary alluvial and wind blown sediment deposits (Barnes 1979, 1983) which range from a few meters thick near the basin edges to several hundred meters towards the basin centers.

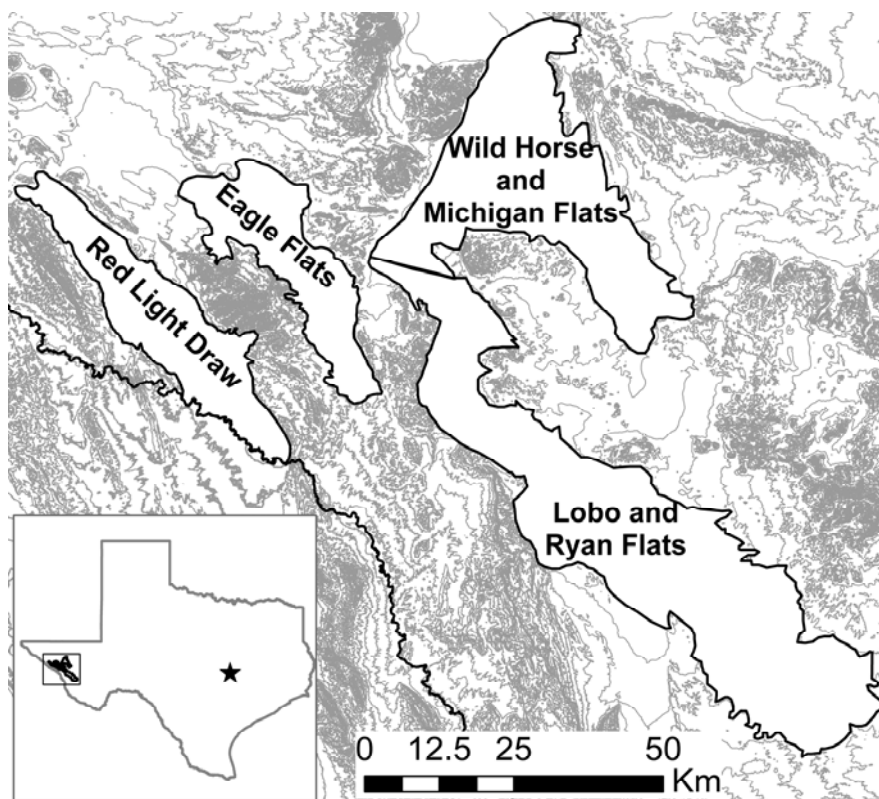


**Fig. 2.1** Location of the four study basins. Contour lines are in 60 m intervals derived from the USGS NED 1/3 arc second dataset.

Climate in the Trans-Pecos region is arid to semi-arid; average annual precipitation is 200-400 mm (NOAA NCDC 2010). Weather patterns in this desert differ from most other North American deserts; the Chihuahan Desert experiences the majority of its precipitation as rain between the months of June and October as a result of convective storm events (Beach et al. 2004, 2008). Rain events tend to be of short duration and high intensity. Precipitation also occurs as snow or ice in the highest elevation regions of the mountains, but is insignificant in the overall water budget for the region (Beach et al. 2008). Because of the high intensity and relatively short duration of the average rainfall event, runoff can be significant in the region.

Four basins in the Trans-Pecos region were selected for this research: Red Light Draw, Eagle Flats, Wild Horse and Michigan Flats, and Lobo and Ryan Flats. Cattle grazing and open rangeland are the most common land use types in all the basins. In both Wild Horse and Michigan Flats and Lobo and Ryan Flats irrigated agriculture was

extensive in the past (up to 13% of basin floor land use circa 1975) and continues to be the third most common land use type. Very little land (<1%) in either Red Light Draw or Eagle Flats has been used for irrigated agriculture.

### **2.3 Conceptualizations of Flow, Groundwater Availability Models (GAMs), and Estimated Age of Groundwater in the Basin Aquifer Systems**

#### *Conceptual Model of Flow and Recharge*

The general conceptual model of the Trans-Pecos region basin aquifers is that they are hydrologically closed systems with extremely limited recharge in which water follows long, slow flow paths (Darling et al. 1998; Uliana 2000; Van Broekhoven 2002; Beach et al. 2004, 2008). The understanding is that most groundwater currently in the basins recharged during the last glacial period (between 15,000 and 20,000 years ago), when the climate of this region was much wetter (Beach et al. 2004, 2008). Little recharge is hypothesized to have occurred in the past 10,000 years and no recharge occurs on the basin floors (Scanlon 1991; Darling et al. 1998; Beach et al. 2004, 2008). The recharge that occurs is assumed to be from two mountain-front recharge (MFR) mechanisms; surface recharge through alluvial fans along the edges of the basins and sub-flow recharge via fractures (Nielson and Sharp 1985; Van Broekhoven 2002; Beach et al. 2004, 2008; Wilson and Guan 2004).

A regional flow path from the southern end of Lobo and Ryan flats northwest towards Wild Horse and Michigan flats is indicated by the slope of the water table (Uliana 2000). Geochemical data also analyzed by Uliana et al. (2007) indicate a hydrologic connection between these basins and springs in the adjacent Toyah basin, although numerical models of the system generally treat the basins as ‘closed’, with groundwater abstraction and evapotranspiration as the only discharge mechanisms (Beach et al. 2004, 2008). Groundwater flow in the basin aquifers is considered to be slow with long residence times (Darling et al. 1998) and recharge is limited to the edges of the basins (Darling et al. 1998; Uliana 2000; Van Broekhoven 2002; Beach et al. 2004, 2008).

### *Texas Water Development Board GAMs*

In Texas, Groundwater Availability Models (GAMs) have been developed by the Texas Water Development Board (TWDB) for major and minor aquifer systems in order to manage current and future water use. The GAMs use information on recharge, discharge, aquifer properties, and pumping practices to determine how much water can be extracted over a period of time and maintain desired conditions within the aquifer (such as volume of future spring discharge or water table levels). There are currently three models for the Trans-Pecos region basin aquifers; one (Beach et al. 2004) for the region containing Lobo, Ryan, Wild Horse and Michigan Flats, one (Beach et al. 2008) for the region containing Eagle Flats and Red Light Draw, and one (Wade 2012) for the Presidio Bolson which is not a part of this study.

These GAMs make several fundamental assumptions:

- 1) All recharge comes from two sources; surface water recharging through alluvial fan deposits and streambeds on the basin edges and sub-flow via fracture networks;
- 2) No recharge occurs on basin floors because the ET demand is too high for the amount of precipitation received to ever reach the water table;
- 3) Recharge does not occur in areas with less than 30.5 cm of precipitation per year because of the ET demand;
- 4) Anthropogenic recharge is negligible - all available water is taken up by crops; and
- 5) Basin sediments are homogeneous and isotropic.

The estimate of recharge used in the GAMs is based upon a percentage value of the amount of precipitation estimated to fall in each basin's recharge zone (adjacent mountains) which is 0-7%, depending on the elevation of the recharge zone (Beach et al. 2004). This estimated amount of annual recharge to the basin aquifers is small; less than 0.5 cm/yr contributed from the mountains surrounding the basins and zero recharge occurring on the basin floors.

Based upon these assumptions and GAM simulations, the conclusion of the GAM is that the water that is being pumped from the basins at a rate of tens to hundreds of

thousands of cubic meters per day during the growing season is “groundwater mining” (i.e., the rate of recharge to the basin floor aquifers is a fraction of the rate of withdrawal). Currently, the desired future conditions set for the Trans-Pecos region basin aquifers are based upon some acceptable rate of drop in the water table over the next several years.

#### *Age Estimates of Basin Groundwater*

Several different methods of estimating groundwater age in the Trans-Pecos basin aquifers have been performed. Carbon-14 and  $^3\text{H}$  dating was used by Darling et al. (1995, 1998); Scanlon et al. (1991) used chloride mass balance in vadose zone sediments as a proxy for basin floor recharge. The age estimates resulting from these methods agree with the conceptual understanding of recharge and the assumptions made for the GAMs. Darling et al. (1995, 1998) estimated the age of groundwater in Eagle Flats and Red Light Draw to be generally between 10,000-20,000 years old, supporting the hypothesis that the majority of recharge had occurred during the last glacial period. From the  $^3\text{H}$  data, Darling et al. were able to determine that some young water is recharging beneath the alluvial fans (MFR source 1) but that it was limited in both amount and spatial distribution. The chloride mass balance method used by Scanlon et al. indicated that minimal downward moisture flux occurred through basin floor sediments during the past 10,000 years. This was the basis for the GAM assumption that no recharge occurs through the basin floor sediments.

## **2.4 Methods**

### **2.4.1 *Historical groundwater geochemical dataset***

Wells were selected for this research based on three main criteria: 1) geographic location (within one of the four basins of interest), 2) drilling record (whether the well was drilled into the basin aquifers of interest or into the underlying systems), and 3) the availability of historical water chemistry data with reliable  $\text{NO}_3^-$  analyses. The list was limited to only water chemistry data deemed to be reliable; which were samples collected by the USGS, samples collected by the TWDB (or predecessor agencies) following



TWDB protocol (e.g., allowing the well to flow prior to sample collection and filtered or preserved samples only), and samples collected for current or past thesis research.

The water chemistry data from each well were imported into a geo-referenced database and assigned a sample decade based on the year of collection. Because the data are temporally sparse, the samples were not analyzed at a time frequency shorter than decadal. In the (rare) case that multiple samples of a single well were collected in one decade, the sample results were averaged together to create a single result for that time period. The  $\text{NO}_3^-$  values from these data were plotted over time to observe the concentration trend. A sample was determined to have a clear upward or downward trend if the change in concentration over time was greater than 1.0 mg/L (as  $\text{NO}_3^-$ ). Samples with less than 1.0 mg/L change in  $\text{NO}_3^-$  concentration were labeled as “no change” and samples that displayed both increases and decreases over time were labeled as “variable”. If variation was present yet an overall trend was still observable (e.g., a sample increased by 7 mg/L between 1970 and 1990, then decreased by 1 mg/L between 1990 and 2000) it was labeled by its dominant trend; this occurred in 4 of the 93 wells examined.

#### **2.4.2 2011 Field Work and Analysis**

##### *Sample Collection and Preservation*

Water samples for cation and anion analyses were collected from wells that were pumped for a minimum of 5 minutes prior to sampling. Samples were collected at the outlet closest to the well, though not all wells had sampling ports installed so some samples were collected from outside faucets or kitchen sinks. All samples were collected from untreated sources. The samples were filtered with disposable 0.45 micron PES filters. A total of 120 mL of sample was collected and filtered from each well. The filtered samples were kept on ice for 24-72 hours and refrigerated upon return to the lab.

Samples from eight wells were collected for CFC-11, CFC-12, CFC-113, and  $\text{SF}_6$  analyses during July 2011. In the case of one open borehole, a Bennett™ pump with nylon tubing was used to collect the sample. The borehole was purged for 1.25 hrs (the time at which temperature, pH, and conductivity readings from discharging water had

been stable for 30 minutes) prior to sample collection. All other samples were collected by connecting copper tubing to sample ports on pumping wells. A flow-through cell was assembled using a 2-liter Pyrex Griffin Beaker and a minimum of 6 liters of water was discharged through the flow cell prior to collection of each bottle of sample. Samples were collected and sealed in 500 mL borosilicate bottles with foil lined caps provided by the University of Miami Tritium Laboratory. All samples were collected in triplicate. Sample bottles were sealed with electrical tape, stored and shipped upside down. Due to problems with shipping two samples (Booth House and Cottrell) were analyzed in duplicate rather than triplicate.

#### *Laboratory Analyses*

Water samples collected during the June and July 2011 were analyzed for major cations and anions using IC. The analyses were performed at The University of Texas Bureau of Economic Geology. Minimum detection level for all analytes was 0.01 mg/L. All results reported were rounded to one decimal value to match with the previously assembled dataset.

The analyses for CFC and SF<sub>6</sub> were performed by the University of Miami Tritium Laboratory. Average annual temperatures and the elevation of the basin floors were provided for the estimation of recharge temperature and recharge elevation. This lab states: “All CFC and SF<sub>6</sub> concentrations are reported on the SIO2005 absolute calibration scale. The atmospheric histories of the CFCs were obtained from Prinn et al. (2000) and Walker et al. (2000) and updated with information from <https://bluemoon.ucsd.edu/pub/cfchist/>. The SF<sub>6</sub> atmospheric history was obtained from [http://cdiac.ornl.gov/oceans/new\\_atmCFC.html](http://cdiac.ornl.gov/oceans/new_atmCFC.html). The temperature, salinity, pressure dependent CFC and SF<sub>6</sub> solubilities were obtained from Warner and Weiss (1985), Bu and Warner (1995), and Bullister et al. (2002). The detection limits for SF<sub>6</sub>, CFC-12, CFC-113, and CFC-11 are 0.05 fmol/kg, 0.010 pmol/kg, 0.010 pmol/kg, and 0.005 pmol/kg respectively.”

## 2.5 Results

### 2.5.1 $\text{NO}_3^-$ trends

During 2011, 80 samples were collected from wells in the four basins. All wells sampled contained measurable levels of  $\text{NO}_3^-$  ( $>0.5$  mg/L as  $\text{NO}_3^-$ ). Concentrations ranged from 1.4 mg/L to 42.2 mg/L (as  $\text{NO}_3^-$ ) with the majority of the wells having  $\text{NO}_3^-$  concentrations in the range of 6.1-9.0 mg/L (Table 2.1). The concentrations of  $\text{NO}_3^-$  are spatially variable, but generally higher in areas of the basins currently used for irrigated agriculture (Fig. 2.2).

Concentration (mg/L - $\text{NO}_3^-$ )	Percent of wells
0.5-3.0 mg/L	12.7%
3.1-6.0 mg/L	8.5%
6.1-9.0 mg/L	47.9%
9.1-12.0 mg/L	19.7%
12.1-15.0 mg/L	1.4%
15.1-18.0 mg/L	5.6%
$>18.1$ mg/L	4.2%

**Table 2.1** Range of concentrations of  $\text{NO}_3^-$  and their relative abundance measured in the 80 wells sampled in 2011.

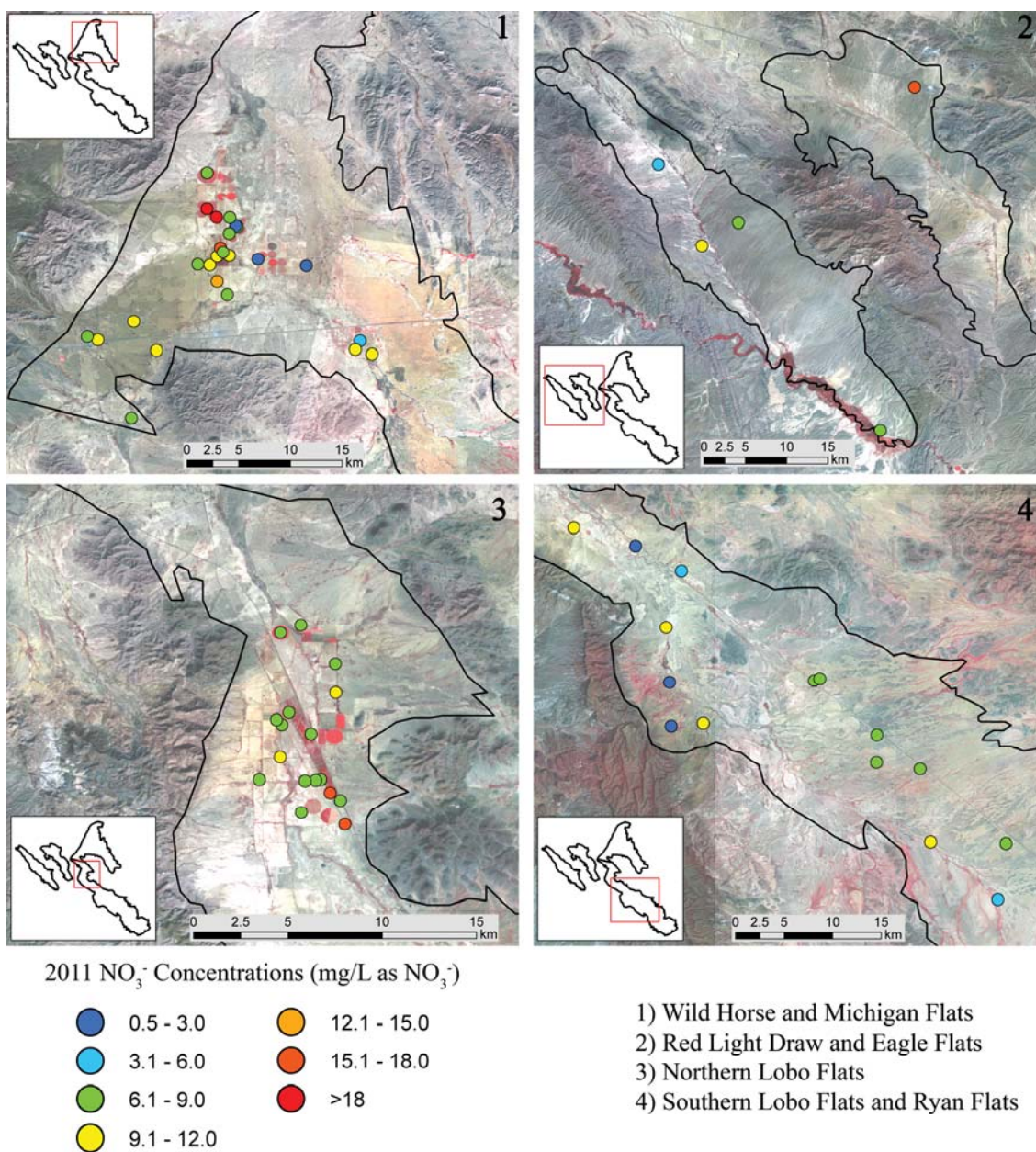
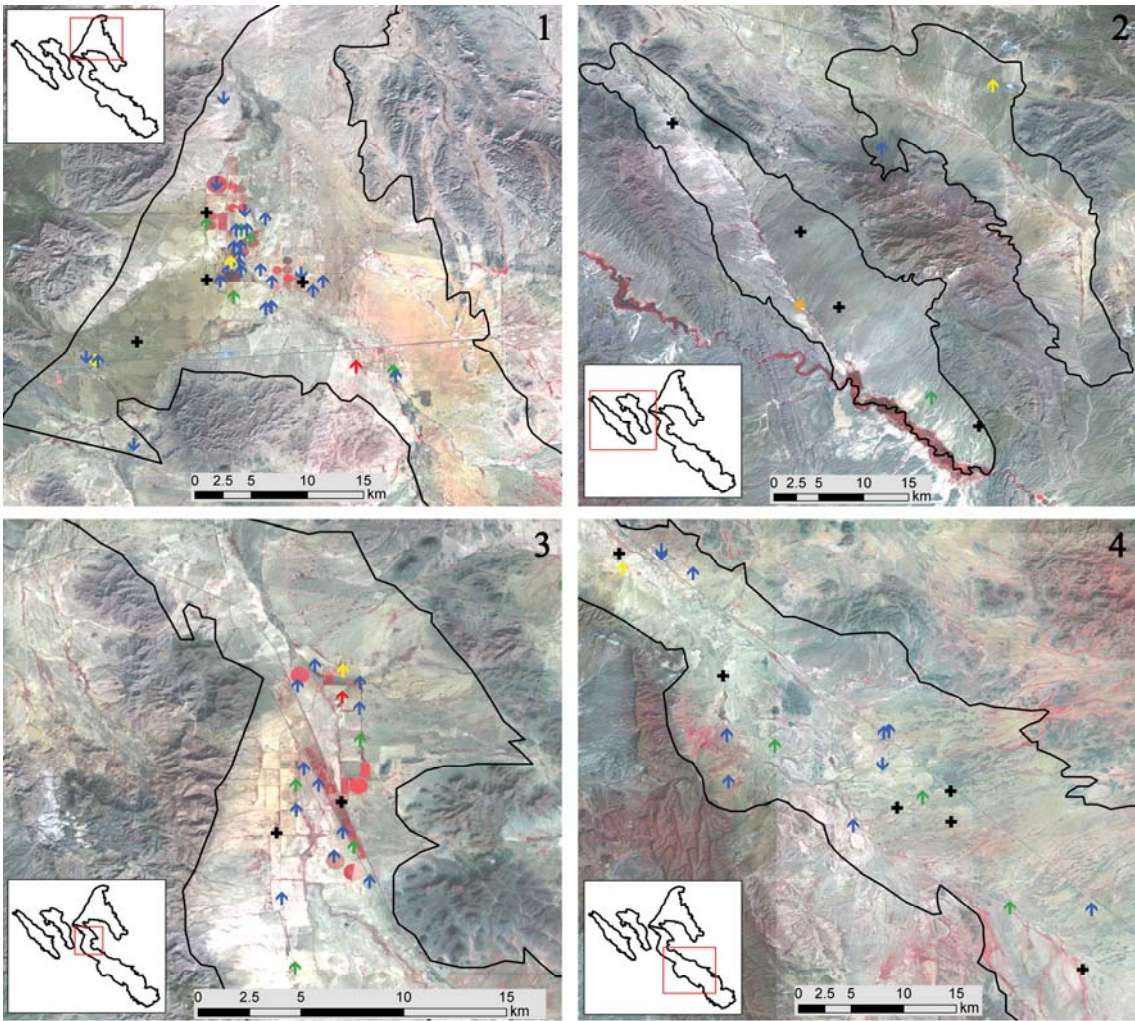


**Fig. 2.2** Map of 2011 NO<sub>3</sub><sup>-</sup> concentrations. Orthoimagery provided by the USGS Landsat Mosaic orthoimagery database, 2000.

Compiling data from the most recent sampling event with the historical groundwater chemistry data, a continuation in the trend of an overall increase of NO<sub>3</sub><sup>-</sup> concentration in basin groundwaters is observed (Fig. 2.3). Previous NO<sub>3</sub><sup>-</sup> concentrations have ranged from 0 mg/L to 100 mg/L (as NO<sub>3</sub><sup>-</sup>), with most samples measuring under 40

mg/L (Fig. 2.4). Median  $\text{NO}_3^-$  concentration in each basin has generally increased over time (from 4.75 mg/L in 1975 to 6.7 mg/L in 2011 in Red Light Draw and Eagle Flats, from 5.25 mg/L in 1945 to 7.8 mg/L in 2011 in Lobo and Ryan Flats, and from 5.25 mg/L in 1955 to 9 mg/L in 2011 in Wild Horse and Michigan Flats) as has the median concentration in the aggregation of the data- from 5.25 mg/L in 1945 to 7 mg/L in 2011 (Fig. 2.5). Of the 93 wells for which multiple data points exist over time, 60 (64.5%) are increasing in  $\text{NO}_3^-$  concentration, 12 (12.9%) are decreasing, 16 (17.2%) are not changing (or have changes of less than 1 mg/L as  $\text{NO}_3^-$ ), and 5 (5.4%) are variable (increasing and decreasing between decades). Of the wells that have had an increase in  $\text{NO}_3^-$  over time (60), the majority have increased between 1-5 mg/L (38 or 63.3%).





$\text{NO}_3^-$  trends (mg/L as  $\text{NO}_3^-$ ): up arrow indicates an increasing trend, down arrow indicates a decreasing trend. Any changes in concentration of  $< 1$  mg/L as  $\text{NO}_3^-$  is considered “no change”



- 1) Wild Horse and Michigan Flats
- 2) Red Light Draw and Eagle Flats
- 3) Northern Lobo Flats
- 4) Southern Lobo Flats and Ryan Flats

**Fig. 2.3** Map of trends in  $\text{NO}_3^-$  concentrations from the 1940's to present. Orthoimagery provided by the USGS Landsat Mosaic orthoimagery database, 2000.

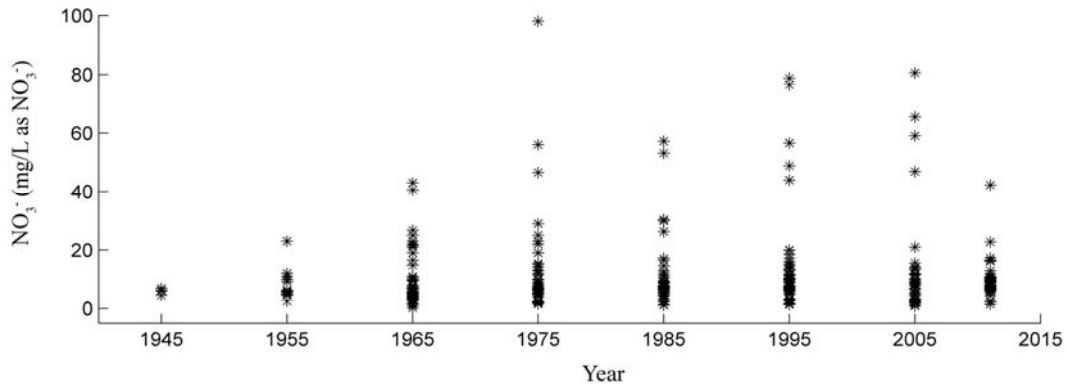


**Fig. 2.4** Scatter plot of NO<sub>3</sub><sup>-</sup> concentrations over time for all wells with available water quality data.

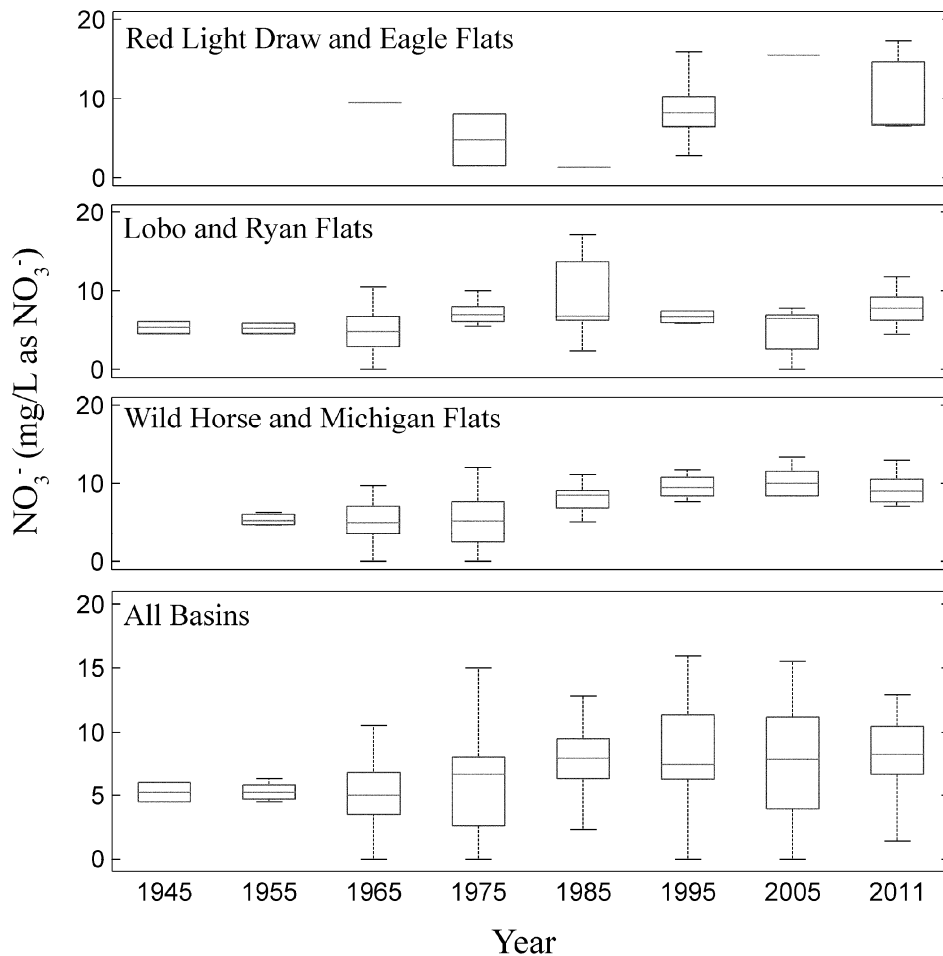


**Fig. 2.5** Box and whisker plots of NO<sub>3</sub><sup>-</sup> concentration by decade. The line inside the box represents the median concentration. The lower and upper extent of the box represent the 25<sup>th</sup> and 75<sup>th</sup> percentile values respectively, and the whisker lines represent the total extent of data points not considered to be outliers. Outlier values not shown on the graphs.

### 2.5.2 CFCs in Basin Groundwaters

Five wells were sampled for CFCs and SF<sub>6</sub> during 2011; two in Wild Horse and Michigan Flats, two in Lobo and Ryan Flats, and one in Eagle Flats. The SF<sub>6</sub> data are not reported because most of the samples were supersaturated with respect to current atmospheric concentrations. This may be due to the water coming in contact with the volcanic/igneous rocks and sediments derived from these rocks. Results from the CFC



analyses are presented in Table 2.2. All of the basin groundwater samples had some amount of CFCs, indicating the presence of young (<70 years old) recharge.

<b>Well ID and Basin</b>	<b>CFC-11</b>	<b>CFC-12</b>	<b>CFC-113</b>
Easley (Lobo/Ryan) – 5110326	47 +/- 2	43 +/- 2	40 +/- 2
Miller (Lobo/Ryan) – 5119902	31 +/- 2	27 +/- 2	26 +/- 2
Brookshier (Wild Horse) – 4759103	55 +/- 2	65 +/- 2	48 +/- 2
Cottrell (Wild Horse) – 4751701	54 +/- 2	65 +/- 2	48 +/- 2
Booth (Eagle Flat) – 4864604	39 +/- 2	31 +/- 2	31 +/- 2

**Table 2.2** CFC results for groundwater collected during 2011.

## 2.6 Discussion

If the residence time of groundwater in these basins is on the order of tens of thousands of years as inferred from models and age-dating, then it is reasonable to assume that the water would be in equilibrium with the surrounding sediments and that significant changes in groundwater chemistry should not be occurring. However, this is not reflected by either the temporal changes in  $\text{NO}_3^-$  concentrations observed over the past six decades or the presence of CFCs in basin groundwater. There are documented patterns of changing  $\text{NO}_3^-$  concentrations in the majority of sampled wells in the four basins. Most of the wells observed have increasing concentrations of  $\text{NO}_3^-$  over time, which leads to two main questions:

- 1) What is/are the source(s) of  $\text{NO}_3^-$  to the basin groundwater?
- 2) How is the  $\text{NO}_3^-$  being transported to the basin groundwater?

### *Hypothesized Sources of $\text{NO}_3^-$*

There exist six probable sources of the  $\text{NO}_3^-$  in the basin aquifers in Trans-Pecos, West Texas. Some of these sources could be major contributors while others could have minor to negligible (or localized) contributions:

- 1) Anthropogenic input via sewage waste from septic tanks/septic fields;
- 2) Atmospheric deposition of reactive nitrogen (N) (anthropogenic, volcanic, and lightning);

- 3) Mobilization of mineralized N (volcanics, meta-sedimentary, and hydrothermal alteration);
- 4) Microbial fixation (biological nitrogen fixation, BNF) of  $N_2$  to reactive N in the soil zone;
- 5) Mobilization of  $NO_3^-$  from a zone of build-up in the desert soils; and
- 6) Anthropogenic input via fertilizer (both synthetic and natural).

Because of the area's sparse population (0.43 people per  $km^2$ ), sewage is not a likely candidate for widespread input to the basin groundwaters. Atmospheric deposition of reactive N may be a significant source of  $NO_3^-$  to the groundwater over very long time scales but the annual mass flux to the groundwater is too small to be a major source of  $NO_3^-$  to the system. Estimates for total atmospheric deposition of reactive nitrogen are between 0.17 and 0.596  $g-N/m^2-yr$  (West 1978). These estimates are reconfirmed by long-term (~30 years) monitoring sites associated with the NADP NTN in two nearby locations, the Guadalupe National Park and Big Bend National Park. The Trans-Pecos region does not contain the rocks that are considered to be major sources of mineralized N, such as shales and coals (Holloway and Dahlgren 2002), but it does contain volcanic and intrusive igneous rocks as well as some outcrops with evidence of hydrothermal alteration (Barnes 1979, 1983); weathering of these rock types is a potential source of  $NO_3^-$  in the groundwater. The relative paucity, spatial variability, and rate of weathering of these rock types make it difficult to predict whether or not they are a major contributor, but the temporal variability in  $NO_3^-$  concentrations make it unlikely.

Fixation of  $N_2$  to reactive N species may be a significant source in the long-term (>1,000 years), but based on BNF rates and estimates of vegetation uptake from other desert soils in the Southwestern United States (Belnap 2002; Peterjohn and Schlesinger 1990) BNF is unlikely to be a significant contributor of  $NO_3^-$  to groundwater on an annual basis. Estimates of BNF for similar grassland systems are around 0.305  $g-N/m^2-yr$  (Cleveland et al. 1999). The maximum potential uptake of reactive N during the growing season of the two most common genera of grass found in the basins (bluestem

and grama) is in the range of 34-85 g-N/m<sup>2</sup>-yr (Levang-Brilz and Biondini 2002). While these grasses are capable of growing and reproducing in environments which are much more N limited, it is possible for vegetation to uptake as much N as BNF provides to the system per year.

This estimate does not discount BNF sourced N as a significant source of reactive N to the groundwater; through assimilation by plants and microbes, reactive N from the BNF process is immobilized in the soil zone. A change in land use from natural vegetation to agricultural use might result in a mobilization of the sequestered N through the breakdown of the organic matter. It is subsequently released back into the vadose zone as reactive N, where it can be transported to the underlying aquifer. This increase of reactive N species beneath cultivated soils has been observed in the High Plains aquifer and was attributed to the mobilization of previously sequestered soil N (Scanlon et al. 2008).

Studies by Walvoord et al. (2002, 2003, 2004) demonstrate that in desert regions NO<sub>3</sub><sup>-</sup> can accumulate at depth in the soil (~10 m) over thousands of years. Concentrations of accumulated NO<sub>3</sub><sup>-</sup> in the vadose zone can be high- NO<sub>3</sub><sup>-</sup> concentrations ranged from 1-258 mg/L as N in (seven) soil cores taken from the Chihuahan Desert depending on the type of overlying vegetation (Walvoord 2002, 2004). Mobilization of this reservoir of NO<sub>3</sub><sup>-</sup> could be a significant contributor to the NO<sub>3</sub><sup>-</sup> concentration in the basin groundwater.

Synthetic and natural (manure-based) fertilizers are the main source of anthropogenic NO<sub>3</sub><sup>-</sup> contamination of groundwater in most of the world (Galloway et al. 2004). Due to timing differences between application and crop demand, some percent of the fertilizer applied can bypass plant uptake and be flushed below the root zone where it can subsequently reach and contaminate the groundwater. N-P-K (nitrogen-phosphorous-potassium) synthetic fertilizers have had widespread use since the 1950s (Galloway et al. 2004). Synthetic fertilizers are the primary choice for crop fertilization in the Trans-Pecos region. Leaching of these fertilizers from the soil zone is a possible source of NO<sub>3</sub><sup>-</sup> contamination within the basin groundwaters because fertilization is

widespread (non-point source) and a seasonally repeated practice. Animal manure is also a possible source of reactive N. Grazing of animals including cattle can increase the manure load to the land surface, particularly around watering troughs where the animals tend to gather.  $\text{NO}_3^-$  contribution from manure is spatially variable.

*Possible Pathways for  $\text{NO}_3^-$  Introduction into the Groundwater*

With the exception of mobilization of mineralized  $\text{NO}_3^-$  from rocks and sediments (a source unlikely to be able to account for the widespread temporal variability in  $\text{NO}_3^-$  in the groundwater of this region), all of the sources of N to the system are located at or near the land surface on the basin floors. The two most probable pathways for the introduction of  $\text{NO}_3^-$  to basin groundwater are:

- 1) Anthropogenically-induced recharge on the basin floor due to irrigation practices; and
- 2) Natural recharge is occurring on the basin floors

In existing models of recharge to these basins, direct recharge via infiltration of precipitation on basin floors is considered negligible because: a) the amount of precipitation on the basin floor is less than the amount occurring in mountain zones; and b) potential evapotranspiration on the basin floor is often high enough most precipitation is likely evapotranspired before it can recharge the groundwater (Winograd 1981; Scanlon et al. 1997). However, this model may need revision in situations where irrigated agriculture occurs on basin floors. Added irrigation water could either mobilize  $\text{NO}_3^-$  in the soils and subsurface during recharge, have high  $\text{NO}_3^-$  concentrations due to the presence of anthropogenic fertilizers, or both (Scanlon et al. 2006). In localized zones of intense agriculture where groundwater is used for irrigation there is a possibility of a temporal increase in TDS as well as  $\text{NO}_3^-$  concentrations resulting from the effects of irrigation return flow (Causape et al. 2004b), though it is unclear whether this phenomenon is occurring in the irrigated areas of the Trans-Pecos.

It is unlikely that most precipitation events within the basins cause widespread recharge given their magnitude, the antecedent conditions, and the geomorphology of the basin floors. An alternative hypothesis to the current model of “zero recharge” on the basin floors is that recharge events on basin floors are the result of infrequent major

precipitation events leading to a flux of both water and solutes to the underlying groundwater (Sami 1992; Lewis and Walker 2002; Herczeg and Leaney 2011). A major rain event that results in the ponding of water in low lying areas could cause a “flushing” of water through the vadose zone, mobilizing soil N and contributing a large flux of  $\text{NO}_3^-$  to the groundwater. Additionally, studies using oxygen and hydrogen isotopes in Australian basins indicate that arid zones may have more basin floor recharge than their semi-arid counterparts due to the paucity of permanent vegetation taking up the available water in the unsaturated zone (Herczeg and Leaney 2011), which questions the assumption of “zero” recharge on the basin floors.

*Increased  $\text{NO}_3^-$  as an indicator of rapid recharge/recharge occurring on the basin floors*

The Trans-Pecos systems offers a unique setting in which  $\text{NO}_3^-$  can be used as an indicator of both decadal scale recharge occurring to deep basin groundwater and the presence of widespread basin floor recharge. All of the sources of  $\text{NO}_3^-$  discussed above are present only on the basin floors, with the possible exception of mobilization of N from rock sources. The lithology of the area makes it unlikely that mobilization of mineralized N from rocks and sediments is a significant contributor of  $\text{NO}_3^-$  to basin groundwater. Because the sources are present only on the basin floors, some mechanism of recharge must be occurring on the basin floors. The fact that groundwater with increasing concentrations of  $\text{NO}_3^-$  is observed in wells in the middle of the basin as well as along the basin edges indicates widespread recharge through the basin floor sediments, not just via alluvial fans and gravel channels on the basin edge.

Transport of  $\text{NO}_3^-$  through the basin aquifers can be treated as conservative because of the properties of the system. Minimal build-up of organic carbon occurs in the basin sediments, the water table is very deep (between 20 m to over 200 m), and there is evidence of oxic groundwater even in the deep wells of the basins. These lines of evidence indicate that denitrification (if it occurs at all) is not a significant sink of N. Beneath the root zone, very little assimilation of  $\text{NO}_3^-$  occurs. Because these two  $\text{NO}_3^-$  sinks are limited within this system,  $\text{NO}_3^-$  can be considered as conservative in the basin

groundwater. Thus, it can be assumed that the  $\text{NO}_3^-$  that reaches the deep groundwater will remain there (absent the abstraction of groundwater via wells).

Based on the observations above (location of possible  $\text{NO}_3^-$  sources and evidence that  $\text{NO}_3^-$  is conservative within the groundwater), a trend of increasing  $\text{NO}_3^-$  over time can be attributed to addition of  $\text{NO}_3^-$  to the groundwater. When the observed increases occur on the decadal scale (as is the case in these basin groundwaters), then the process(es) responsible for the  $\text{NO}_3^-$  transport (recharge mechanisms) must be decadal in scale as well. Irrigation return flow is one possible mechanism of relatively rapid recharge to basin aquifers; it has been observed to increase  $\text{NO}_3^-$  and salt concentrations in groundwater in similar systems, such as the High Plains aquifer (Gurdak and Qi 2006) and the Murray River basin in Australia (Beare and Heaney 2001) as well as many others. However, irrigation return flow cannot account for all of the observed increases in groundwater  $\text{NO}_3^-$  in the West Texas basins, especially not in basins with little or no irrigated agriculture (i.e., Eagle Flats and Red Light Draw). Natural recharge must be occurring on relatively rapid (decadal or shorter) time scales in order to account for the decadal scale changes in  $\text{NO}_3^-$  concentration observed in wells throughout all of the basins.

#### *Evidence of Preferential flow paths*

Anecdotal evidence of preferential flow paths in basin sediments has been documented in multiple basins examined for this study. While there remains the challenge of how to quantify the presence of these flow paths and their effects on groundwater flow within the basins, they are inferred to have some impact on groundwater flow and solute transport within these systems. Three examples of preferential flow paths in the basin sediments are described in Northern Lobo Flats, Wild Horse Flats, and Michigan Flats.

In Northern Lobo Flats, the Easley well (well ID 5110326) is an irrigation well that provides water to two 0.64 km<sup>2</sup> fields. Estimated pumping rate from the well is ~110 m<sup>3</sup>/hour. Maintenance on the pump was performed during the summer of 2011. While the pump was out of the well, a video camera was put down hole to determine if any

sections of the well casing needed to be repaired or replaced. The camera operators observed that particulate matter in the water column was moving rapidly in a horizontal direction through the well casing; furthermore, it was moving quickly enough that it did not have time to fall out of suspension before it exited. The authors infer that the well is pumping from a coarse gravel channel that is highly conductive relative to the surrounding sediments.

In Michigan Flats, the Koehn irrigation well (well ID 4760401) pumps progressively fresher water throughout the season. Measurable decreases in salinity can be observed in the discharging water days to weeks after pumping has commenced. This observation indicates that this well is possibly receiving lateral inflow from fresher water sources.

In Wild Horse Flats, during major rain events, discharge through the ephemeral Wild Horse Creek, Hurds Pass Draw, and Clayton Draw can be observed disappearing along stretches of the channels. The presence of high permeability zones in the underlying strata that conducts some of the overland flow into the subsurface has been inferred.

#### *Revised Conceptual Model of Flow*

The authors propose a revised conceptual model of recharge and groundwater flow in these basins based upon the trends in water chemistry, apparent age results from dissolved gas collection, and the anecdotal evidence of preferential flow paths in basin sediments. Existing numerical models of these systems assume homogeneity and isotropy of basin sediments, that no recharge occurs on basin floors, and that groundwater in these systems is very old (>10,000 years old).

There is no dispute that recharge occurs by sub-flow and overland flow from the adjacent mountain blocks, but these recharge sources alone cannot account for the variability in groundwater chemistry and the presence of young water in wells kilometers away from mountain front recharge zones. There is no significant source of  $\text{NO}_3^-$  in the mountainous recharge zones so recharge from these areas cannot account for the changes observed in  $\text{NO}_3^-$  concentrations over the past decades. In light of these observations, the

authors propose that recharge occurs on the basin floors as a result of both anthropogenic and natural processes.

Although its occurrence may be temporally and spatially variable, recharge certainly occurs beneath land used for irrigated agriculture. Irrigation of crops on the basin floor is mobilizing two possible sources of  $\text{NO}_3^-$  to basin aquifers by transporting synthetic fertilizers beneath the root zone of the plants and into the groundwater and by mobilizing  $\text{NO}_3^-$  salts from the deep vadose zone to the underlying groundwater.

Variability in water chemistry in wells in basins with no past or present irrigated agriculture and in sections that have not been used for irrigated agriculture in the past 30 years indicate that natural recharge is also occurring on the basin floors. Not all precipitation that falls on the basin floors recharges the underlying aquifers; the high PET in this region causes much of the precipitation to be evapotranspired before it can reach the water table. However, the Trans-Pecos region is known for its large magnitude, short duration convective storm events that have a potential to result in some recharge to the groundwater. Large desiccation cracks in basin sediments (Goetz 1985) as well as other preferential flow paths can transport water beneath the root zone. These “flushing” precipitation events could mobilize  $\text{NO}_3^-$  from both surface sources and the deep vadose zone and transport  $\text{NO}_3^-$  to the underlying groundwater.

### *Implications*

Several implications arise from the data collected and the observations made in this research. First, there is more water recharging through the basin floor to the underlying aquifers than is commonly assumed, and second, irrigation return flow to the basin groundwater is a process of concern in this system because of the resulting increases in  $\text{NO}_3^-$  and salinity in basin groundwater. Consideration of these processes is integral to the sustainable use and management of these aquifers. Beyond local implications, these results raise questions about the validity of similar assumptions made in conceptual and quantitative models in other arid basin systems.



## 2.7 Conclusions

This research documents an overall trend of increasing groundwater  $\text{NO}_3^-$  concentration from the 1950s to present in the basin aquifers of Trans-Pecos Texas and the presence of young (<70 year old) water in these basins. These observations lead to the conclusion that there exist mechanism(s) of relatively rapid recharge to the groundwater and that the(se) mechanism(s) are occurring not only along the mountain front zones but are also widespread across the basin floors. Both natural and anthropogenic mechanisms are likely occurring; the source of natural recharge is most likely large magnitude, short duration rainfall events and anthropogenic recharge is occurring via irrigation return flow. The source(s) of  $\text{NO}_3^-$  to the basin groundwater are likely both natural and anthropogenic including mobilization of N from the soil zone, synthetic fertilizers, and manure. Such trends are important to consider when addressing water quality and sustainable use policies here and in similar systems around the world.

**Chapter 3:** Estimates of recharge in two arid basin aquifers: a model of spatially variable net infiltration and its implications (Red Light Draw and Eagle Flats, Texas, USA)

**Abstract**

Methods of estimating recharge in arid basin aquifers (such as the 1% rule, Maxey-Eakin method, storm-runoff infiltration and others) overlook the potential contribution of direct recharge on the basin floors. In the Trans-Pecos region of West Texas, USA, this has resulted in potential recharge and solute flux to basin aquifers being ignored. Observed trends in groundwater nitrate ( $\text{NO}_3^-$ ) concentrations and the presence of young (<70 year old) water in the basins indicate that recharge is occurring through the basin floors. A spatially variable net infiltration model (INFIL 3.0.1) was used to estimate the volume and spatial distribution of potential recharge to two basins: Red Light Draw and Eagle Flats. The INFIL model provides insight into the mechanisms by which recharge and solute flux occurs in arid basin systems. This method demonstrated that recharge is widespread; it is not limited to the mountainous areas and mountain-front recharge mechanisms, and up to 15% of total potential recharge in these basins occurs across widespread areas of the basin floors. Models such as this should improve scientific understanding and sustainable management of arid basin aquifers in Texas and elsewhere.

**3.1 Introduction**

Water quality and availability in arid regions is a concern due to increasing population and demand for potable water both for drinking and other purposes (i.e., irrigated agriculture and animal husbandry). In the Trans-Pecos region of West Texas, USA, scientists and water management authorities have been attempting to address these issues for the past three decades (e.g., Gates et al. 1980; Darling et al. 1998; Beach et al. 2004, 2008). To date, the modeling and management approaches taken for this region have been based on a widely used conceptual model for groundwater recharge in arid basin systems: In this model, there is minimal modern recharge that occurs to the basin aquifers, the main source(s) of that recharge are via mountain front recharge mechanisms, and negligible recharge occurs on the basin floors away from the mountain blocks and

alluvial fan deposits (Darling et al. 1998; Uliana 2000; Van Broekhoven 2002; Walvoord et al 2002; Wilson and Guan 2004; Beach et al. 2004, 2008). These assumptions simplify the system for modeling and management but do not reflect the changes observed in groundwater chemistry over the past six decades (Robertson and Sharp 2012) and limit their applicability to these basins. A more sophisticated modeling approach- one that accounts for spatial and temporal variability in precipitation, runoff, potential evapotranspiration, and watershed properties is needed to address the question of where and how much recharge occurs to the basin aquifers. In this paper, the INFIL model, a spatially variable net infiltration model, is applied to examine the spatial distribution of potential recharge to the Red Light Draw and Eagle Flats basins.

### **3.2 Site Description**

The Trans-Pecos basin aquifers of West Texas, USA are located in far west Texas, bordered to the north by the New Mexico-Texas border and to the south by the Rio Grande (Fig. 3.1a). The eastern-most expression of the Basin and Range province, the basins were created during the Late Cretaceous Laramide Orogeny and subsequent Tertiary rifting processes (Barnes 1979, 1983). As part of the Chihuahan desert, the climate of the region is arid with average annual precipitation being between 220-360 mm on the basin floors and between 500-700 mm in the adjacent mountainous areas. The majority of precipitation in the region occurs as a result of convective summer storm events occurring between June and October; the storms tend to be of large magnitude and short duration. Limited snowfall does occur within the region but is considered negligible in the context of total precipitation (Beach et al. 2004, 2008). There are two groundwater systems in the basins; the unconfined aquifers in the unconsolidated quaternary fill (known as the basin aquifers) and the underlying confined Cretaceous system (Beach et al. 2008). Depth to water within the basin aquifers varies depending on distance from the adjacent mountains with typical depths of 8-10 m close to the edges of the mountain front to depths of 130-140 m towards the centers of the basins. The natural vegetation types are blue stem, grama, lechuguilla, and creosote bush within the basins with limited juniper growing in the mountains at higher elevations. Vegetation typically

covers between 10-35% of the land area; bare soil is dominant in most areas (McMahon et al. 1984; Schmidt 1995; Beach et al. 2008). In the basins of Red Light Draw and Eagle Flats, most of the land is used for grazing of cattle or left as natural scrubland. Very little (<3%) has been used for irrigated agriculture in the past five decades and almost all irrigated agriculture occurring in Red Light Draw is along the Rio Grande and uses river water. This practice has ceased as water quality and supply have diminished in the Rio Grande (Miyamoto et al. 1995; Levings et al. 1998; Bennett 2006). There are no urban areas within either basin. Some industry, a talc mine and a processing facility, is present in Eagle Flats. This facility does not use the unconfined basin groundwater as the well that supplies water is screened only in the underlying Cretaceous carbonate aquifer. Overall due to the low population and limited industry the water demands in these two basins are small; currently an estimated 400 ac-ft per year ( $4.9 \times 10^5$  m<sup>3</sup>/yr) is withdrawn (Beach et al. 2008). This withdrawal rate has remained consistent from the mid 1980's to present (Beach et al. 2008).

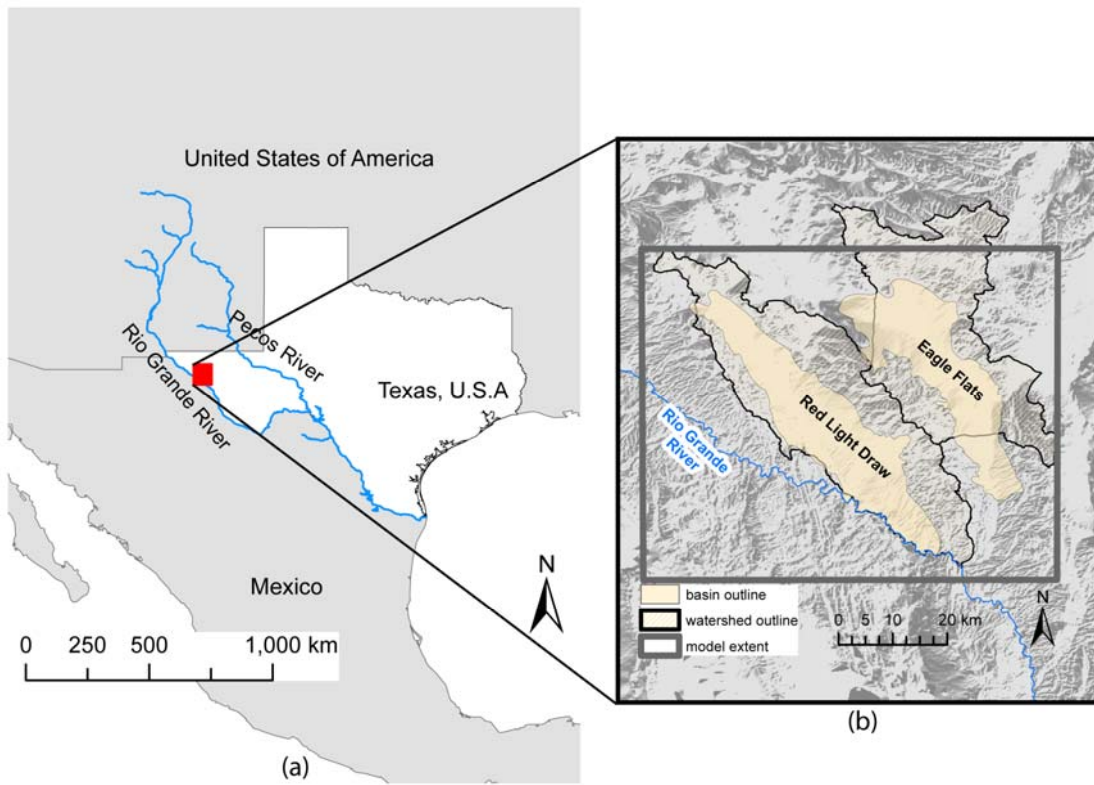


**Fig. 3.1** (a) Map of the area of interest within the Trans-Pecos Region of Texas, USA. (b) Location of the modeled area; Red Light Draw and Eagle Flats basins and their contributing watersheds.

### 3.3 Previous Estimates of Recharge

Several recharge estimates using a variety of methods have been made for these basins during the course of research and water management studies in the region over the past 30 years. In 1992 Eagle Flats was a proposed location for a low-level radioactive waste repository and in that context detailed research was performed on the hydrology of the area (Darling et al. 1994). Groundwater availability models were created for both Red Light Draw and Eagle Flats in the context of a state-wide survey of available water resources of Texas. These recharge values have been used to estimate the volume of water available for extraction and inform management practices in the basins.

The first recharge estimates made for the Red Light Draw and Eagle Flats basins were based on the 1% rule (Gates et al. 1980). These estimates assume that 1% of annual

precipitation becomes recharge, regardless of basin characteristics such as geology or topography. Spatial distribution of recharge is not considered with this model; it only provides an estimate of recharge volume to the basin. Using this model the estimate for Red Light Draw recharge was 2,000 ac-ft/yr ( $2.47 \times 10^6$  m<sup>3</sup>/yr) and for Eagle Flats was 3,000 ac-ft/yr ( $3.7 \times 10^6$  m<sup>3</sup>/yr) (Gates et al. 1980). A modification of this method was used by LGB-Guyton et al. (2001) which accounted only for precipitation falling at higher elevations and not on the basin floors where annual evapo-transpirative demand is much greater than annual precipitation; this modification led to an estimate of recharge for Red Light Draw of 700 ac-ft/yr ( $8.6 \times 10^5$  m<sup>3</sup>/yr) and an estimate of 1,000 ac-ft/yr ( $1.2 \times 10^6$  m<sup>3</sup>/yr) for Eagle Flats.

In 2001, a storm runoff infiltration model was used to estimate recharge to Eagle Flats which assumed that a runoff generating event occurs once every two years, of which 35% became recharge. It did not take into account any watershed or basin characteristics and it did not account for recharge occurring at higher elevations. The storm runoff model estimated that for Eagle Flats there would be the equivalent of 4,119 ac-ft/yr ( $5.1 \times 10^6$  m<sup>3</sup>/yr) of recharge that would occur (Finch and Armour 2001). A modification to the 2001 estimate was performed in 2004 which took into account basin floor characteristics and potential recharge zone to account for heterogeneity in storm water runoff and infiltration. It mapped the location and hydrologic properties of alluvial fan deposits (assumed to be the areas where recharge could occur (Scanlon et al. 2001; Finch and Armour 2001)) and used elevation to predict where runoff would accumulate (Beach et al. 2004). This model estimated that 3036 ac-ft/yr ( $3.7 \times 10^6$  m<sup>3</sup>/yr) of recharge was occurring in Eagle Flats; a decrease from the previous storm runoff infiltration model (Beach et al. 2004).

In 2008 the Texas Water Development Board created a Groundwater Availability Model for the Red Light Draw, Eagle Flats and Green River Valley basin aquifers that included recharge estimates based on a conceptual model that 1) assumed all recharge comes from two sources; surface water recharging through alluvial fan deposits and streambeds on the basin edges and sub-flow via fracture networks, 2) no recharge occurs

on basin floors because the ET demand is too high for the amount of precipitation received to ever reach the water table, 3) anthropogenic recharge is negligible - all available irrigation water is taken up by vegetation, and 4) basin sediments are homogeneous and isotropic. The method of recharge estimation used was a modified Maxey-Eakin approach combined with a storm runoff re-distribution model. It assumed that in areas of the basin with fewer than 12 in (305 mm) of annual precipitation that zero recharge would occur and increasing amounts of recharge would occur with increasing precipitation up to 12% at over 20 in (508 mm) of annual precipitation (Beach et al. 2008). This approach resulted in an estimate for recharge in Red Light Draw of 1,631 ac-ft/yr ( $2.0 \times 10^6$  m<sup>3</sup>/yr) and 2,869 ac-ft/yr ( $3.5 \times 10^6$  m<sup>3</sup>/yr) in Eagle Flats.

Field studies performed by Darling et al (1995, 1998) looking at tritium (<sup>3</sup>H) and carbon 14 (<sup>14</sup>C) and by Scanlon (1991) using the chloride (Cl<sup>-</sup>) mass balance approach align with the recharge estimates made in the past models and a groundwater age of between 10,000 and 20,000 years old in the basin aquifers. Darling et al (1995, 1998) found <sup>14</sup>C ages between 10,000 and 20,000 years old in the basins and were only able to detect <sup>3</sup>H beneath the alluvial fans along the edges of the basins. Scanlon (1991) used Cl<sup>-</sup> concentrations in the unsaturated zone and calculated moisture flux based on a steady-state flow model. Downward soil moisture flux through the upper one meter of the unsaturated zone was approximately 0.1 mm/yr using this method so it was concluded that minimal recharge has occurred in the basin during the last 10,000 years (Scanlon 1991).

The modified one percent rule (LGB-Guyton et al. 2001), the storm runoff infiltration model (Finch and Armour 2001), the storm runoff distribution model (Beach et al. 2004), and the Texas Water Development Board Groundwater Availability Model (Beach et al. 2008) all assume that recharge from direct precipitation on the basin floors is negligible and is not included in the recharge estimates. All of the methods used to estimate recharge in the Red Light Draw and Eagle Flats basins conclude (or assume) that minimal recharge occurs to these basins during present-day time, that the limited recharge which is occurring occurs mountain front/mountain block recharge and along

the edges of the basins (Scanlon et al. 2001; Finch and Armour 2001; Wilson and Guan 2004), and that no widespread recharge is occurring on the basin floors.

### **3.4 Nitrate Variability and Apparent Age of Groundwater in Red Light Draw and Eagle Flats**

Trends in groundwater chemistry (specifically  $\text{NO}_3^-$ ) indicate that the conclusion drawn by previous research of zero recharge on the basin floors is incorrect (Robertson and Sharp, 2012). Within Red Light Draw and Eagle Flats, there are eight wells for which there are water quality data for multiple decades (including  $\text{NO}_3^-$  concentrations). In four of these eight wells,  $\text{NO}_3^-$  concentrations have been increasing over time. The average increase in  $\text{NO}_3^-$  concentration for Red Light Draw is 8.6 mg/l (as  $\text{NO}_3^-$ ) over 30 years (0.29 mg/l per year) and 6.75 mg/l (as  $\text{NO}_3^-$ ) over twenty years (0.34 mg/l per year) in Eagle Flats. The most likely source of  $\text{NO}_3^-$  to the basin aquifers is mobilization of  $\text{NO}_3^-$  from a zone of build-up in the vadose zone of the basin floor sediments (Walvoord et al. 2003; Robertson and Sharp 2012; Robertson et al. 2012), not in the adjacent mountains where depths to bedrock are shallow and soil horizon development is limited (Beach et al. 2004, 2008). Additionally, chlorofluorocarbon (CFC) dating of a well in Eagle Flats (TX well ID 4864604) has an apparent age of 39 years (+/- 2 yrs) based on CFC-11 and 31 years (+/- 2 yrs) based on CFC-12 and CFC-113, which indicate the presence of young water in the basin.

These observations conflict with the past estimates of recharge and the current GAMs because they indicate that widespread modern recharge is occurring on the basin floors. The increase in groundwater  $\text{NO}_3^-$  concentrations from the 1950's to present are indicative of this because 1) there are no significant sources of N in the thin soils of the adjacent mountain ranges and 2) the increase in  $\text{NO}_3^-$  concentrations in wells kilometers removed from the mountains and mountain front zones is not likely caused by infiltration of runoff that rarely reaches further than the distal extent of alluvial fan deposits adjacent the mountains and does not reach the middle of the basin 10 to 15 km away (Wilson and Guan 2004). The presence of young water within the basin aquifer (based on CFC sampling) far (approximately 12 km) from the adjacent mountains add additional



evidence that indicates recharge from direct precipitation occurs on the basin floors. The 1% rule, Maxey-Eakin method, storm-runoff infiltration model and the other methods of estimating recharge that have been used in this region do not adequately characterize the complexities of these systems.

### 3.5 Methods

#### 3.5.1 Model Description

A different approach to estimating recharge in the Red Light Draw and Eagle Flats basins was selected in order to evaluate if widespread recharge could occur on the basin floors as is indicated by the trends in  $\text{NO}_3^-$  and presence of CFCs in basin groundwater. The INFIL 3.0.1 model is a grid cell based distributed parameter watershed model that estimates net infiltration beneath the root zone on daily time scales (Hevesi et al. 2002; U.S. Geological Survey Staff 2008). The total net infiltration is calculated for each grid cell using precipitation (rain and snow), ET, runoff, surface water run-on, infiltration of water into the root zone, and changes in near surface water content:

$$NI_d^i = RAIN_d^i + MELT_d^i + Ron_d^i - Roff_d^i - \sum_{j=1}^6 (\Delta W_d^i)_j - ET_d^i \quad (1)$$

Where  $N_d^i$  is the net infiltration for day  $d$  and grid cell  $i$  (mm),  $RAIN_d^i$  is precipitation occurring as rain for day  $d$  and grid cell  $i$  (mm),  $MELT_d^i$  is snowmelt for day  $d$  and grid cell  $i$  (mm),  $Ron_d^i$  is infiltration to the root zone due to surface water run-on for day  $d$  and grid cell  $i$  (mm),  $Roff_d^i$  is the surface water runoff for day  $d$  and grid cell  $i$  (mm),  $\sum (\Delta W_d^i)_j$  is the total change in root zone water storage for all six model layers ( $j = 1 - 6$ ) for day  $d$  and grid cell  $i$  (mm), and  $ET_d^i$  is the total bare-soil evaporation and root zone transpiration for all six root zone layers for day  $d$  and grid cell  $i$  (mm). Net infiltration is defined as the flux of water across the lower boundary of the root zone, which estimates potential recharge. The lower boundary of the root zone is assumed to be the depth beneath which evapo-transpirative processes have no effect and thus water beneath this zone will move downward and become recharge. Grid cell area can be determined by the user and up to six discrete vertical layers within the vadose zone (five soil types and one

bedrock type) can be delineated. This model has been used successfully to estimate net infiltration and recharge in Joshua Tree, CA (Nishikawa et al. 2004), in Death Valley, NV and CA (Hevesi et al. 2002, 2003), and in Riverside County, CA (Rewis et al. 2006).

INFIL 3.0.1 is unique from the models used previously to estimate recharge in these basins in that it simulates spatially distributed precipitation, ET, and infiltration processes on a daily time scale rather than on an annual scale averaged across the entire watershed area. Models used by Gates et al. (1980), Finch and Armour (2001), and LBG-Guyton et al. (2001) included no way to quantify spatial or temporal variability in potential recharge; precipitation was not represented either spatially within the catchment or temporally distributed to represent the variability in magnitude and duration of storm events. The INFIL model interpolates spatially distributed precipitation and PET values on a daily, monthly, and annual time scale based on data from weather stations within and surrounding the model extent. This enables the estimates of potential recharge to reflect spatial and temporal variability within the catchment, unlike the models used by Gates et al. (1980), Finch and Armour (2001) and LBG-Guyton et al. (2001).

The storm water redistribution model developed by Beach et al. (2004) does improve upon the past modeling efforts in that it attempts to account for spatial distribution of potential recharge. However, this model is based upon flawed (and arguably arbitrary) assumptions (e.g., no recharge occurs as a result of direct precipitation, no recharge can occur in areas with less than 12 in (305 mm) of annual precipitation) that limit the locations where recharge could potentially be occurring rather than modeling the processes which govern moisture flux on the surface and in the root zone. It treats the infiltration, ET, water storage, and moisture flux processes as a lumped system and assumes based on average annual ET demand versus average annual precipitation that net flux beneath the root zone in most of the catchment area is zero (Beach et al. 2004). The INFIL model improves on Beach et al. because it models precipitation, surface flow processes, ET, water storage, moisture fluxes and the interaction between them for each grid cell; it spatially and temporally distributes these

processes throughout the catchment. The INFIL model provides a more accurate estimation of the spatial distribution of potential recharge to the Red Light Draw and Eagle Flats aquifers.

### **3.5.2 Model Set-up**

For the study of Red Light Draw and Eagle Flats a model of 15,600 grid cells measuring 500 m by 500 m, in 130 columns and 120 rows was developed that encompasses all of both basins and most of the contributing watershed area (Fig. 3.1b). Elevation changes within the mountain ranges and variability of basin floor lithology largely dictated the spatial resolution for the model area. Two vertical layers were delineated within the root zone; one soil layer and one rock layer, selected because of the thin (typically less than 1 m thick, maximum thickness of ~1.8 m) soil horizons within the model extent (Beach et al. 2008, Soil Survey Staff accessed June 2012) and lack of detailed vertical profiles of soil type (Soil Survey Staff accessed June 2012).

Several datasets were used in order to create the model inputs required to run the INFIL model. Digital elevation models (DEM) and slope/aspect values were created based on the 30m National Elevation Dataset (Gesch 2002, 2007). Soil type, thickness, and properties were obtained through the U.S. General Soils Map and the Soil Survey Geographic Database (Soil Survey Staff accessed June 2012) and the field capacity, wilting-point, and drainage coefficient variables were assembled based on literature values (Jury et al. 1991; Hornberger et al. 1998; Dingman 2002). Geological data were taken from the Geological Atlas of Texas (Stoeser et al. 2007) and the associated values for porosity and hydraulic conductivity were assembled from representative published values (Freeze and Cherry 1979; Domenico and Schwartz 1997; Custodio 2007). Data on vegetation cover were gathered from The Vegetation Types of Texas map (McMahon et al. 1984), vegetation density was estimated using the Landsat 7 Enhanced Thematic Mapper Plus (ETM+) imagery available for the field area on 12 June – 19 June 2000 (NASA Landsat Program accessed June 2012) and root-zone thickness variables were estimated based on similar plant types used in previous studies (Hevesi et al. 2002; Nishikawa et al. 2004; U.S. Geological Survey Staff 2008). For the section of the model

located in Mexico, limited data on geology, soils, and vegetation were available. The gaps in these data were filled in by using known values and comparing them to locations of similar elevation and slope on the U.S. side of the border to extrapolate out vegetation, soil, soil thickness, and rock type.

Climate data were assembled from long term weather station data in the National Oceanic and Atmospheric Administration's National Climatic Data Center database (NOAA NCDC accessed June 2012). Five stations were used; Fort Hancock (USC00413266), Sierra Blanca (USC00418305), Van Horn (USC00419295), Valentine (USC00419275), and Candelaria (USC00411416). Stations were selected for their proximity to the model extent and their availability of data (10 years or more during the 60 year model simulation). All of the stations selected had records of air temperature (max and min), rainfall, and snowfall. The precipitation input for this model simulation was rainfall only; snowfall was infrequent (7 recorded days with snowfall at Sierra Blanca and 84 days with recorded snowfall at Van Horn out of 21901 simulation days) and its depth minimal when it was recorded (typically less than 10% of precipitation) and was thus not added.

Sixty years of data were provided as input for this model simulation (1 January 1950- 1 January 2010). A spin-up time of 5 years was allotted to give the system an opportunity to equilibrate before data were incorporated into the output. Thus the modeled output values of net infiltration are average annual values for the time period between 1 January 1955 and 1 January 2010. An output interval of 1 year was specified and the date of December 31 was used to report average annual results.

In this simulation, the SNOW subroutine, which is responsible for simulating snowfall, snow accumulation, snowmelt, and sublimation of snow, was turned off. This was done because 1) recorded snowfall events during the time period of the model simulation were infrequent, and 2) snowfall depth was minimal in comparison to total precipitation. Three of the five weather stations (Sierra Blanca, Fort Hancock, and Candelaria) did not record any snowfall during the simulation period, and the two that did record precipitation as snowfall (Van Horn and Valentine), the amount was negligible

(0.06% and 0.1% of average annual precipitation). Unlike in other mountainous regions where this model has been used previously (e.g., Hevesi et al. 2003), snowpack is not a significant contributor to runoff or recharge processes in the Trans-Pecos basins (Beach et al. 2008).

Model input values used to simulate evapotranspiration were set to the values consistent with those used in previous modeling studies of similar field sites. The empirical adjustment factor of potential evapotranspiration was maintained at 0.16 (Hevesi et al. 2003). Values for the  $\beta$  variable used in the modified Priestley-Taylor equation for evapotranspiration off of bare soil, bare rock, and soil layers with vegetation were all set to a value of -10 and values for the  $\alpha$  parameter were set to 1.04 (bare soil), 1.50 (rock matrix), and 1.50 (soil matrix) respectively (Flint and Childs 1987; Hevesi et al. 2003). These are standard initial values of the  $\alpha$  and  $\beta$  parameters in arid and semi-arid regions and have been used effectively in past studies in regions with climates similar to Trans-Pecos, TX (De Bruin 1998; Stannard 1993; Hevesi et al. 2003).

Values for the skyview and the 36 ridge blocking angles for each grid cell were determined by inputting the DEM values into SKYVIEW, a preprocessing routine that calculates the blocking-ridge angles by examining the distance and elevation differences between the grid cell of interest and surrounding grid cells in an increasing radius of distance (Flint and Childs 1987; U.S. Geological Survey Staff 2008). A maximum search radius of 10,000 m was used when defining the blocking-ridge angles for the SKYVIEW routine. The SKYVIEW code was provided by Alan Flint of the U.S. Geological Survey.

In order to calculate infiltration capacities from the input values of soil and bedrock hydraulic conductivity the duration of storm events for the summer and winter seasons were set to 2 and 12 hours, reflective of the short duration convective storm events that dominate summer precipitation and the longer lasting fronts which occur in the winter months (Beach et al. 2004, 2008). These values are also the same time lengths used in the simulations of previous research (U.S. Geological Survey Staff 2008). The start date for the beginning of summer storms was set to May 1 (day 119) and the end date was set to September 30 (day 273) to coincide with the timing of convective summer

storm events in the Trans- Pecos. The input variables that define stream channel characteristics and stream channel infiltration capacity (*ichanmod*, *chan1*, *chan2*, *chan3*, *chan4*, *ikschnmod*, *kschn1*, *kschn2*, and *kschn3*) were set to 1, 0.20, 500, 0.8, 2.0, 0, 50.0, 2000.0, and 5.0 respectively, consistent with the values used in previous studies (Hevesi et al. 2003; Nishikawa et al. 2004; Hevesi et al. 2008). Each of these variables is used in the modeling of the difference in total grid cell area to the wetted grid cell area during periods of surface runoff (U.S. Geological Survey Staff 2008). These parameters are not expected to be significantly different in the Trans-Pecos than in the previous study locations as the dimensions of the known washes in Eagle Flats are of the same order as those documented in Joshua Tree, CA (Nishikawa et al. 2004).

### **3.5.3 Model Calibration**

In previous work using the INFIL model (e.g., Hevesi et al. 2003; Nishikawa, et al. 2004; U.S. Geological Survey Staff 2008) model output was calibrated against gaged stream flows within the catchment/model extent, which was not feasible for this study. The only perennial river or stream within the model extent is the Rio Grande River, along the southwestern edge of the Red Light Draw basin and the only gaging station downstream of the model extent is approximately 125 km away near Presidio, TX (there is also a gaging station approximately 50 km upstream of the Red Light Draw watershed at Fort Quitman, TX). There are a few springs within the model extent (e.g., Indian Hot Springs at latitude 30°47' N, longitude 105°10' W) but they are small- discharge is not sufficient to maintain stream flow. Because calibrating to surface water discharge was not possible, this model was calibrated with another model of precipitation, the PRISM dataset, and with estimates of PET calculated using the Thornthwaite equation (1948).

The INFIL modeled precipitation was calibrated using the 1981-2010 PRISM (Parameter-elevation Regressions on Independent Slopes Model) 30 arc-second (800m) precipitation dataset (the PRISM Climate Group at Oregon State University 2012). Elevations and monthly average precipitation at each weather station were combined with 21 additional points representing a range of elevations from the DEM (952 m to 2173 m- the full range) and precipitation values from the PRISM dataset. Quadratic regression

was the best fit for these data ( $R^2$  from 0.742 to 0.939 depending on month) and so this model was used. The INFIL modeled precipitation provides a range of annual values from 238-511 mm (versus 210-501 mm modeled by the PRISM dataset) (Figs. 3.2 and 3.3). A set of 148 control points (see inset Fig. 3.4) distributed across the model extent was selected to compare values of PRISM modeled precipitation to the INFIL modeled precipitation where the centroids of the INFIL grids cells were within 50 m of the centroids of the PRISM grid cells. The values of precipitation at these points correspond with a reasonable fit ( $R^2$  of 0.864) (Fig. 3.4). The values of modeled precipitation near the weather station at Sierra Blanca and Van Horn locations correlate well to measured values and the values for PRISM and INFIL modeled precipitation are well matched throughout the model extent where elevation is between 1,100 and 1,450 m, which accounts for 66% of the grid cells. There some contrast is present in the spatial distribution of precipitation at the low and high ends of the range (Figs. 3.2 and 3.3); the PRISM precipitation values are notably lower than the INFIL model in two low lying areas (one within the Red Light Draw watershed) and higher in the three regions of highest elevation (the Eagle Mountains between the two basins, the Carizo Mountains northeast of Eagle Flats, and the Van Horn Mountains on the eastern edge) within the model extent. The values of modeled precipitation near the weather station at Sierra Blanca and Van Horn locations correlate well to measured values. Overall, the two models have sufficient agreement in both spatial distribution and magnitude in order to be used to model precipitation for the INFIL simulations.

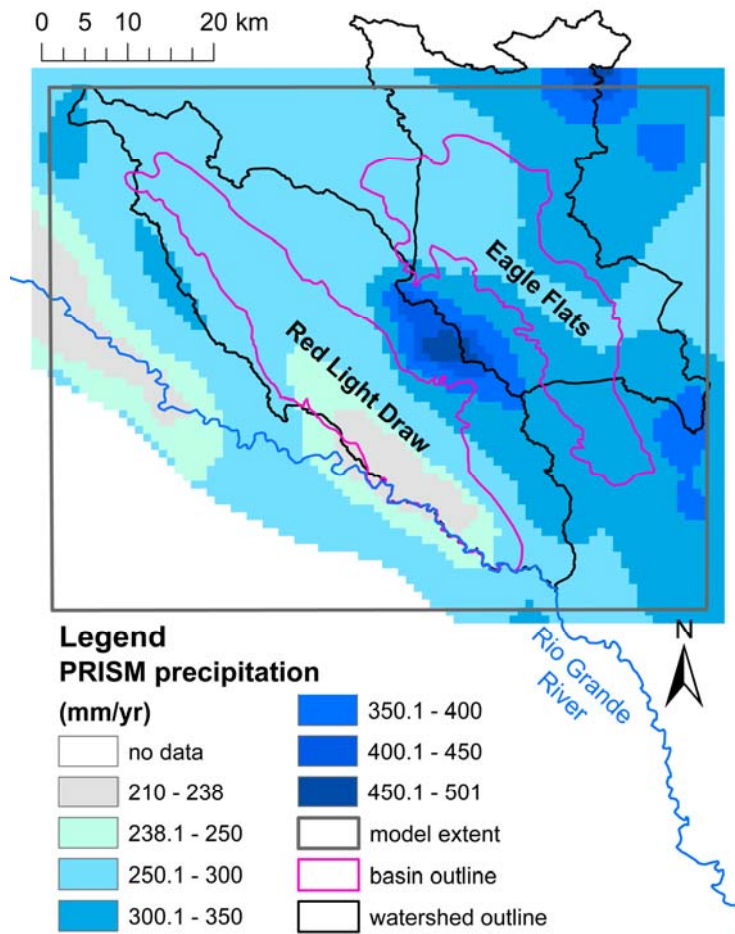


**Fig. 3.2** Map of precipitation distribution modeled by PRISM for the area of interest.



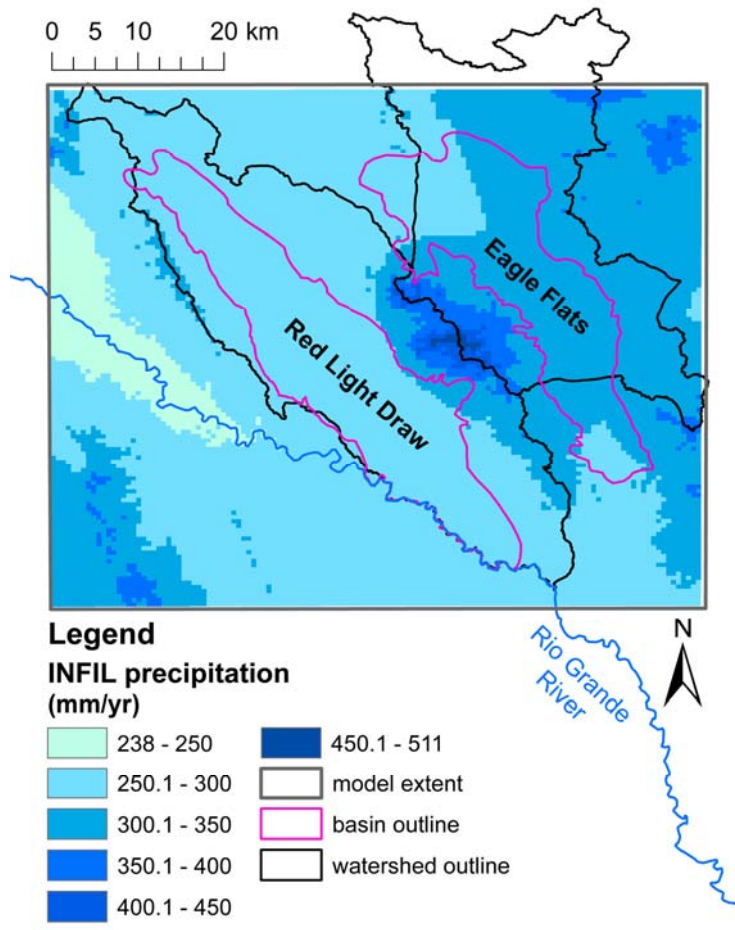


**Fig. 3.3** Distribution of precipitation using the quadratic regression method in the INFIL model.

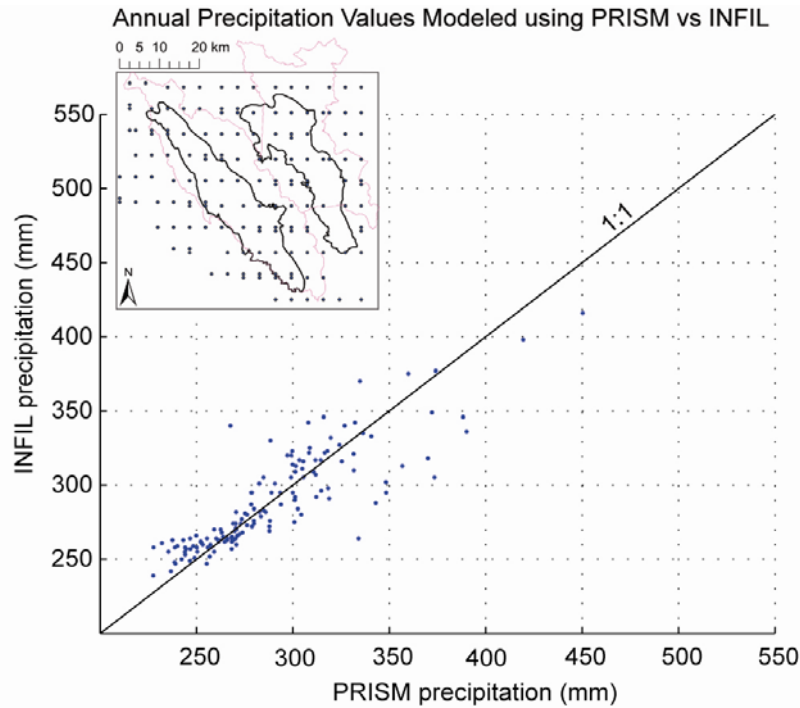


**Fig. 3.4** Plot of PRISM modeled precipitation values versus INFIL modeled precipitation values for the 148 control points across the model extent. Inset: location of the 148 control points used to compare PRISM and INFIL modeled precipitation (Red Light Draw and Eagle Flats basins are outlined).

A model of daily potential evapotranspiration (PET) was calculated using Thornthwaite (1948). This empirical equation uses temperature, day length, and saturation vapor pressure to estimate PET:

$$PET_H = 29.8 \cdot D \cdot \frac{e_a^*(T_a)}{T_a + 273.2} \quad (2)$$

Where  $D$  is the day length in hours,  $e_a^*(T_a)$  is the saturation vapor pressure at the mean daily temperature (in °C) in kilopascals. Thornthwaite is a temperature based model that does not take into account the surface properties (e.g., vegetation type, density, surface albedo). The INFIL model uses a modification of the Priestley-Taylor equation to estimate PET for each grid cell on a daily time scale (U.S. Geological Survey Staff 2008). This equation includes corrections to account for the PET of different surfaces- bare soil versus soil with vegetation:

$$(PET3)_d^i = \{(VEGCOV^i)(SOILET2)+(1-VEGCOV^i)(BARSOIL2)\}(PET)_d^i \quad (3)$$

Where  $PET_d^i$  is the unadjusted PET value calculated by the Priestley-Taylor equation in mm for a given day  $d$  and a given grid cell  $i$ ,  $VEGCOV^i$  is the estimated vegetation cover for a given grid cell  $i$  in decimal percent,  $SOILET2$  is the  $\alpha$  soil-transpiration coefficient (dimensionless), and  $BARSOIL2$  is the  $\alpha$  bare soil coefficient (dimensionless). The daily values of INFIL modeled PET were compared to the daily values of PET using Thornthwaite. The INFIL modeled PET values were consistently higher than the Thornthwaite values, especially in the middle of the PET value range between 2-5 mm (Fig. 3.5). A linear calibration factor of 0.90 was applied to the INFIL PET to produce the modeled values that were used which better matched the lower and middle range values (Fig. 3.6). The calibrated INFIL PET values are overall still higher but generally match well with the trend and magnitude of the values from the Thornthwaite model ( $R^2 = 0.864$ ).

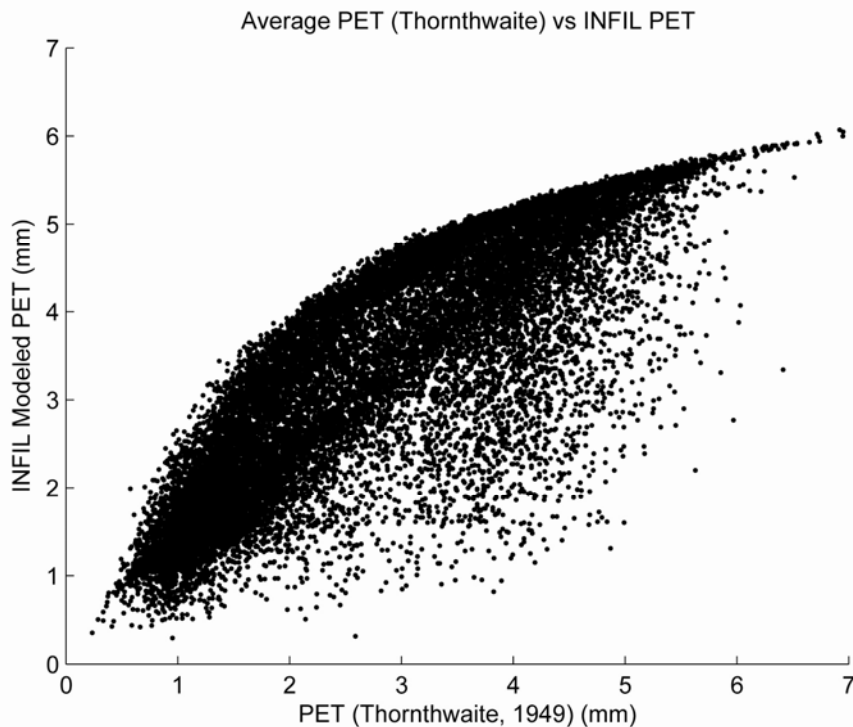


**Fig. 3.5** Crossplot of Thornthwaite estimated PET versus INFIL estimated PET.

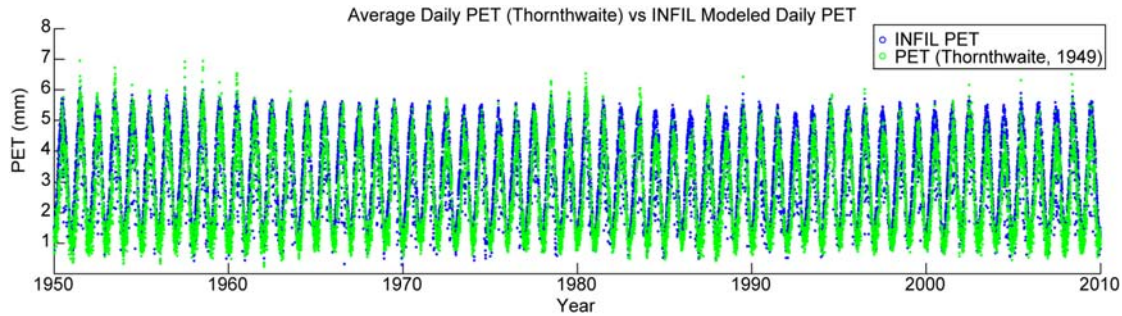


**Fig. 3.6** Daily PET for the Thornthwaite and calibrated INFIL models.

### 3.6 Results

#### 3.6.1 Sensitivity Analysis

One-at-a-time sensitivity analyses were run for model parameters including PET, soil thickness, vertical hydraulic conductivity of the rock layer (Krock), and vertical hydraulic conductivity of the soil layer (Ksoil). Each parameter was tested over its anticipated range; PET of 0.7-1.3 x the defined model values, soil thickness of 0.5 to 2 x the defined model values, Krock of 0.01-100 x the defined model values, and Ksoil of 0.01-100 x the defined model values. The parameters the model was most sensitive to were PET and soil thickness, which has been found to be the case in previous studies using the INFIL model (Rewis et al. 2006; U.S. Geological Survey Staff 2008). A 10% increase in PET resulted in a 15.5% decrease in estimated net infiltration, whereas a 10% decrease in PET resulted in a 25% increase in estimated net infiltration. The range of estimated net infiltration values for the model extent in response to PET changes of 0.7 to 1.3 was  $\sim 1.5 \times 10^7 \text{ m}^3/\text{yr}$  to  $\sim 2.8 \times 10^6 \text{ m}^3/\text{yr}$ . When the thickness of the soil layer was increased by a factor of 2, the estimated net infiltration decreased by 28.7% (from  $\sim 7.5 \times 10^6 \text{ m}^3/\text{yr}$  to  $\sim 3.0 \times 10^6 \text{ m}^3/\text{yr}$  for all cells) and when the thickness of the soil layer was decreased by a factor of 0.5, estimated net infiltration increased by 77.5% (from  $\sim 7.5 \times 10^6 \text{ m}^3/\text{yr}$  to  $\sim 2.6 \times 10^7 \text{ m}^3/\text{yr}$  for all cells). The model demonstrated less sensitivity to Krock and Ksoil, requiring a change of 1-2 orders of magnitude in these parameters to produce a change in estimated net infiltration that was on the same order as those observed in the sensitivity analysis for PET and soil thickness. The range of estimated net infiltration for changes in Krock was  $\sim 2.1 \times 10^6 \text{ m}^3/\text{yr}$  to  $\sim 8.9 \times 10^6 \text{ m}^3/\text{yr}$  for all grid

cells and the range for changes in  $K_{\text{soil}}$  was  $\sim 4.1 \times 10^6 \text{ m}^3/\text{yr}$  to  $\sim 2.5 \times 10^7 \text{ m}^3/\text{yr}$  for all grid cells.

### 3.6.2 Model Results

The INFIL model estimates that an average of  $1.53 \times 10^6 \text{ m}^3$  (1237.6 ac-ft) of potential recharge could occur per year within the modeled contributing area of Red Light Draw, with  $\sim 10\%$  of that potential recharge ( $1.5 \times 10^5 \text{ m}^3$  (121.4 ac-ft)) occurring on the basin floor. In Eagle Flat, there is an estimated  $2.48 \times 10^6 \text{ m}^3$  (2010.7 ac-ft) of annual potential recharge occurring within the modeled contributing area, with  $\sim 15.5\%$  of that potential recharge ( $3.85 \times 10^5 \text{ m}^3$  (312.3 ac-ft)) occurring on the basin floor (Table 3.1). Average rates of potential recharge ranging from 0 mm/yr to 36.3 mm/yr are predicted within the model extent. This model demonstrates that potential recharge is spatially variable but nonetheless widespread through the catchment areas and on the basin floors as the result of run-off from the adjacent mountain blocks and from recharge due to direct precipitation on the basin floors (Fig. 3.7). More potential recharge is modeled at higher elevation, which is consistent with the orographic effect observed in the precipitation data and the geologic composition of the mountains adjacent to the basins (fractured igneous rocks and karstified limestone). On the basin floors of both Eagle Flats and Red Light Draw lithology appears to control the lower end of the spectrum for rates of annual potential recharge; negligible potential recharge ( $< 0.005 \text{ mm/yr}$ ) occurs through the basin sediments with high clay content (e.g., the northern end of Eagle Flats). Adjacent areas with more sand material (e.g., the eastern side of Eagle Flats and the northern section of Red Light Draw) were estimated to have some measurable net infiltration. Infiltration from runoff and surface water channeling does appear to be significant in Eagle Flats; the line of blue (4.01-15.0 mm of annual net infiltration) grid cells running diagonally through the center of Eagle Flats is aligned with the location of the arroyo (dry wash) that is present in the basin. No similar zone of increased modeled infiltration along mapped channels is observed within Red Light Draw. Net infiltration as a result of direct precipitation is modeled in both basins; net infiltration is modeled as occurring (up to 0.25 mm/yr) in the middle of the Red Light

Draw basin and throughout much of the Eagle Flats basin kilometers away from the mountain fronts.

<b>Estimation Method</b>	<b>Red Light Draw</b>	<b>Eagle Flats</b>
One Percent Rule (Gates et al., 1980)	2,000 ac-ft/yr ( $2.47 \times 10^6 \text{ m}^3/\text{yr}$ )	3,000 ac-ft/yr ( $3.7 \times 10^6 \text{ m}^3/\text{yr}$ )
Radioactive Isotopes (Darling, 1997)	280 ac-ft/yr ( $3.45 \times 10^5 \text{ m}^3/\text{yr}$ )	430 ac-ft/yr ( $5.3 \times 10^5 \text{ m}^3/\text{yr}$ )
Modified One Percent Rule (LBG-Guyton Associates et al., 2001)	700 ac-ft/yr ( $8.6 \times 10^5 \text{ m}^3/\text{yr}$ )	1,000 ac-ft/yr ( $1.2 \times 10^6 \text{ m}^3/\text{yr}$ )
Storm Runoff Infiltration (Finch and Armour, 2001)	N/A	4,119 ac-ft/yr ( $5.1 \times 10^6 \text{ m}^3/\text{yr}$ )
Runoff Redistribution (Beach et al., 2004)	N/A	3,036 ac-ft/yr ( $3.7 \times 10^6 \text{ m}^3/\text{yr}$ )
Modified Maxey-Eakin and Storm Runoff Redistribution (Beach et al., 2008)	1,631 ac-ft/yr ( $2.0 \times 10^6 \text{ m}^3/\text{yr}$ )	2,869 ac-ft/yr ( $3.5 \times 10^6 \text{ m}^3/\text{yr}$ )

**Table 3.1** Previous estimates of annual recharge volume in the Red Light Draw and Eagle Flats basins, Trans-Pecos, Texas, USA.

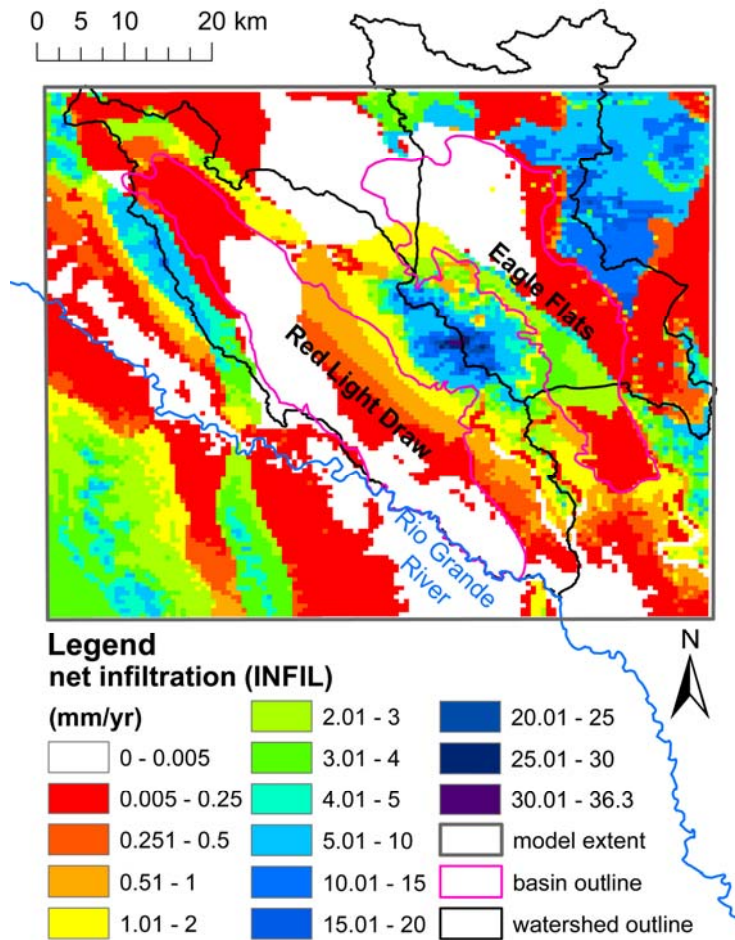


**Fig. 3.7** Average values of annual net infiltration estimated using the INFIL model.

### 3.7 Discussion

#### 3.7.1 Limitations of the INFIL model

The rates of annual potential recharge estimated by the INFIL model are not reflective of the amount of water reaching the water table on a yearly basis. The values provided by the INFIL model at the end of a model run are annual averages of net infiltration from 55 years of simulations. These values indicate, on average, how much water has moved beneath the root zone. In arid regions, thick unsaturated zones can increase travel time of moisture and solute flux to the water table by years or decades. Conversely, travel time in some discrete zones may be much more rapid than can be modeled with INFIL; large desiccation cracks and high permeability channels (Goetz 1985; Van Broekhoven 2002) have been documented in the Trans-Pecos basins. These

features may transport water and solute quickly past the root zone but will not be reflected at the scale of the INFIL model. Though it is a significant step forward from the estimates of recharge made from empirical equations (e.g., Maxey-Eakin) and from lumped parameter models (e.g., storm water runoff model) because of its ability to model spatially distributed daily fluxes, the time scales and spatial resolution that can be modeled using INFIL still does not capture the full complexity of the system and the processes that govern water flux. INFIL simulations should not be taken as absolute annual recharge but rather as an indicator of the presence of potential recharge and possibly a general idea of its magnitude and relative importance to the water budget.

Specifically for this INFIL model, the values for hydraulic conductivity assigned to the different lithology types are conservative. Low-end (one to two orders of magnitude below average) to average values were selected for each of the porous media represented and low-end (two orders of magnitude below average) values were selected for fractured media from published data. This likely had limited effect on the volume of potential recharge estimated to occur on the basin floors as 1) the majority of precipitation did not fall on the basin floors, 2) the published values for hydraulic conductivity have a relatively small range (typically 3 or 4 orders of magnitude), and 2) the downward velocities are all slow enough that the model is much more sensitive to PET rates than to a ten fold change in hydraulic conductivity as was demonstrated by the sensitivity analyses. The volume of potential recharge is likely underestimated for the catchment as a whole because the mountainous areas receive the greatest proportion of precipitation, and the mountains are fractured and karstified which results in a skewed range of hydraulic conductivity values. Additionally the mountainous areas have the thinnest soil horizons. Combined with a fractured/karst terrain, this suggests that downward velocities may be much more rapid than those in the basin floor vadose zone.

The sensitivity analyses demonstrated that net infiltration is sensitive to soil thickness and PET, as has been observed in previous studies (e.g., Revis et al. 2006). The sensitivity to soil thickness is not considered to be a major factor affecting the INFIL model of Red Light Draw and Eagle Flats because soil thickness within the model extent



was well characterized (Soil Survey Staff accessed June 2012), though it is possible that local variability of soil thickness not described at the scale of the soil data set could affect net infiltration rates and thus potential recharge. The INFIL model's sensitivity to small changes in PET does, in the case of this model, likely cause under-estimation of net infiltration. This is because the INFIL modeled PET was overall slightly higher than the estimate of PET using Thornthwaite, even after calibration (Fig. 3.6). As a result, the volumes of potential recharge both on the basin floors and in the catchments are valuable as conservative estimates.

### **3.7.2 Comparison to Previous Models**

The volume of potential recharge modeled using the INFIL approach is within the range of values predicted by previous research (Table 3.2, Fig. 3.8). The current INFIL model does not predict a significant increase in total recharge to either Red Light Draw or Eagle Flats basins over what has been previously modeled ( $3.45 \times 10^5 - 2.47 \times 10^6 \text{ m}^3/\text{yr}$  for Red Light Draw and  $5.3 \times 10^5 - 3.7 \times 10^6 \text{ m}^3/\text{yr}$  for Eagle Flats) though with less conservative values for hydraulic conductivity and/or PET that could change. Spatial variability in potential recharge as indicated by the INFIL results does demonstrate that the practice of extrapolating site specific recharge estimates like Cl<sup>-</sup> profiles (Scanlon 1991) and <sup>14</sup>C / <sup>3</sup>H age dating (Darling et al. 1995, 1998) to the basin scale is overly simplified. While it is apparent that in some parts of Red Light Draw and Eagle Flats there is no significant recharge occurring, it is not the case everywhere. Three important inferences that the INFIL model establishes which were missing from previous methods are that, 1) there is significant spatial variability in the magnitude of potential recharge to the basins, 2) that widespread recharge can occur from direct precipitation on the basin floors as well as from runoff, and 3) that widespread recharge on the basin floors is a potentially significant (accounting for 10-15% of total recharge) source of water and mechanism for solute flux to the Red Light Draw and Eagle Flats basin aquifers.

Basin	Recharge on Basin Floor	Recharge in Watershed
Red Light Draw	121 ac-ft/yr ( $1.5 \times 10^5 \text{ m}^3/\text{yr}$ )	1238 ac-ft/yr ( $1.52 \times 10^6 \text{ m}^3/\text{yr}$ )
Eagle Flats	312 ac-ft/yr ( $3.9 \times 10^5 \text{ m}^3/\text{yr}$ )	2011 ac-ft/yr ( $2.5 \times 10^6 \text{ m}^3/\text{yr}$ )

**Table 3.2** Estimates of annual recharge volume on the basin floors and for the watersheds of Red Light Draw and Eagle Flats basins using the INFIL model.

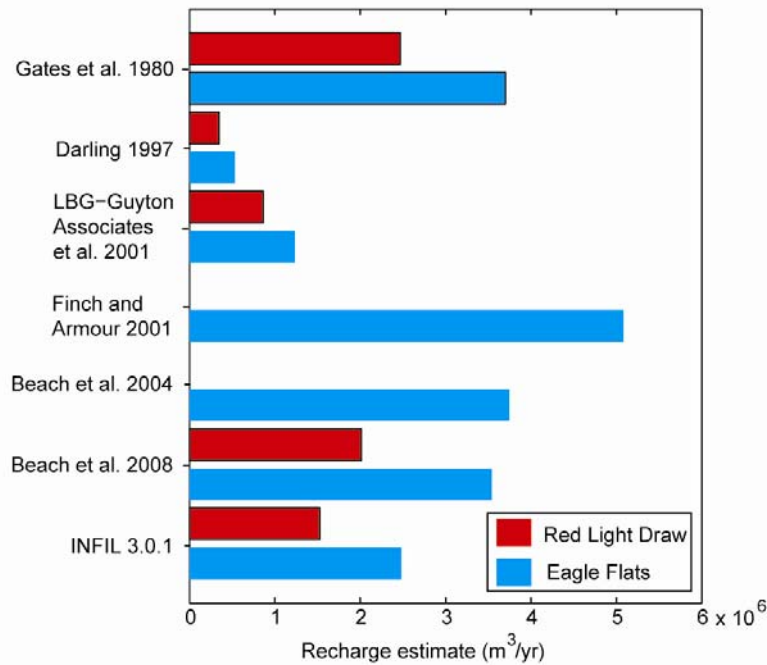


**Fig. 3.8** Bar graph of recharge estimates for Red Light Draw and Eagle Flats.

### 3.7.3 Implications

The INFIL modeling approach independently confirms observed water chemistry data, increases the validity of the conceptual model proposed by Robertson and Sharp (2012), illustrates the spatial variability of potential recharge, and models a mechanism by which vadose zone  $\text{NO}_3^-$  (and other solutes) may be reaching the groundwater within this system. Changes in groundwater  $\text{NO}_3^-$  concentration, the presence of CFCs at depth in the groundwater, and the results of the INFIL model simulation for Red Light Draw and Eagle Flats demonstrate that recharge to the basin groundwater is occurring through

widespread infiltration on the basin floor in addition to the recharge that occurs in the mountains and adjacent alluvial fans.

The conceptual model discussed in Robertson and Sharp (2012) includes widespread recharge on basin floors as a mechanism of solute and water flux to arid basin groundwater. This process may be occurring in other similar systems around the world such as other basins in the Western USA, the Murray-Darling Basin in Australia, and arid/semi-arid catchments in China. Additionally, the changes in  $\text{NO}_3^-$  concentration and the presence of CFCs at depth indicate that other solutes or contaminants may also be transported by the same mechanism to basin groundwater in these systems; this raises serious concerns about long-term water quality and vulnerability of these resources, especially in regions where groundwater is the sole or primary source of drinking water.

### **3.8 Conclusions**

The INFIL 3.0.1 model could be used as an effective approach to modeling the spatial variability of potential recharge in arid basin aquifers. It is more data and time intensive than are most of the other methods of recharge estimation (e.g., Maxey-Eakin, 1% rule) but provides insight into the distribution and mechanisms of potential recharge and solute flux. Previous modeling approaches estimated similar volumes of recharge to these systems, but do not capture the distribution of recharge. The long held conceptual model of recharge mechanisms to arid basin aquifers upon which these estimates are made cannot account for observed changes in groundwater chemistry; important system processes are being missed. This could have significant implications for recharge, solute transport, and resource management. Spatial variability is integral because the distribution of solutes and potential recharge within the basins will control the flux of constituents like  $\text{NO}_3^-$  into the groundwater. Understanding the complex nature of recharge and solute flux in arid basin aquifers is key to their sustainable use and it is necessary to develop and use more detailed modeling approaches (such as INFIL) in order to accomplish this goal.

**Chapter 4:** Estimates of potential recharge in arid basins and impacts on infiltration processes and solute flux due to land use and vegetation change

**Abstract**

Human impacts on land use and vegetation regime in arid basins have, in some regions, significantly altered hydrological processes and groundwater chemistry. However, some modeling approaches currently used do not account for these effects. In the Trans-Pecos region of Texas the presence of modern water and increasing  $\text{NO}_3^-$  concentrations belie the notion that basin groundwater is unaffected by overlying land use and vegetation change. Recharge to the Trans-Pecos basins is spatially and temporally variable, and due to human impacts (namely human-induced woody vegetation encroachment and the presence of irrigated agriculture), potential recharge to the basin aquifers has likely changed since pre-western settlement time (circa 1850's). By using a spatially distributed model of net infiltration (INFIL 3.0.1), the volume and spatial distribution of net infiltration was examined for two basins, Wild Horse/Michigan Flats and Lobo/Ryan Flats. The effects of irrigation return flow and of woody vegetation encroachment were examined. Insight into recharge mechanisms, impacts from anthropogenic processes, and solute flux in arid basin systems was gained. Model results indicate that recharge to the basins is not limited to mountain-front zones and discrete features (i.e., alluvial channels), rather, infiltration on the basin floors results from irrigation return flow (as much as  $6.3 \times 10^7 \text{ m}^3$  of net infiltration over 40 years) and direct precipitation (between 7 and 11.5% of annual recharge). Net infiltration may also be higher under current vegetation regimes than in pre-western settlement conditions; the removal of thick dense grasslands through over-grazing, fire suppression, and climate change may have enhanced net infiltration by 48% or more. Results from distributed models (like INFIL) improve upon the scientific understanding of the links between vegetation regime and hydrological processes; this is important for the sustainable management of arid basin aquifers in Texas and elsewhere.

**4.1 Introduction**

The sustained availability of clean, potable water in arid regions across the globe is an issue of pressing concern due to population expansion and increased demand for

resources. The question of how to manage limited groundwater resources has arisen in the Trans-Pecos region of West Texas, USA, where groundwater is used for irrigated agriculture, animal husbandry, and as domestic water supply. Groundwater is the sole source of water for drinking, industry, and agriculture (Beach et al., 2004, 2008; Scanlon et al., 2006; Mahlknecht et al., 2008). Past water crises have hit the region hard and best management practices have been a topic of discussion for over three decades; one major uncertainty is quantifying recharge to basin aquifers. The models for water budgets and recharge used have been based upon a common conceptual model for groundwater recharge in arid basin aquifers, wherein the basins receive minimal modern recharge, there is no diffuse recharge on basin floors, and no recharge occurs from anthropogenic sources (i.e., irrigation return flow) (Maxey 1967; Adar and Neuman 1988; Darling et al., 1998; Uliana and Sharp, 2001; Van Broekhoven 2002; Walvoord et al., 2002; Beach et al., 2004, 2008; Flint et al. 2004; Wilson and Guan, 2004; Pool and Dickinson 2006; Uliana et al., 2007). This conceptual model describes a system where basin floor surface processes (i.e., alteration of vegetation type and density due to grazing practices and intensive agricultural activities) are disconnected from the underlying groundwater due to thick vadose zones and annual evapo-transpirative (ET) demand exceeding annual precipitation. These assumptions are helpful for management policy because they simplify a complex system, but they are limited in their applicability; in these basins there is evidence of widespread modern recharge (Robertson and Sharp, 2012) in contradiction with the underlying assumptions of the management models. Increases in groundwater  $\text{NO}_3^-$  concentrations and the presence of CFCs point to recharge in the basins more recently (<70 years) than had been documented (e.g., Darling et al. 1998) or modeled (e.g., Scanlon et al. 2001, 2006; Beach et al. 2004, 2008) in previous studies, where the vast majority of recharge was assumed to have occurred during the last glacial maximum (10,000-20,000 years ago). Changes to the natural vegetation regime after western settlement (e.g., increases in bare ground cover, woody vegetation encroachment (Buffington and Herbel 1965; Grover and Musick 1990)) have significantly altered hydrological fluxes within the system, and irrigated agriculture (circa 1950's to present)

introduced additional sources of water (through irrigation return flow) and labile N (through the application of synthetic and manure based fertilizers). These impacts to the physical properties of the surface of the basin floor are relevant for both groundwater quantity (amount of recharge) and groundwater quality (mobilization of solutes from the vadose zone). A different approach to estimating recharge is needed; one that can account for spatial variability in watershed properties and can reflect anthropogenic impacts such as changes to vegetation regime and intensive irrigation.

#### **4.1.1 Site description**

The basins of Wild Horse/Michigan Flats and Lobo/Ryan Flats are part of the Trans-Pecos basin aquifer system located in far west Texas (Fig. 4.1) (Sharp 2001). Resulting from the Late Cretaceous Laramide Orogeny and subsequent Tertiary rifting, these basins are the eastern-most expression of the Basin and Range province (Barnes 1973, 1983). The climate of the Trans-Pecos region is arid to semi-arid, with average annual precipitation ranging between 220-360 mm on the basin floors and between 500-750 mm in the adjacent mountainous areas (Beach et al. 2004, 2008). Some snowfall does occur in the region, particularly at higher elevations during the winter months, but the majority of the precipitation results from convective storm events that occur between June and October. The Trans-Pecos basin aquifer system consists of a series of unconfined basin aquifers underlain by Permian and Cretaceous aged bedrock (Beach et al. 2004, 2008). There is strong evidence for hydrologic connectivity between the basins (Sharp 1989, 2001); regional flow of basin groundwater is from south to north in Lobo/Ryan Flats, entering Wild Horse/Michigan Flats through the southwest limb before turning east and entering the Apache Mountains (karstified limestone)(Sharp 1989). The unsaturated zone within the basins is typically thick (depths to water range from 10-225 m (Beach et al. 2004)); soil horizons are thin (typically less than 1.5 m (Soil Survey Staff accessed July 2012) and are underlain by unconsolidated basin fill consisting of alluvial and wind-blown deposits (Barnes 1979, 1983) with some volcanoclastic sediments present at depth in southern section of Ryan Flats (Beach et al. 2004).

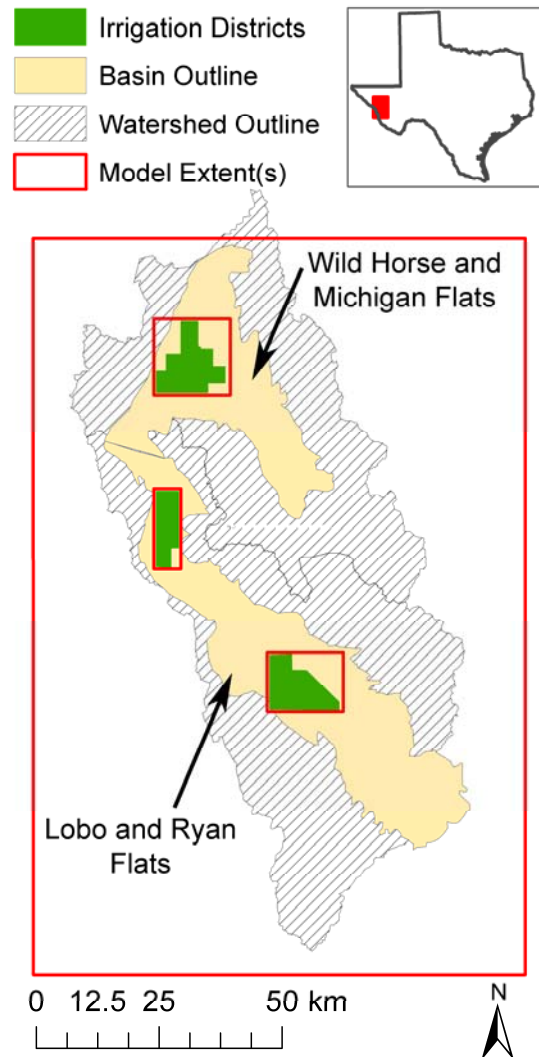


**Fig. 4.1** Map of the area of interest within the Trans-Pecos Region of Texas, USA with outlines of the basins, their contributing watersheds, and model extent(s).

The current vegetation regime consists of blue stem, grama, lechuguilla, and creosote bush at low elevations and juniper at higher elevations; bare soil and rock are dominant with typical vegetation coverage between 10-35% (McMahon et al. 1984; Schmidt 1995; Beach et al. 2008). Prior to western settlement (pre 1860's), the basins were covered in thick, dense grasslands (Humphrey 1958) with sparse shrubs and succulents. Extensive grazing in the Trans-Pecos occurred in the 1880's (sheep and cattle) and continued through the 1940's, resulting in a marked decrease to the rangeland productivity, an increase in bare ground cover, and the proliferation of woody vegetation

species (Humphrey 1958; Johnston 1963); the effects of over-grazing combined with fire suppression practices and climatic shifts in the desert Southwest have resulted in regional loss of grasslands and rise in woody vegetation encroachment (Archer 1994; Van Auken 2000 and others). Between the early 1950's and 2010 the region experienced another series of major land use changes. The production of inexpensive synthetic fertilizers post-World War II caused a boom in development of land for intensive irrigated agriculture. Basin wells produced  $2.5 \times 10^7 - 4.2 \times 10^7$  m<sup>3</sup>/yr from the 1950's to the 1960's; extraction peaked in the 1970's to early 1980's at  $6.2 \times 10^7 - 6.8 \times 10^7$  m<sup>3</sup>/yr (Beach et al. 2004). During peak production, approximately 20% of the land was used for irrigated agriculture; pecans, cotton, and alfalfa were the primary crops. Towards the late 1970's-early 1980's irrigated agriculture had resulted in a drop of up to 25 m in the basin water table levels. It became economically unviable to produce irrigation water from some wells and many farmers went bankrupt, sold their land, or switched to raising cattle. In 2010, only 5-7% of the land was being used for irrigated agriculture; the remainder was used for grazing or left fallow, allowing native and invasive species to re-colonize. From peak water demands, current extraction has significantly decreased; an estimated  $3.8 \times 10^7$  m<sup>3</sup>/yr of water is withdrawn from the basins each year, down to the range of extraction rates of the early 1960's (Beach et al. 2004). In most of the measured wells (8 of 12 monitored wells), water table levels have not yet fully recovered to pre-irrigation withdrawal levels; they remain 3-19 m lower than their measured level in 1950 (Beach et al. 2004).

#### **4.1.2 Previous Studies**

Several estimates of recharge have been calculated for Wild Horse/Michigan Flats and Lobo/Ryan Flats (Gates et al., 1980; Mayer 1995; Mayer and Sharp 1998; Finch and Armour 2001; Beach et al. 2004). With the exception of the 1% rule (i.e., 1% of precipitation in the catchment results in recharge (Gates et al. 1980)), which does not use any watershed parameter beyond precipitation to estimate recharge, all the methods are based upon the prevailing assumptions that on the basin floors 1) diffuse recharge does not occur, 2) recharge as a result of direct precipitation does not occur because the



average annual ET demand of native vegetation is much greater than average annual precipitation, and 3) anthropogenic impacts on the basin floor surface (i.e., irrigated agriculture and alteration of the vegetation regime) do not alter recharge processes. The assumption that when annual (or monthly) ET demand exceeds precipitation it is indicative of negligible potential recharge is widespread in research studies of arid (and some semi-arid) systems (e.g., Maxey 1967; Adar and Neuman 1988; Flint et al. 2004; Seyfried et al. 2005). Recharge in the previous models, when spatially distributed, was limited on the basin floors to discrete features (e.g., dry washes, alluvial fans) located along the edges of the basins and from infiltration at higher elevations. Age dating ( $^{14}\text{C}$ ,  $^3\text{H}$ ) of groundwater in some of the Trans-Pecos basins indicates that the majority of basin groundwater recharged during the last glacial maximum (10,000-20,000 years ago) (Darling et al. 1998; Uliana et al. 2007).

Much of the research into recharge processes in this and similar systems has concluded that there is minimal modern recharge (Flint et al. 2000; Finch and Armour 2001; Wilson and Guan 2004; Newman et al. 2006; Pool and Dickinson 2006; Scanlon et al. 2001, 2006), and that no widespread modern recharge occurs on the basin floors from either natural (i.e., precipitation) or anthropogenic (i.e., irrigation return flow) sources, however, there have been some studies undertaken in analogous systems that have arrived at different conclusions. In the Avra Valley, Arizona and in the Rio Grande Valley, irrigation return flow was identified as a contributing source of recharge to the basin valley aquifer (Hanson et al. 1990; Ellis et al. 1993); direct recharge from precipitation was also identified in sections of the Rio Grande Valley with higher annual precipitation (mostly in Colorado), but was considered negligible in the drier regions (i.e., New Mexico and Texas, which have ranges of mean annual precipitation [ $\sim 250$ - $410$  mm/yr on the basin floors] similar to the Trans-Pecos region of Texas). In the High Plains aquifer (mean annual precipitation  $\sim 420$ - $500$  mm/yr), both irrigation return flow and enhanced infiltration due to changes in land use (from natural vegetation to rain fed agriculture) have been identified as potential sources of recharge, though an increase in recharge rate due to grazing was not identifiable in either the Central or the Southern

High Plains (McMahon et al. 2006; Scanlon et al. 2008). This research indicates the potential for changes to basin floor land use to impact recharge processes (and solute flux) in the Trans-Pecos basin aquifers.

#### **4.1.3 Nitrate Variability and Apparent Age of Groundwater in Wild Horse/Michigan Flats and Lobo/Ryan Flats**

Increases in  $\text{NO}_3^-$  concentrations of basin groundwater from the 1960's to 2010 belie the assumption from the original Trans-Pecos basin conceptual model that no widespread recharge occurs (Robertson and Sharp 2012). Within these basins there are 79 wells for which water quality data (including  $\text{NO}_3^-$  concentrations) are available for multiple decades. In Lobo/Ryan Flats median  $\text{NO}_3^-$  concentration has increased by approximately 3 mg/L (as  $\text{NO}_3^-$ ), and in Wild Horse/Michigan flats median  $\text{NO}_3^-$  concentration has increased by approximately 4 mg/L (as  $\text{NO}_3^-$ ) since the 1960's. The major source of  $\text{NO}_3^-$  to the groundwater in the basins is mobilization of labile N that had previously been sequestered in the vadose zone beneath the roots of native basin floor vegetation (Walvoord et al. 2003; Robertson and Sharp 2012; Robertson et al. 2012). This source of labile N is absent from the adjacent mountains where depths to bedrock are shallow, soil horizon development is limited, and vegetation is sparse (Beach et al. 2004, 2008). The effects of over-grazing, regional climatic shifts, and fire suppression have resulted in woody vegetation encroachment on the basin floors, an increase in bare ground cover in the basins, and decreases in rooting depth and root density in grass cover in the grasslands (Humphrey 1958; Buffington and Herbel 1965; Grover and Musick 1990). Irrigated agriculture (utilizing groundwater) has further altered the basin floor environment by changing rooting depths, vegetation type, and density as well as adding N to the system (from fertilizer). These changes may have significant impacts on water and N fluxes in the basin system and may be driving some of the observed trends in the basin groundwater.

In addition to the observed trends in groundwater  $\text{NO}_3^-$  concentration, chlorofluorocarbon (CFC) dating of four wells within the basins (TX well IDs 5110326, 5119902, 4759104, and 4751701) have apparent ages between 26 and 65 years (+/- 2

yrs), which indicates the presence of modern water (Table B.1). Irrigation in the basins uses groundwater, which means that not all of the CFCs in the basin groundwater are attributable to infiltration of precipitation; it is likely that a combination of precipitation and irrigation return flow are the sources of modern water to the basin aquifers. However, CFCs were measured both in wells beneath irrigated lands and in wells beneath land used solely for grazing, indicating that the modern recharge is related to more than just contributions from irrigation return flow.

The conflict between these observations and past assumptions of recharge processes is apparent; both increases in  $\text{NO}_3^-$  concentration and presence of modern water at depth in wells several km (3 to 15 km) away from the mountains indicate widespread modern recharge is occurring in the basins. The majority of groundwater in the basins may have recharged during the last glacial maximum but the impacts of vegetation change and agricultural practices on recharge processes in the basins should not be ignored. The 1% rule, modified Maxey-Eakin, storm-runoff infiltration, and runoff redistribution methods that have been used to estimate recharge in this system do not adequately characterize the complexity in this system (Robertson and Sharp 2013) and because these methods do not account for the possibility of increased recharge post-vegetation disturbance or of recharge through irrigation return flow, potential sources of water and solute (e.g.,  $\text{Cl}^-$  and  $\text{NO}_3^-$ ) to the basin aquifers are not evaluated in the current management plans.

## **4.2 Methods**

### **4.2.1 Model Description**

The increase in  $\text{NO}_3^-$  concentrations and the presence of CFCs in basin groundwater indicate recharge occurs on the basin floors. In order to evaluate if 1) basin floor recharge from direct precipitation is occurring, 2) basin floor recharge could have increased infiltration due to changes in vegetation regime, and 3) irrigation return flow is contributing to recharge in Wild Horse/Michigan and Lobo/Ryan Flats, a different approach to quantifying infiltration and estimating recharge was selected. The INFIL 3.0.1 model is a grid-cell-based distributed parameter watershed model developed by the

U.S. Geological Survey; it calculates net infiltration beneath the root zone on a daily time scale (Hevesi et al. 2002; U.S. Geological Survey Staff 2008). Total net infiltration (defined as the flux of water across the lower boundary of the root zone and used in this paper to estimate potential recharge) is calculated for each grid cell by combining precipitation (rain and snowfall), ET, runoff, surface water run-on, infiltration of water into the root zone, and changes in near-surface water content. Grid cell area is defined by the user and a maximum of six vertical layers may also be defined within the vadose zone; five soil types and one bedrock type. Previous research has estimated net infiltration and recharge using INFIL in California (Nishikawa et al. 2004, Rewis et al. 2006), Death Valley (CA and NV) (Hevesi et al. 2002, 2003), and in two adjacent basins in west Texas Trans-Pecos basin aquifer system (Robertson and Sharp 2013).

The INFIL model allows for the examination of infiltration processes detached from the assumptions of previous models of this system, i.e., that there is no recharge on the basin floor as a result of direct precipitation and that recharge processes are not altered by human impacts on the system (either from changes to the vegetation regime or irrigation practices). It also has the ability to incorporate daily precipitation and evapotranspiration into the climate model and account for spatial variability in physical properties of the system (such as lithology, vegetation, soils, etc.); this was not done in previous Trans-Pecos models. Additionally, by treating irrigation water as precipitation during the growing season, INFIL can be used to estimate increases in net infiltration due to irrigation. INFIL improves on existing models of the Trans-Pecos region because it examines the spatial distribution of net infiltration and potential recharge as well as examining potential effects of anthropogenic processes on the system while making use of the available datasets (spatial and temporal) without introducing uncertainty into the modeling process associated with utilizing a model for which the input data are scarce or are unavailable.

Previous research and hydrological models of the Trans-Pecos basin aquifers (and other analogous systems) assumed that negligible recharge occurs on the basin floors as a result of direct precipitation (Nielson and Sharp 1985; Ellis et al. 1993; Finch and

Armour 2001; Scanlon et al. 2001; Wilson and Guan 2004); this assumption is based upon the observation that mean annual PET is much greater than mean annual precipitation (1570 mm PET vs. 250-350 mm precipitation); therefore any direct precipitation on the basin floors is evapotranspired before it can infiltrate beneath the root zone. Within the Trans-Pecos region, however, this assumption may not hold due to the magnitude and intensity of storm events. The majority of precipitation within the catchment area results from summer convective storm events which are large magnitude and short duration. When plotted against estimates of daily or monthly PET, it becomes apparent that many storm events could result in infiltration and potentially recharge (Figs. 4.2 and 4.3). A comparison of the range of storm magnitudes during the past 7 decades to two estimates of PET demonstrate that while not every storm event is capable of being a recharge generating event, some clearly are (Table 4.1) and considering antecedent conditions (Fig. 4.3), the summer months with regular convective storm events may result in more infiltration beneath the root zone than previously thought. Because the temporal resolution of INFIL incorporates daily weather conditions into the climate model, the variability of storm events and ET demand can be incorporated into model simulations rather than relying on monthly or annual averages.

<b>Precipitation (mm)</b>	<b>Number of days (TWDB average PET of 3.8 mm/day) for total water loss</b>	<b>Number of days (Thornthwaite average PET of 2.3 mm/day) for total water loss</b>
average: 9.1	2.4	4.0
minimum: 0.3	0.1	0.1
maximum: 95.0	25.0	41.3
25 <sup>th</sup> percentile: 2.5	0.7	1.1
75 <sup>th</sup> percentile: 12.2	3.2	5.3

**Table 4.1** Range of storm event magnitudes at Valentine, TX and the number of days required (at two estimates of average daily PET) for total water loss via evapotranspiration.

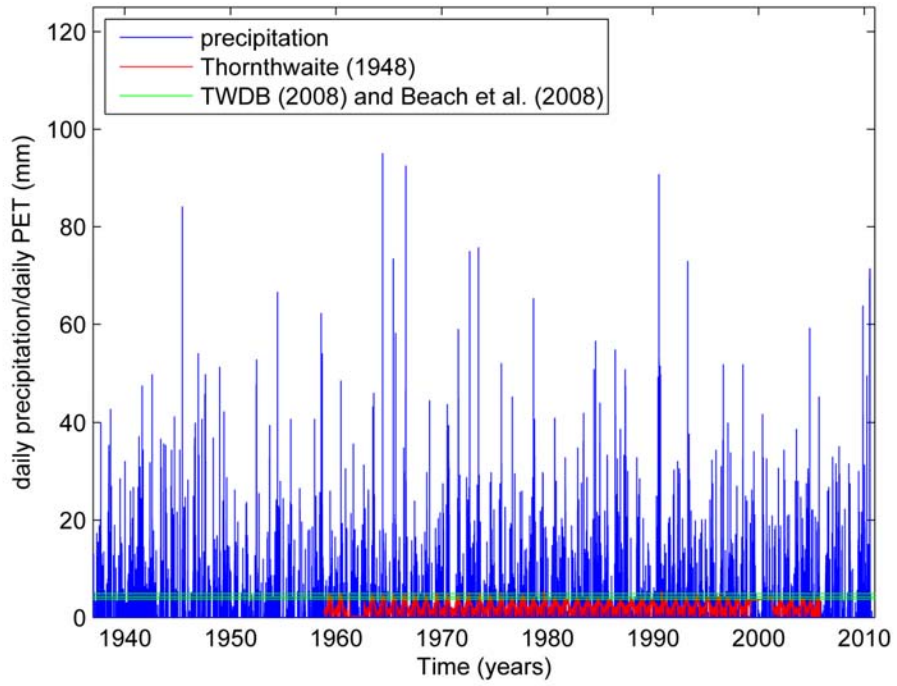


**Fig. 4.2** Plot of PET estimates and precipitation from 1937 to 2010 in Valentine, TX (located in the Lobo/Ryan Flats basin).

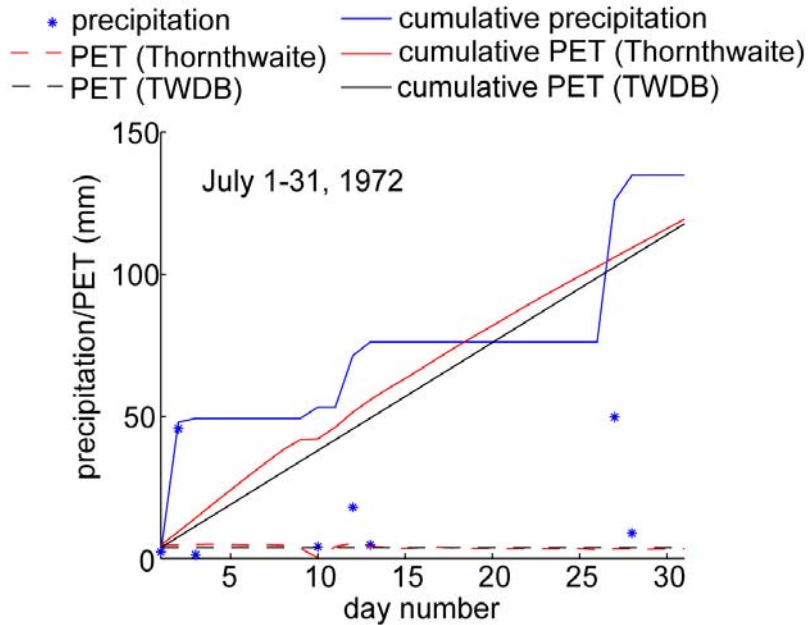


**Fig. 4.3** Plot of daily and cumulative precipitation and PET for the month of July 1972 in Valentine, TX (located in Lobo/Ryan Flats basin). The magnitude (and regularity) of convective storm events result in an amount of precipitation that is not overcome by ET demand for most of the month. 1972 was an average year for precipitation at Valentine (319 mm vs 320 mm average annual precipitation).

Spatial variability in vegetation, soil type, and lithology are also incorporated using INFIL; these parameters were not accounted for in previous Trans-Pecos models. Past models either disregarded physical properties of the system entirely (i.e., the 1% rule, Maxey-Eakin) or treated the basins as a lumped systems. The storm-water runoff redistribution model attempted to address the spatial variability of recharge by delineating where runoff is more likely to infiltrate by outlining discrete alluvial channels and less likely to infiltrate by identifying zones along the basin edges where caliche or clay layers are present (Beach et al. 2004), however it did not account for vegetation type or coverage, it treated the mountain block, mountain front, and basin floor as lumped elements, and assumed no recharge as a result of direct precipitation on the basin floors. By not examining the spatial distribution of physical properties in the system, there is a

possibility that processes with significant implications for recharge are not being considered or quantified.

Temporal variability of ecosystem properties (such as vegetation change), while not directly addressed in the INFIL model set-up, can also be examined using INFIL. In previous models of the Trans-Pecos basins, the only system changes that were examined were predictions of aquifer response to different pumping regimes; physical properties of the system were assumed to be static, including water loss due to evapo-transpiration (Beach et al. 2004). It is clear from historical narrative that the vegetation regime within the basins has undergone significant alteration; ET demand has likely not remained static through time, which could impact infiltration rates and recharge processes within the system.

Finally, an additional source of potential recharge is irrigation return flow, which has not been considered in any model undertaken for this region. Because intense irrigation has been practiced on much of the basin floor, the potential impact of irrigation return flow on recharge and solute transport processes should not be discarded. From 1960 to 1980, an average  $4.8 \times 10^7$  m<sup>3</sup>/yr of groundwater was used for irrigation within the basins. Irrigation return flow is not 'new' water to system (as irrigation in these basins uses groundwater) but it does represent less water 'lost' from the water budget due to groundwater extraction and subsequent ET. It may also have a significant impact on groundwater quality (as has been observed in other arid and semi-arid regions (Schmidt and Sherman 1987; Simpson and Herczeg 1991; Beare and Heaney 2001; Smedema and Shiati 2002; Causape et al. 2004; Derby et al. 2009).

The ability of the INFIL model to incorporate daily weather data, spatial variations in basin properties, and anthropogenic impacts allows for significant improvements in understanding recharge processes in the Trans-Pecos basins. Examining net infiltration in a spatially distributed model, detached from the governing assumptions of the previously used conceptual model, and the impacts of anthropogenic activities on infiltration processes will help to improve the aquifer water budget and examine potential risks to long-term water quality within the basins.



#### **4.2.2 Model Set-up**

For this study, both natural and anthropogenic processes driving infiltration were modeled. One large model was developed covering the extent of both basins and the majority of their catchment areas (Fig. 4.1) to model net infiltration resulting from direct precipitation and runoff. In addition to modeling net infiltration under current the current vegetation regime (i.e., sparse grass cover, woody vegetation encroachment on the basin floors), it was also modeled under a scenario where grassy vegetation is thicker and denser and where scrubland (encroached areas) was replaced by thick, dense grassland. These simulations were intended to provide a range of net infiltration estimates dependent on the vegetation regime and provide insight into how human impacts on vegetation could potentially alter infiltration and recharge processes within the basins. Three smaller models covering the three main irrigation districts were also developed to simulated net infiltration and potential recharge resulting from irrigation return flow (Fig. 4.1).

Grid cell size in all models was 500 m x 500 m. Two vertical layers were delineated; a single soil layer and a rock (either the unconsolidated basin sediments or bedrock) layer. This was done because the soils within the model extent are typically thin (0.75-1.5 m) (Beach et al. 2008, Soil Survey Staff accessed July 2012). Several datasets and input parameters were used in order to create the model inputs required to run the INFIL model (Table 4.2). Where the large model extended across the U.S. Mexico border, gaps in datasets (i.e., lithology, soils, and vegetation) were filled in using values from grid cells on the U.S. side that had similar elevation and slope values.

<b>INPUT(S)</b>	<b>DATASET(S) USED</b>	<b>REFERENCE(S)</b>
elevation, slope, aspect	30m National Elevation Dataset	Gesch 2002 and Gesch 2007
soil type, soil thickness, soil physical characteristics	U.S. General Soils Map and Soil Survey Geographic Database	Soil Survey Staff (accessed June 2012)
geology	Geological Atlas of Texas	Stoesser et al. 2007
vegetation type	The Vegetation Types of Texas Map	McMahon et al. 1984
vegetation density	Landsat 7 Enhanced Thematic Mapper Plus (ETM+) 19-28 of June 2000	NASA Landsat Program (accessed July 2012)
climatic data (precipitation, minimum daily temperature, maximum daily temperature)	National Oceanic and Atmospheric Administration Climatic Data Center	NOAA NCDC (accessed June 2012)
<b>PARAMETER</b>	<b>VALUE(S)</b>	<b>REFERENCE(S)</b>
field capacity	0.09-0.18	Jury et al. 1991; Hornberger et al. 1998; Dingman 2002
wilting point	0.02-0.085	Jury et al. 1991; Hornberger et al. 1998; Dingman 2002
soil-drainage-function coefficient	3.02-5.71	Jury et al. 1991; Hornberger et al. 1998; Dingman 2002
rock hydraulic conductivity	0.01-150000.00 mm/day	Freeze and Cherry 1979; Domenico and Schwartz 1997; Custodio 2007
rock porosity (root zone)	0.10-0.43	Freeze and Cherry 1979; Domenico and Schwartz 1997; Custodio 2007
empirical adjustment factor of PET- for cloud cover + rain	0.16	Hevesi et al. 2003
$\beta$ parameter (PET)	-10 for bare soil, bare rock, and soil with vegetation	Flint and Childs 1987 and Hevesi et al. 2003
$\alpha$ parameter (PET)	1.04 (bare soil), 1.50 (bare rock), 1.50 (soil with vegetation)	Flint and Childs 1987 and Hevesi et al. 2003
length of storm events first and last days of summer	2hrs (summ.), 12hrs (wntr) May 1 (day 119) and Sept 30 (day 273)	U.S. Geological Survey Staff 2008 and NOAA NCDC (accessed June 2012)
stream channel characteristics and infiltration capacity (ichanmod, chan1, chan2, chan3, chan4, ikschnmod, kschn1, kschn2, kschn3)	1.0, 0.20, 500, 0.8, 2.0, 0, 50.0, 2000.0, and 5.0 (respectively)	U.S. Geological Survey Staff 2008

**Table 4.2** List of datasets and input values (and their sources) used in INFIL model simulations

Long term climatic data were assembled from the National Oceanic and Atmospheric Administration's National Climactic Data Center database of weather stations (NOAA NCDC accessed June 2012). Eight stations were used; Fort Hancock (USC00413266), Sierra Blanca (USC00418305), Van Horn (USC00419295), Valentine (USC00419275), Candelaria (USC00411416), Fort Davis (00413262), Kent (USC00414767), and Marfa (USC00415589). Stations were selected for their proximity to the model extent and their availability of data (10 years or more during the 60 year model simulation). All of the stations selected had records of air temperature (max and min), rainfall, and snowfall. The precipitation inputs for this model simulation were combined values for rainfall and snowfall. For all models, sixty years of data (1 January 1950- 1 January 2010) were used as input. An output interval of 1 year was specified and the date of December 31 was used to report average annual results. A quadratic regression was used for the interpolation of air temperature and precipitation values calculating the spatial distribution over the model domain. The large models had a 5 year spin-up time to allow for equilibration. The small models had a 10 year spin up time; 5 years with only natural precipitation (same as the large models) and 5 years with added irrigation water.

#### *Large Model*

In part due to the limited availability of long-term climatic data in the Trans-Pecos region (only eight stations with records greater than 10 years were available inside the model extent and within a ~60 km radius outside the model extent), the 1981-2010 PRISM 30 arc-second (800m) precipitation dataset (the PRISM Climate Group at Oregon State University 2012) was used as an additional input for precipitation in the INFIL model. The INFIL modeled precipitation provides a range of annual values from 259-743 mm (versus 250-681 mm modeled by the PRISM dataset). A set of 600 control points (see inset Fig. 4.5) distributed across the model extent was selected to compare values of PRISM modeled annual precipitation to the INFIL modeled annual precipitation. The values of precipitation at these points correspond with a fit of 0.68 (Fig. 4.5); 76% (443/600) of the INFIL modeled annual precipitation values are within 50

mm of the PRISM modeled values. The values of modeled precipitation near the weather stations at Valentine, Van Horn, Marfa, and Fort Davis match well (within 3-16 mm of mean annual precipitation). Within the basins and their catchment areas there is acceptable agreement and overall the two models have sufficient agreement in both spatial distribution and magnitude in order to be used to model precipitation for the INFIL simulations.

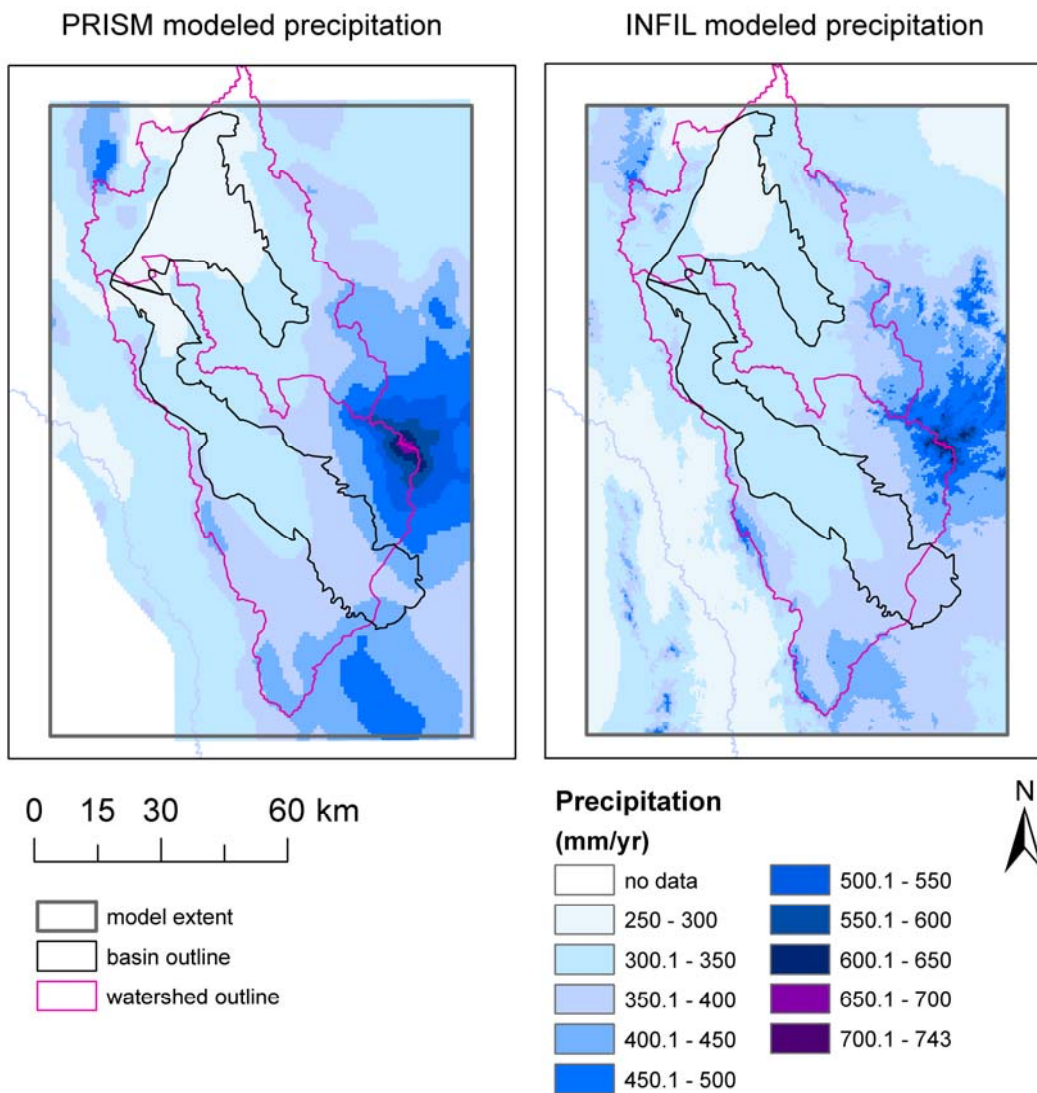


**Fig. 4.4** Map of precipitation distributions using PRISM and INFIL models. The maps show average annual precipitation (in mm/yr) during the simulation period (1981 to 2010 for PRISM, 1955 to 2010 for INFIL)

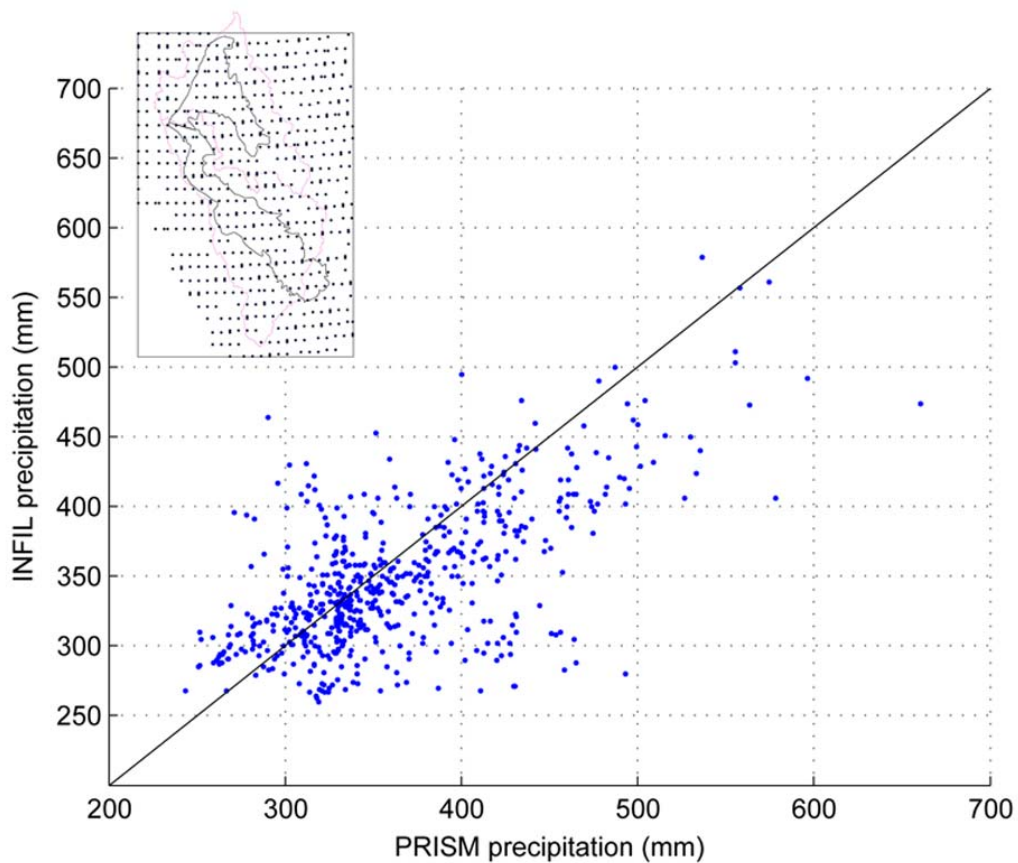


**Fig. 4.5** Plot of PRISM modeled precipitation values versus INFIL modeled precipitation values for the 600 control points across the model extent. Inset: locations of the 600 control points used to compare PRISM and INFIL modeled precipitation

Simulations of net infiltration were estimated under three different vegetation scenarios. Scenario one is a vegetation regime based on current conditions; sparse vegetation density in the grasslands, increased bare ground cover, and woody vegetation encroachment (increased scrubland) on the basin floors. Under this scenario, mapped grasslands were assigned a vegetation density of 15% (85% bare ground cover) and scrublands (regions with mixed woody and herbaceous vegetation) were assigned a vegetation density of 20% (80% bare ground cover) (density estimates were based on Landsat 7 imagery (NASA Landsat Program, accessed July 2012)). Scenario two is a vegetation regime where the mapped grasslands have a vegetation density of 50% (scrubland is left unaltered in spatial distribution and density from scenario one); this was

designed to simulate un-grazed grasslands. Finally, scenario three is a vegetation regime where mapped scrubland has been replaced in the model with grassland and the vegetation in the grasslands is assigned a density of 50%; this was designed to simulate the pre-western settlement vegetation where basin grasslands were unperturbed by over-grazing, fire suppression, and climate change.

#### *Smaller Models of Irrigation Districts*

The three largest irrigation districts (Wild Horse, North Lobo, and Antelope Valley) within Wild Horse/Michigan and Lobo/Ryan Flats basins were modeled to examine the impact of irrigation return flow on net infiltration. The application of irrigation water was simulated by adding weather stations with irrigation water simulated as daily precipitation to each small model (Fig. 4.6). The amount of irrigation water was taken as the annual extraction rates from the basin aquifers using the Texas Water Development Board's extraction data from 1955 to 2000. In this region, farmers typically irrigated their crops between June 1 and September 1 of each year; irrigation water was applied as daily precipitation during this time frame. An even daily distribution of irrigation water was applied to all grids cells within each small model with irrigated agricultural land use.

The first attempt to incorporate irrigation water into INFIL in this study attempted to use the framework of the single large model (discussed above). This was unsuccessful; the presence of multiple false weather stations with added irrigation water at low elevations caused an over-estimate of precipitation at the higher elevations; INFIL uses elevation based regression and inverse-distance-squared interpolation to model precipitation at each grid cell (see U.S. Geological Survey Staff 2008 for detailed description), and applying irrigation water as precipitation at low elevations (on the basin floors) caused excess runoff and infiltration throughout the model extent. Adjustments to the interpolation equation that was used to estimate grid-cell precipitation could not counter the effect. As a result, three smaller models covering the three main irrigation districts were developed instead of incorporating irrigation into the large INFIL model. The INFIL model relies upon elevation, change in slope, and flow path routing to

determine grid cell run-on and runoff; this impacts net infiltration (U.S. Geological Survey Staff 2008). The cells within the smaller models:

- 1) Receive minimal run-on from the adjacent cells outside the extent of the smaller models,
- 2) Contribute minimal runoff to the adjacent cells outside the extent of the smaller models, and
- 3) There is minimal change in the net infiltration (resulting from natural precipitation) between the extents when they are analyzed as a part of the larger model and when they are run independently of the larger model (Table 4.3)

These qualifications make the estimates of net infiltration from the smaller models applicable in the context of the large basin-wide model. After it was established that the results from the smaller models and the large model were comparable, irrigation water was applied using the weather stations inside the irrigated areas (Fig. 4.6). The spatial effect of the irrigation water was limited within each model by surrounding the irrigated zones with additional false weather stations without added irrigation water, with the intention to distribute irrigation water as evenly as possible on to grid cells with irrigated agriculture and maintain the cells outside of the irrigated area at precipitation values similar to the natural distribution (Fig. 4.10). When net infiltration was calculated after the addition of irrigation water, all grid cells where a false weather station was located were removed in case the presence of the false station created erroneously high or low net infiltration values (Fig. 4.10).



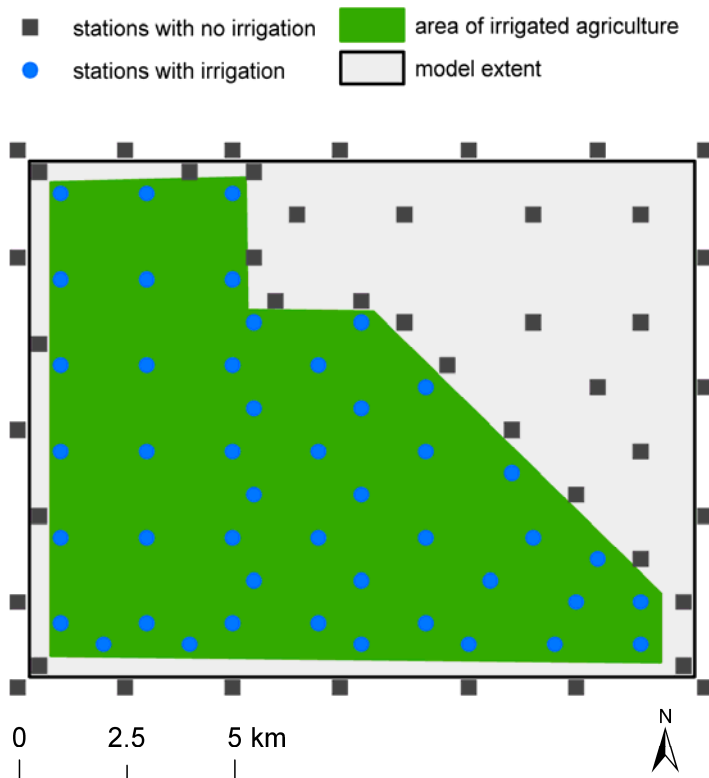


**Fig. 4.6** Map of the distribution of false weather stations in the Antelope Valley irrigation district model. The blue circles are weather stations with added irrigation water and the gray squares are stations with no added irrigation

	<b>run-on from cells adjacent to irrigation district (large model) (mm/yr)</b>	<b>run-off to cells adjacent to irrigation district (large model) (mm/yr)</b>	<b>% difference in net infiltration between large and smaller models</b>
Wild Horse	24.9	24.1	11.9
N. Lobo	4.0	0.0	1.78
Antelope Valley	36.7	0.02	13.5

**Table 4.3** Values for run-on, run-off, and % difference in net infiltration used to determine that the smaller models of irrigation districts can be evaluated independent of the influence from adjacent cells (in large model).

### 4.2.3 Model Calibration

Past research using INFIL to estimate net infiltration calibrated model output against measured stream flow within the catchment/model extent (Hevesi et al. 2003;

Nishikawa, et al. 2004; U.S. Geological Survey Staff 2008). This was not feasible in this study; the only perennial river within the model extent is the Rio Grande River, which is located southwest of LR flats outside the extent of both basins and their catchment area. Because calibrating to surface water discharge was not possible, the large model was calibrated with estimates of daily PET calculated using the Thornthwaite equation (1948). Thornthwaite is a temperature based approach for estimating evapo-transpiration for a reference crop (Thornthwaite 1948). Because it uses latitude of the study area and air temperature, it can provide a daily value for PET based on available historical datasets; this allows for an estimate of PET without introducing uncertainty related to assigning values to input parameters (such as wind speed or surface temperature) needed with other approaches. While not well suited to all conditions (e.g., open ocean evaporation, oasis evapotranspiration), Thornthwaite can be an effective method in a range of climatic conditions (Fitzgerald and Rickard 1960; Pereira and Paes De Camargo 1989). The Thornthwaite calibration approach was used in an INFIL model for two adjacent basins; Red Light Draw and Eagle Flats, TX (Robertson and Sharp 2013). PET was estimated at three weather stations within the model extent; these values were compared to the INFIL modeled daily PET estimates for the grid cells in which the weather stations were located. When compared to the values estimated using the Thornthwaite equation the INFIL modeled  $PET_d^i$  ( $PET_d^i$  is the potential evapotranspiration at grid location  $i$  and day  $d$ ;  $i$  values in this case were equal to 11928- Van Horn, 31628- Valentine, and 58565- Marfa) values were consistently higher throughout the majority of the  $PET_d^i$  value range (1-5mm) (Fig. 4.7). A linear calibration factor of 0.85 was applied to the INFIL PET to produce the modeled values that were used which better matched the lower and middle range values (Fig. 4.8). The calibrated INFIL  $PET_d^i$  values are overall still higher but generally match well with the trend and magnitude of the values from the Thornthwaite model ( $R^2 = 0.859$ ).

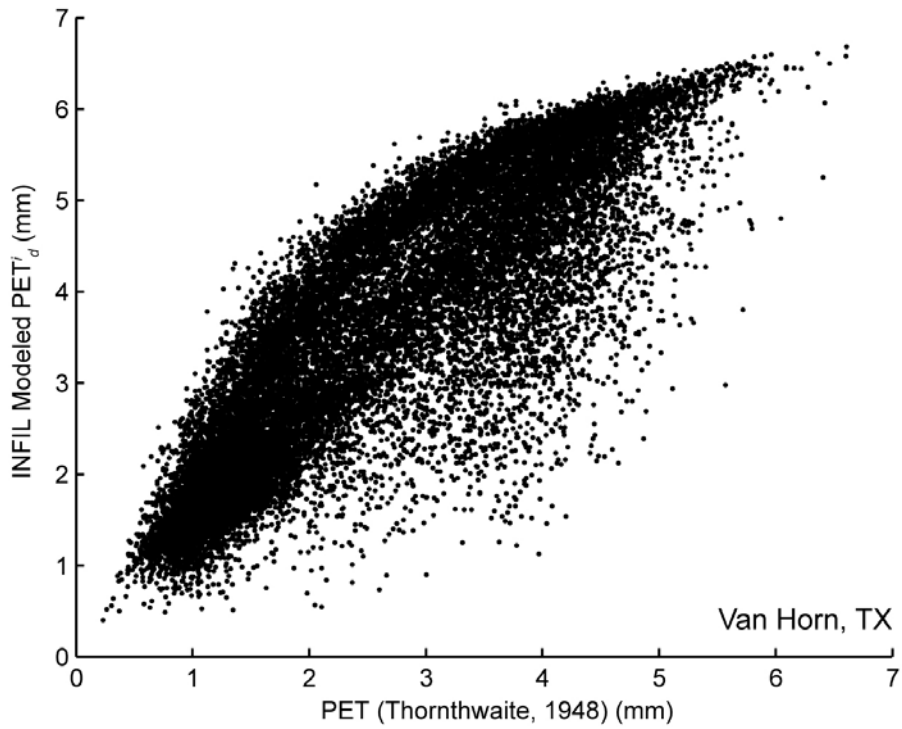


**Fig. 4.7** Crossplot of Thornthwaite estimated PET versus INFIL estimated  $PET_d^i$  at Van Horn, TX (grid cell ID: 11928)

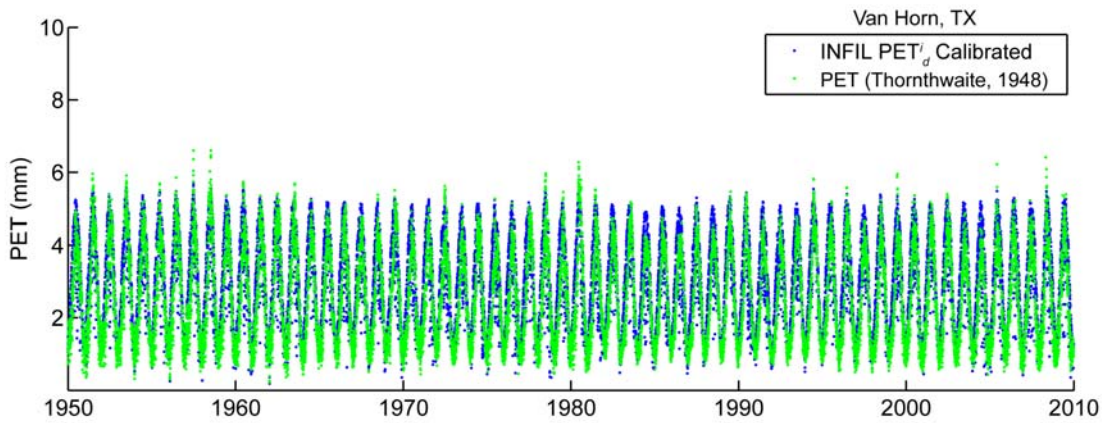


**Fig. 4.8** Daily PET for the Thornthwaite and calibrated INFIL models at Van Horn, TX (grid cell ID: 11928)

## 4.3 Results

### 4.3.1 Sensitivity Analysis

Model parameters  $PET_d^i$  (scaled using the evapotranspiration scaling factor, *etfact*), soil depth (using the soil depth scaling factor, *sdfact*), bedrock vertical hydraulic conductivity (using the rock vertical hydraulic conductivity scaling factor, *imbfact*), and soil vertical hydraulic conductivity (using the soil vertical hydraulic conductivity scaling factor, *sksfact*) were analyzed for model sensitivity using one-at-a-time sensitivity analysis on the large model. The parameters were tested over their anticipated ranges and produced variability in net infiltration from 1-512% of modeled values (Table 4.4). The model was most sensitive to changes in  $PET_d^i$  and soil depth; for example, a 5% increase in  $PET_d^i$  resulted in a 14.9% decrease in average annual net infiltration and a 25% increase in soil thickness resulted in a 52.5% decrease in average annual net infiltration. Model sensitivity to changes in hydraulic conductivities of the rock and soil layers was significantly less (e.g., an order of magnitude decrease in bedrock and soil K resulted in a 34.7 and 42% (respectively) decrease in net infiltration); this sensitivity pattern in the model has also been documented in previous studies (Rewis et al. 2006; U.S. Geological Survey Staff 2008; Robertson and Sharp 2013).

parameter	range examined	net infiltration (m <sup>3</sup> /yr)	% change
$PET_d^i$ ( <i>etfact</i> )	0.8-1.2	$2.68-7.38 \times 10^7$	-57 to +17
soil depth ( <i>sdfact</i> )	0.25-5	$7.2 \times 10^5 - 3.84 \times 10^8$	-98 to +511
soil K ( <i>sksfact</i> )	0.01-100	$1.7 \times 10^7 - 1.8 \times 10^8$	-72 to +195
rock K ( <i>imbfact</i> )	0.01-100	$1.98 \times 10^7 - 6.8 \times 10^7$	-68 to +8

**Table 4.4** Results of one-at-a-time sensitivity analyses

### 4.3.2 Large Model

The results from the large INFIL model demonstrate that in both Wild Horse/Michigan and Lobo/Ryan Flats, there is significant potential for recharge resulting from mountain front/mountain block sources, from runoff, and from diffuse infiltration on the basin floors (Fig. 4.9). Approximately 7% ( $6.8 \times 10^5$  m<sup>3</sup>, 0.74 mm/yr) of potential recharge to Wild Horse/Michigan Flats and 11.5% ( $1.45 \times 10^6$  m<sup>3</sup>, 1 mm/yr) to

Lobo/Ryan Flats is basin floor recharge (Table 4.5). Average rates ranging from 0 mm/yr to 160 mm/yr are predicted within the model extent; on the basin floors net infiltration rates ranges from 0-15 mm/yr. There is an increase in net infiltration with increased elevation; this is consistent with the orographic effect that is observed in the precipitation data and with the geologic composition of the mountains (fractured igneous rocks, fractured sandstones, and karstified limestone). On the basin floors the soil type appears to control the spatial variability in potential recharge; where the Redona-Verhalen-Musquiz soils (US key s7598) are present (along the western side of Wild Horse/Michigan Flats and in central and northern Lobo/Ryan Flats), there is low to negligible modeled net infiltration. This is likely due to the high clay content (up to 60%) and resulting low hydraulic conductivity and high water retention capability of these soils (Soil Survey Staff accessed July 2012). Net infiltration as a result of direct precipitation is modeled within both basins; in Wild Horse/Michigan Flats it is up to 4.0 mm/yr and within Lobo/Ryan Flats it is between 0.5-2.0 mm/yr kilometers away from the mountain front zones (Fig. 4.9).

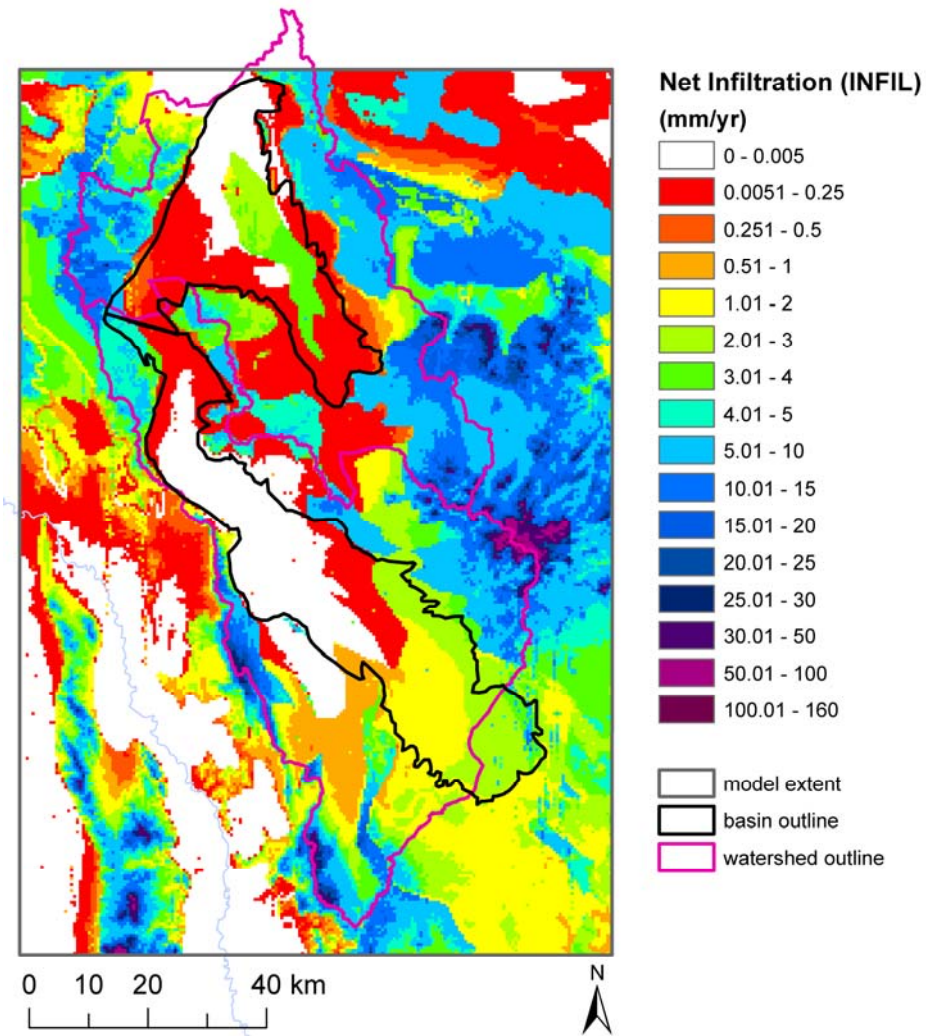


**Fig. 4.9** Average values of annual net infiltration estimated using the INFIL model

<i>Large model</i>			
	<b>net infiltration in watershed</b>	<b>net infiltration on basin floors</b>	<b>% of recharge occurring on basin floors</b>
Wild Horse/ Michigan Flats	$1.03 \times 10^7$ m <sup>3</sup> /yr (11.2 mm/yr)	$6.8 \times 10^5$ m <sup>3</sup> /yr (0.74 mm/yr)	~6.7
Lobo/Ryan Flats	$1.26 \times 10^7$ (8.6 mm/yr)	$1.45 \times 10^6$ (1.0 mm/yr)	~11.5
<i>Smaller models of irrigation districts</i>			
	<b>cumulative (1960-2010) net infiltration (m<sup>3</sup>) with NO irrigation water</b>	<b>cumulative (1960-2010) net infiltration (m<sup>3</sup>) with irrigation water 1960-1985</b>	<b>cumulative (1960-2010) net infiltration (m<sup>3</sup>) with irrigation water 1960-2000</b>
Wild Horse	$1.3 \times 10^6$	$3.06 \times 10^7$	$6.03 \times 10^7$
N. Lobo	$1.89 \times 10^4$	$4.27 \times 10^5$	$1.27 \times 10^6$
Antelope Valley	$1.17 \times 10^5$	$6.2 \times 10^5$	$3.04 \times 10^6$
	<b>sum (m<sup>3</sup>)</b>		
	$1.43 \times 10^6$	$3.16 \times 10^7$	$6.48 \times 10^7$
	---	$-1.43 \times 10^6$	$-1.43 \times 10^6$
	<b>net infiltration from irrigation return flow</b>		
		$3.02 \times 10^7$ m <sup>3</sup> /25 yrs (104.25 mm/25 yrs in the irrigation districts)	$6.33 \times 10^7$ m <sup>3</sup> /25 yrs (218.5 mm/25 yrs in the irrigation districts)

**Table 4.5** Estimates of net infiltration from INFIL model simulations

There is also evidence that the changes in natural vegetation regime (increases in bare ground cover and encroachment of woody vegetation into grasslands) driven by human activities during the past 130 + years (over grazing, fire suppression, and climate change) in the basins has impacted net infiltration rates and recharge processes. By altering vegetation density in the grasslands and replacing scrubland (encroached areas) with grasses, it becomes apparent that net infiltration on the basin floors would be significantly less during the modeled time period of 1955-2010 if the vegetation regime had remained consistent with pre-western settlement reports (i.e., thick, tall grasses interspersed with occasional scrub (Humphrey 1958) (Fig. 4.10). In the maximum

change scenario examined (i.e., an increase in grass density to 50% coverage and replacement of scrubland with grassland), net infiltration decreased by 40% in the Wild Horse/Michigan Flats watershed and by 48% in the Lobo/Ryan Flats watershed (Table 4.6). Similar decreases were modeled on the basin floors.

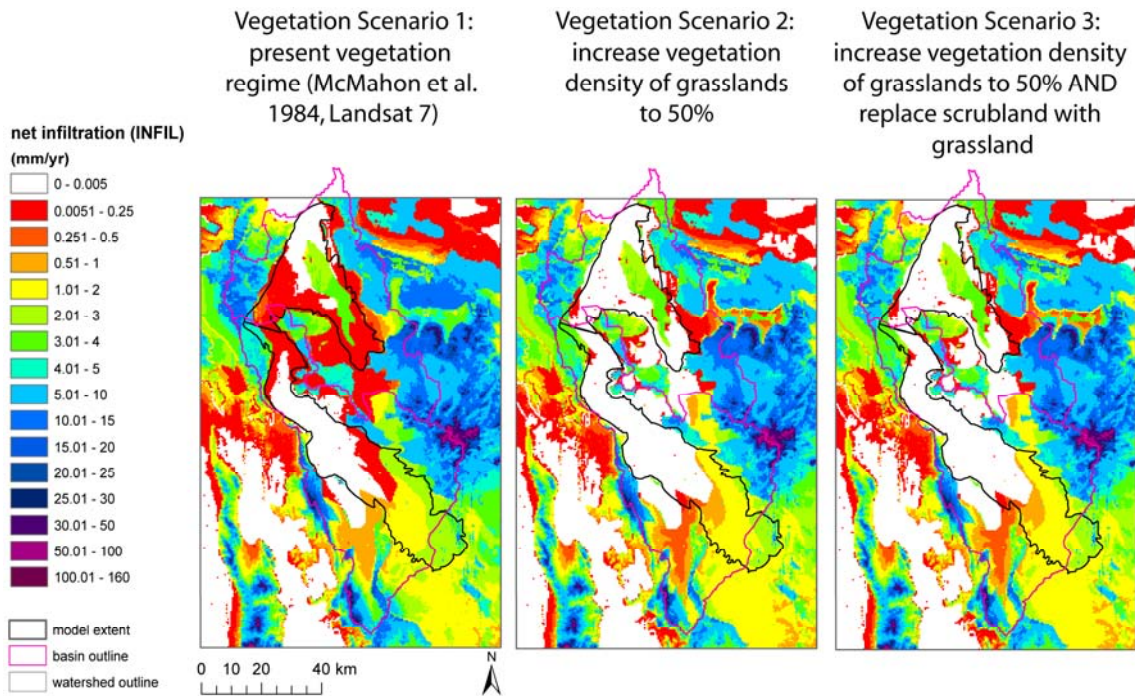


**Fig. 4.10:** Comparison of net infiltration in the Wild Horse/Michigan Flats and Lobo/Ryan Flats INFIL model (large model) with 3 separate vegetation regime scenarios.



	<b>Wild Horse / Michigan Flats watershed</b>	<b>Wild Horse / Michigan Flats basin floor</b>	<b>Lobo / Ryan Flats watershed</b>	<b>Lobo / Ryan Flats basin floor</b>
Vegetation Scenario 1	$1.03 \times 10^7$ m <sup>3</sup> /yr (11.2 mm/yr)	$6.8 \times 10^5$ m <sup>3</sup> /yr (0.74 mm/yr)	$1.26 \times 10^7$ (8.6 mm/yr)	$1.45 \times 10^6$ (1.0 mm/yr)
Vegetation Scenario 2	$8.87 \times 10^6$ m <sup>3</sup> /yr (9.6 mm/yr)	$6.07 \times 10^5$ m <sup>3</sup> /yr (0.66 mm/yr)	$1.09 \times 10^7$ m <sup>3</sup> /yr (7.5 mm/yr)	$1.11 \times 10^6$ m <sup>3</sup> /yr (0.76 mm/yr)
<i>difference V1 and V2</i>	-16.7%	-12.1%	-14.7%	-31.6%
Vegetation Scenario 3	$7.37 \times 10^6$ m <sup>3</sup> /yr (8.0 mm/yr)	$4.64 \times 10^5$ m <sup>3</sup> /yr (0.5 mm/yr)	$8.4 \times 10^6$ m <sup>3</sup> /yr (5.8 mm/yr)	$1.07 \times 10^6$ m <sup>3</sup> /yr (0.74 mm/yr)
<i>difference V1 and V3</i>	-40%	-48%	-48.2%	-35.1%

**Table 4.6** Comparison of net infiltration rates in Wild Horse/Michigan Flats and Lobo/Ryan Flats basins with varying vegetation regime.

#### 4.3.3 Smaller Models of Irrigation Districts

The INFIL model results from all three of the smaller models indicate that irrigation return flow is contributing to potential recharge in Wild Horse/Michigan and Lobo/Ryan flats (Fig. 4.11). The amount of net infiltration is spatially variable and is most dependent on soil and bedrock type; for example, high clay content in Redona-Verhalen-Musquiz soils limits infiltration in the Northern Lobo irrigation district and zones of unconsolidated sands and gravels increase net infiltration on the eastern and western sides of the Wild Horse irrigation district. Regardless, examining net infiltration in the districts with and without irrigation water clearly demonstrates that net infiltration increases with the addition of irrigated agriculture (Table 4.5); in the Wild Horse irrigation district there is potential for more than 10 mm/yr of net infiltration with the addition of irrigation return flow. Between 1950 and 2000, most fields in the irrigation districts were irrigated for between 25 and 40 years. The INFIL model predicts that between  $3.0 \times 10^7$  (25 years of irrigation) and  $6.3 \times 10^7$  m<sup>3</sup> (40 years of irrigation) of potential recharge resulting from irrigation return flow has occurred (sum of all three irrigation districts).

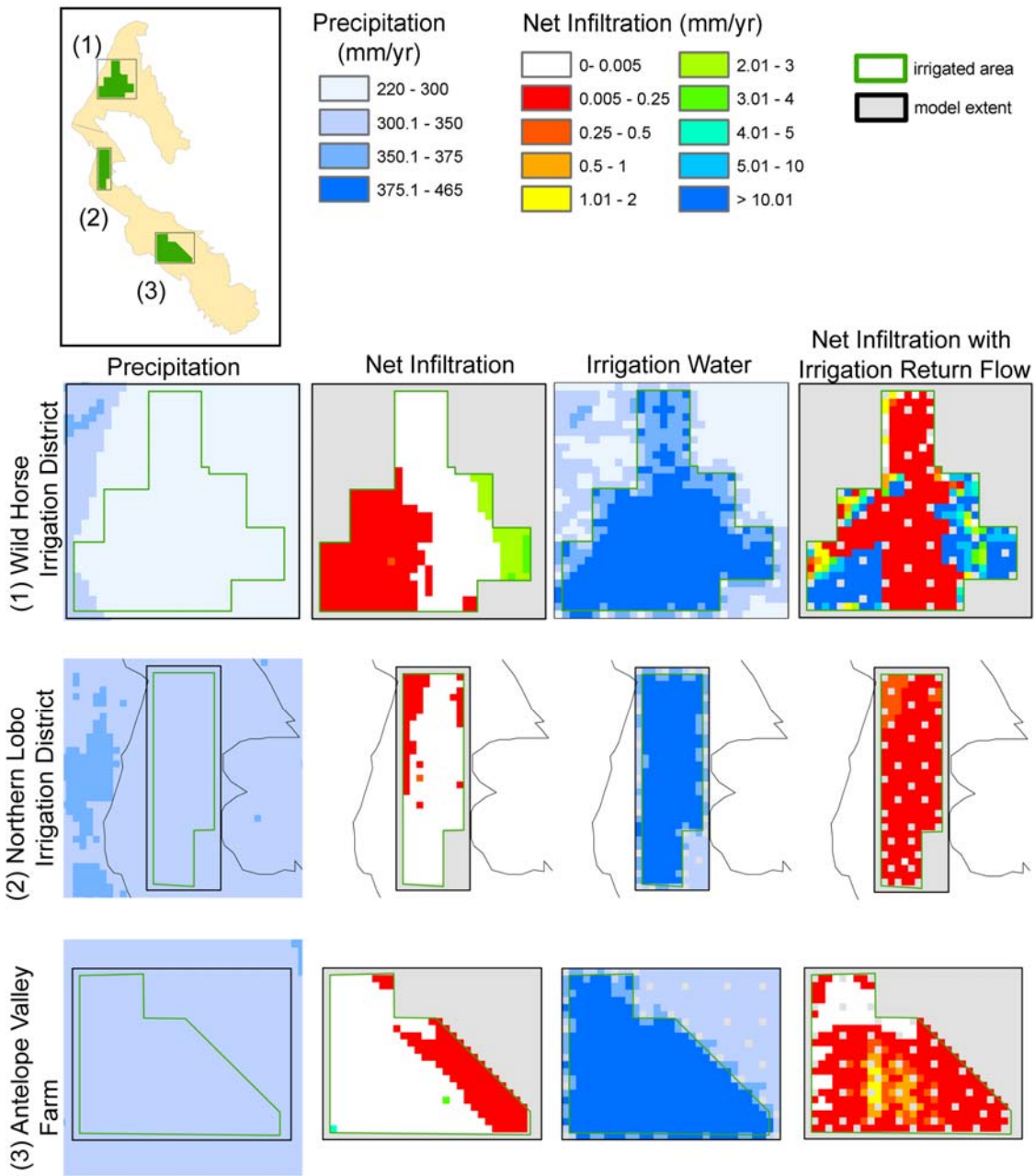


**Fig. 4.11** Diagram displaying precipitation distribution and net infiltration with (right center and far right) and without (far left and left center) added irrigation water for the three smaller models of irrigation districts

## **4.4 Discussion**

### **4.4.1 Limitations**

The estimates of potential recharge produced by the INFIL model are annual averages of net infiltration, not the absolute amount of water reaching the water table on a yearly basis. Thick unsaturated zones typical of arid regions can slow travel time of water and solute by years or decades. Conversely, there is also evidence of preferential flow paths (desiccation cracks, high permeability channels) in discrete areas of the Trans-Pecos basins which are not reflected in the scale of the INFIL model; these features will transport water and solute much more rapidly (Goetz 1985; Van Broekhoven 2002).

There is also uncertainty associated with the spatial resolution of both geological and soil data. Heterogeneity in soil type and lithology of the basin floors of both Wild Horse/Michigan Flats and Lobo/Ryan Flats occur at smaller scales than is recorded in the data that were used to map geology (Stoeser et al. 2007) and soil type (Soil Survey Staff accessed July 2012). A long hypothesized recharge feature, the Van Horn alluvial fan (Gates et al. 1980; Beach et al. 2004) does not appear as a distinct geologic formation within the geological data used because its size was not large enough to be captured on the scale at which the geological data were mapped. This feature and others of similar size within the basins may affect potential recharge in discrete areas in a way that is not reflected in the estimates of potential recharge of the INFIL model.

All PET estimation methods have limitations; over and under-estimation has been documented using temperature-based methods (including Thornthwaite) in comparison with direct measurements of evapo-transpiration (Fitzgerald and Rickard 1960; Pereira and Paes De Camargo 1989; Trajkovic 2005). This contributes to uncertainty in the modeled net infiltration results because for the Trans-Pecos region, there exist few data on which to base a PET measurement, and no published direct measurements of evapo-transpiration are available to which long-term estimates of PET can be compared. As was demonstrated in the sensitivity analysis, the system is more sensitive to PET than to most other parameters. Future research should incorporate the collection of ET

measurements in a range of vegetation regimes so that a more accurate water budget can be developed.

Even distribution of irrigation water in the small models could also cause uncertainty in the estimates of net infiltration from irrigation return flow. This distribution does not reflect daily variations in water application throughout the season or in the ET demand of the crops. As a result, net infiltration due to irrigation return flow may be either over or under-estimated in the small models.

Treating vegetation regime as a static property in the INFIL model may lead to errors in estimation of net infiltration over the course of long-term models. The scenarios examined in this study represent a range of potential vegetation patterns, however, they are not necessarily reflective of real-world conditions and they do not account for transition (i.e., from bare ground to encroachment, fire damage, etc.); it is not clear how important transition times for vegetation change are in the context of infiltration and recharge processes in the Trans-Pecos. The complex interactions between changes to vegetation and hydrological processes are a field of growing interest in arid/semi-arid regions (e.g., Bellot et al. 1999; Veatch et al. 2009; Gustafson et al. 2010; Royer et al. 2011 and others) and in wetter climates (e.g. Frankl and Schmeidl 2000; Brown et al. 2005; Wilcox et al. 2006 and others); incorporation of these processes into regional scale models may prove helpful in prediction of ecohydrological responses to disturbance and change moving forward.

Two improvements that could be made to the INFIL model setup are: 1) allowing for the input of spatially distributed precipitation and 2) allowing for temporal variation in vegetation cover. The current INFIL precipitation input uses long term weather data and climate regression models to estimate precipitation for each grid cell. A mechanism to accept spatially distributed precipitation as input could provide more flexibility to the model; it would allow for inputs like irrigation water to be added to larger scale models and it could potentially provide more usability of the model in regions where weather stations with long-term data sets are scarce. It would also be beneficial to model adaptability if the INFIL model could be altered to accept temporal changes in vegetation

cover. In the Trans-Pecos region (and other arid and semi-arid regions worldwide) changes in woody-herbaceous vegetation dynamics have altered rooting depths and vegetation densities (e.g., Breshears et al. 2005; Newman et al. 2006; Naito and Carins 2011).

#### **4.4.2 Comparison to Previous Research**

Because the delineated contribution areas used in previous research efforts (i.e., the entirety of the Salt Basin extending into southern New Mexico for some models) are not comparable to the model extent used in this study there is little insight gained by directly comparing recharge estimates between the methods. Instead, it is more useful to examine the results of INFIL in the context of how it improves (conceptually) upon the existing models of the Trans-Pecos region; by examining spatial distribution of potential recharge and the impacts of anthropogenic processes on basin hydrology, the INFIL model can explain the presence of modern water and increasing  $\text{NO}_3^-$  concentrations that could not be accounted for by previous research. The modeling efforts using INFIL have demonstrated that modern recharge resulting from natural and anthropogenic sources can occur on the basin floors and that anthropogenic land use and vegetation change are likely impacting infiltration (and thus potential recharge) in the basins.

The spatial distribution of potential recharge estimated using the INFIL model is variable, but it is not limited to the edges of the basins or discrete features as assumed by previous research (Mayer 1995; Mayer and Sharp 1998; Finch and Armour 2001; Beach et al. 2004). It is also likely that net infiltration on the basin floors has increased significantly as a result of changing the native vegetation regime from thick, dense grasslands to its present state. The INFIL results also demonstrate that irrigation return flow is a potential source of water and solute to basin groundwater.

#### **4.4.3 Implications**

That the INFIL model simulates potential recharge on the basin floors as a result of direct precipitation and irrigation return flow and that the simulations indicate changes to vegetation regime alter net infiltration is important in the context of understanding system processes and for prediction of future conditions. The results of the INFIL model

simulations can help to explain transport processes that were in conflict with the models from previous research. They enlighten the spatial variability of potential recharge within the basins, demonstrate the potential for irrigation return flow, and highlight the potential impact of changes to vegetation regime on net infiltration and solute flux within the basins. The INFIL approach allows for the modeling of mechanisms by which vadose zone  $\text{NO}_3^-$  (and other solutes) may be reaching the groundwater within this system. These processes are likely not unique to the Trans-Pecos region and may in fact be occurring in other similar systems around the world such as the Western USA, the Murray-Darling Basin in Australia, and arid/semi-arid catchments in China. Additionally, the trends in  $\text{NO}_3^-$  concentration and the presence of modern water in the basin aquifers indicate a potential risk to water quality; other solutes or contaminants may also be transported by the same mechanisms to basin groundwater in these systems. As arid and semi-arid environments continue to host growing populations worldwide and groundwater is increasingly relied upon as a sole or primary source of drinking water these issues must be addressed.

#### **4.5 Conclusions**

Results from the INFIL model simulations demonstrate that in addition to recharge sourced from the mountains, recharge occurs to basin groundwater through widespread diffuse infiltration on the basin floors and through irrigation return-flow. Annual estimates of potential recharge from natural sources are  $1.03 \times 10^7$  to Wild Horse/Michigan Flats and  $1.26 \times 10^7 \text{ m}^3$  to Lobo/Ryan Flats, of which 7 and 11.5% (respectively) occurs through the basin floors. An additional  $9.5 \times 10^6$  to  $5.2 \times 10^7 \text{ m}^3$  of potential recharge to basin groundwater has occurred since 1960 as a result of irrigation return-flow. INFIL model simulations also indicate that human-induced changes to vegetation regime in the Trans-Pecos basins (through over grazing, fire suppression, and climate change) have also altered infiltration; increases of as much as 48% between pre-western settlement vegetation scenarios and current vegetation regime are modeled. The spatial distribution of potential recharge across the basin floors could explain the

temporal changes in  $\text{NO}_3^-$  concentrations of groundwater and the presence of modern water in the basins that could not be accounted for using models from previous research.

Using INFIL 3.0.1 to model net infiltration and potential recharge is effective in arid basin systems (including the Trans-Pecos region) and this model set-up improves significantly the ability to quantify the spatial distribution of potential recharge and to examine the potential impacts that anthropogenic processes may have on net infiltration within these basins. Recommended adjustments to INFIL to make the model more adaptable to a range of complex arid and semi-arid basin systems would be to 1) allow the input of spatially distributed precipitation and 2) allow for temporal variability in vegetation cover. While the INFIL modeling approach is more data and time intensive than the other methods of recharge estimation used in previous research (e.g., modified Maxey-Eakin, 1% rule) it provides important insight into the distribution and mechanisms of potential recharge and solute flux as well as demonstrating the impact of anthropogenic processes on arid basin systems. Improved understanding of these factors is integral in accurately modeling both recharge and water quality and will aid in the development of sustainable water management policy for these resources.

**Chapter 5:** Impacts of land use and vegetation change on vadose zone and groundwater nitrate concentrations in desert basin aquifers of the Southwestern U.S.

### **5.1 Introduction**

The role of anthropogenically induced land use and vegetation changes on groundwater recharge processes and regional groundwater quality in arid and semi-arid climates is a topic of research which has gained prominence in recent years (e.g., Newman et al. 2006). The impacts of irrigated agriculture on groundwater availability and quality are well documented; the effects range from drastic drops in water table levels (Luckey et al. 1981; Rodell and Famiglietti 2002; Scanlon et al. 2006) to contamination with agrochemicals and labile nitrogen (N) species (Hadas et al. 1999; Oren et al. 2004; McMahon et al. 2006). These effects are a pervasive threat to groundwater sustainability world wide (Llamas and Martinez-Santos 2005). Additionally, shifts in woody-herbaceous vegetation dynamics driven by grazing practices, fire suppression, and climate change alter water balances and water quality in impacted areas (Covington and Sackett 1986; Bellot et al. 1999; Evans and Belnap 1999; Adams et al. 2012). Arid and semi-arid regions are particularly susceptible to human impacts on vegetation and water resources; 2.1 billion people currently live in drylands (i.e., arid to sub-humid climates) around the globe and ongoing climate change is already having measureable impacts on the ecosystems and water resources of these environments (Millennium Ecosystem Assessment 2005; Scanlon et al. 2006). It is imperative that the relationships between land use/vegetation changes, water quality, and water availability in these systems are well understood.

Studies in semi-arid climates with relatively shallow water tables (typically less than 20 m) have demonstrated significant impacts on the vadose zone and underlying groundwater resulting from irrigated agriculture: irrigation 1) enhances recharge; 2) can lead to degradation of underlying groundwater quality; and 3) can have significant impacts on vadose zone salinity (Beare and Heaney 2001; Causape et al. 2004; McMahon et al. 2006; Scanlon et al. 2010). Less research has been done to examine the impact of anthropogenically induced vegetation change (without irrigated agriculture) on water



quality and availability, though studies of rain-fed agriculture have noted similar impacts in these systems as are observed in irrigated areas (i.e., full or partial flushing of  $\text{NO}_3^-$  and  $\text{Cl}^-$  in the vadose zone, enhanced recharge (Scanlon et al. 2008)). Research on the impacts of land use/vegetation changes in semi-arid and arid regions with thicker vadose zones (up to 150 m) has largely been limited to detailed examinations of the vadose zone (Walvoord and Philips 2004; Scanlon et al. 2005); this arises from the often cited hypothesis that as a result of large annual evapo-transpirative demand, low annual precipitation, and thick unsaturated zones, changes on the land surface are often considered disconnected from the underlying groundwater in arid and semi-arid regions (e.g., Adar and Neuman 1988; Walvoord et al. 2002a, 2002b; Wilson and Guan 2004; Pool and Dickinson 2006). This assumption may not hold in some cases (e.g., Stonestrom et al. 2003; McMahon et al. 2004; McMahon and Böhlke 2006a, 2006b; Robertson and Sharp 2012, 2013) and the risk for adverse groundwater quality impacts resulting from changes in vegetation and land use in arid and semi-arid regions is especially high. Long-term (10,000-20,000 yr) accumulation of large reservoirs of salts (including  $\text{Cl}^-$  and  $\text{NO}_3^-$ ) beneath the root zone in arid and semi-arid regions is a well documented phenomenon (Walvoord et al. 2003; Scanlon et al. 2005); if these deposits are mobilized, they could negatively impact groundwater quality.

Alteration of the vegetation regime in arid and semi-arid regions can have significant impacts on hydrological processes. Over-grazing of grasslands thins plant density, decreases root density and depth, increases bare ground cover, and allows for woody vegetation encroachment (Archer 1994; Van Auken 2000; Naito and Cairns 2011). Decreased plant density and the increase of bare ground cover leads to lower ET demand and increases in soil moisture content. A decrease in root density and depth decreases the volume of water available for ET; these translate to an increase in downward moisture flux (and potentially recharge). Woody vegetation encroachment can compound this by contributing to an overall decrease in vegetation density and increase in bare ground cover as woody plants out-compete grasses for water and nutrients (Archer 1994; Newman et al. 2006). When land is used for the cultivation of

non-native species, especially in the context of irrigated agriculture, hydrological processes in the system are both directly and indirectly impacted. Native vegetation is replaced by crop species, altering plant density, rooting depths, ET and nutrient demand. The addition of irrigation water and amendments (specifically fertilizers) further disrupts the natural system.

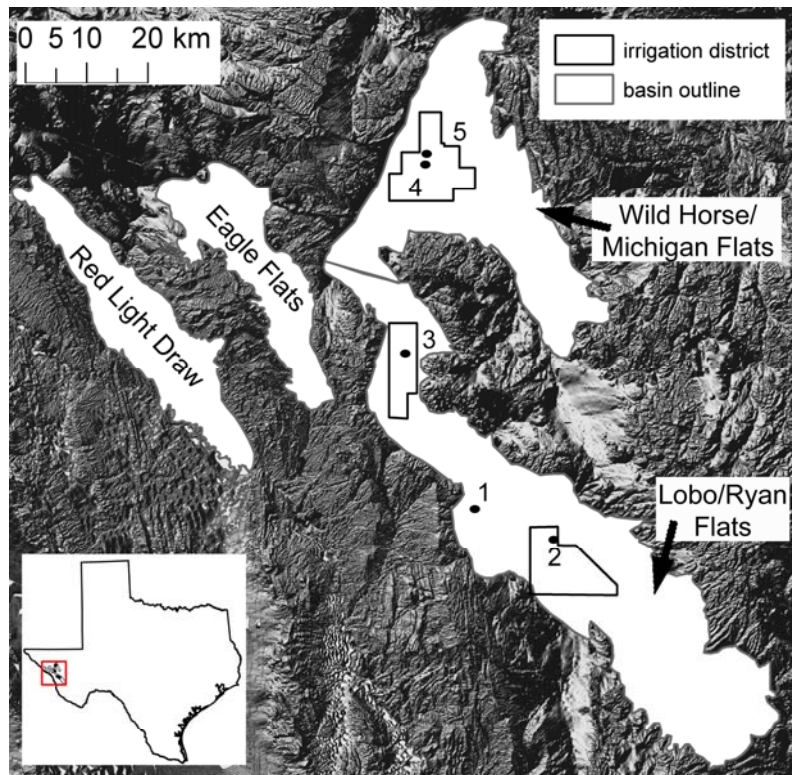
## **5.2 Objectives**

This study was undertaken to: 1) assess the impact of anthropogenically induced vegetation changes in the form of animal grazing and irrigated agriculture on physical and chemical properties of the vadose zone; 2) examine how changes in agricultural use types over time (i.e., irrigated row crops to grazing use, irrigated row crops to irrigated orchards) have impacted vadose zone properties; and 3) establish a link between changes in land use and vegetation regime and the observed changes in basin groundwater quality in arid and semi-arid regions with thick unsaturated zones overlying unconfined aquifers. The study location is a series of basins in the Trans-Pecos region of Texas, an arid region (mean annual precipitation of 220-360 mm/yr) with thick unsaturated zones. Similar studies have been undertaken to address land use change induced impacts (such as enhanced recharge, alteration of labile N species and Cl<sup>-</sup> in the vadose zone, and impacts on groundwater quality) in semi-arid regions of the High Plains and California, however these systems were generally wetter (310-500 mm precipitation /yr), had more shallow depths to water table (7-60 m) than are observed in the Trans-Pecos region, and focused largely on the impact of irrigated agriculture (McMahon and Böhlke 2006; Scanlon et al. 2010). Previous studies within the Trans-Pecos and in Nevada (110-330 mm precipitation /yr and 10-150+ m vadose zones) focused mainly on moisture and solute flux in the vadose zone and estimates for enhanced infiltration due to irrigation return flow; they did not examine links between basin floor land use and vegetation, alteration of vadose zone properties, and changes in regional groundwater quality (Walvoord and Philips 2004; Scanlon et al. 2005). The Trans-Pecos provides a unique opportunity to examine land use impact on groundwater quality because of the availability of long-term water quality data (from ~1950's to present). Results from the region may be broadly

applicable; similar shifts in vegetation and land use are currently occurring in analogous systems in the Southwestern U.S., China, Australia, and elsewhere. In order to manage arid and semi-arid groundwater resources effectively in the face of ongoing land use and climatic change, it is important to understand how these processes are linked.

### **5.3 Site Description**

The Trans-Pecos basin aquifer system is located in far west Texas; the area is part of the Chihuahan Desert and has an arid to semi-arid climate (Fig. 5.1). Average annual precipitation on the basin floors ranges from 220-360 mm/yr and increases with elevation in the adjacent mountains up to 760 mm/yr (Beach et al. 2004, 2008). The unconsolidated basin aquifers are comprised of late Tertiary and Quaternary alluvial and wind blown sediments (Barnes 1979, 1983). Soil horizons in the region are typically thin (1-1.5 m on the basin floors) (Soil Survey Staff, accessed 2012). Depth to water in the basins ranges from ~10 m near the edges to greater than 150 m in the basin centers (Beach et al. 2004, 2008). The basin aquifers are hydrologically connected; flow between Eagle Flats and Red Light Draw, between Wild Horse Flats and Eagle Flats, and from Lobo/Ryan Flats to Wild Horse/Michigan Flats have been documented by previous research (Sharp 2001; Beach et al. 2004, 2008, Uliana et al. 2007). Groundwater residence times in the basins are on the order of thousands of years (Darling et al. 1998; Uliana et al. 2007). Underlying the unconfined basin aquifers are confined units consisting of Permian and Cretaceous sedimentary and Tertiary volcanic rocks (Beach et al. 2004, 2008). Studies of the vadose zone (in un-irrigated regions of the basins) have documented presence of caliche and high concentrations of  $\text{Cl}^-$  and  $\text{NO}_3^-$  beneath the root zones, high matric potential, and low water content, all of which indicate negligible downward moisture flux and recharge on the basin floors and which have been linked to the high ET demand of native vegetation and small annual input of precipitation (Scanlon et al. 1991; Walvoord and Philips 2004).



Core Locations - 1: Miller 1 and Miller 2 (GR),  
 2: Antelope Valley (IRC → GR), 3: BVH (IRC → IO),  
 4: Brookshire 1 and Brookshire 2 (IO),  
 5: Cottrell 1 and Cottrell 2 (IRC)

**Fig. 5.1** Map of the study site in the Trans-Pecos region of west Texas including basin names, locations of core samples, and outlines of irrigation districts within the basins.

Historic accounts of vegetation cover from the first Anglo explorers of the region describe a vegetation regime far different than the one found today. Dense grassland with sparse interspersed shrubs and succulents was the native vegetation regime on the basin floors. A combination of over-grazing (beginning in the 1880's), fire suppression, and regional climatic shifts have led to woody vegetation encroachment, an increase in bare ground cover, and decreases in rooting depth and root density in grass cover on the basin floors during the past century (Humphrey 1958; Buffington and Herbel 1965; Grover and Musick 1990). In addition, irrigated agriculture (utilizing groundwater) has changed rooting depths, vegetation type, and density as well as adding N to the system (from fertilizer). Between the 1950's and late 1970's a large boom in irrigated agriculture

(~20% of basin floor land use in Wild Horse/ Michigan Flats and Lobo/Ryan Flats basins) removed natural vegetation from large swaths of the basins; replacing it with cotton, hay, and pecan trees. Basin groundwater was the source of water for irrigated agriculture. This led to a water crisis in the late 1970's when the water table in some areas of the basins was drawn down by as much as 25 m (Beach et al. 2004). Subsequently, much of the irrigated land was converted to grazing land for cattle or allowed to revert to pre-agricultural vegetation. As of 2006, only ~5% of the basins are used for irrigated agriculture, with row crops covering a larger percentage (91% of irrigated agriculture) than pecan orchards (9% of irrigated agriculture) (Fry et al. 2006). Vegetation cover in some areas with changing land use over time (ex: those with past irrigated agriculture, present grazing/range land) is still distinct from areas that were never irrigated; 20-30 years after their last use, irrigation pivot 'scars' are still visible (grass cover is generally more dense in former irrigated areas) and shrub encroachment is less common.

Despite the presence of thick unsaturated zones (10-150+m) and mean annual PET greatly exceeding mean annual precipitation on the basin floors (1570 mm/yr vs 230-350 mm/yr), it appears that changes to basin groundwater quality (specifically  $\text{NO}_3^-$  concentrations) are related to basin floor surface processes. Median  $\text{NO}_3^-$  concentrations in basin groundwater have increased between 3-4 mg/l (as  $\text{NO}_3^-$ ) during the period of record (~1950-2011) and spatially distributed models of net infiltration (potential recharge) estimate a significant portion of recharge enters through the basin floors (Fig. 5.2) both from natural (i.e., precipitation) and anthropogenic (i.e., irrigation return flow) sources; the shifts in vegetation regime and increase in bare ground cover likely increases the amount of net infiltration (Robertson and Sharp 2013; Robertson and Sharp *in review*). Overall, there are larger magnitude increases in  $\text{NO}_3^-$  concentration beneath land with ongoing or past irrigated agricultural activity (Fig. 5.3), but increases have also been documented beneath land used solely for grazing purposes (Robertson and Sharp 2012). The increases in  $\text{NO}_3^-$  concentration of basin groundwater impact all four basins (Wild

Horse/Michigan Flats, Lobo/Ryan Flats, Eagle Flats, and Red Light Draw) and pose a risk to long-term groundwater sustainability in the region.

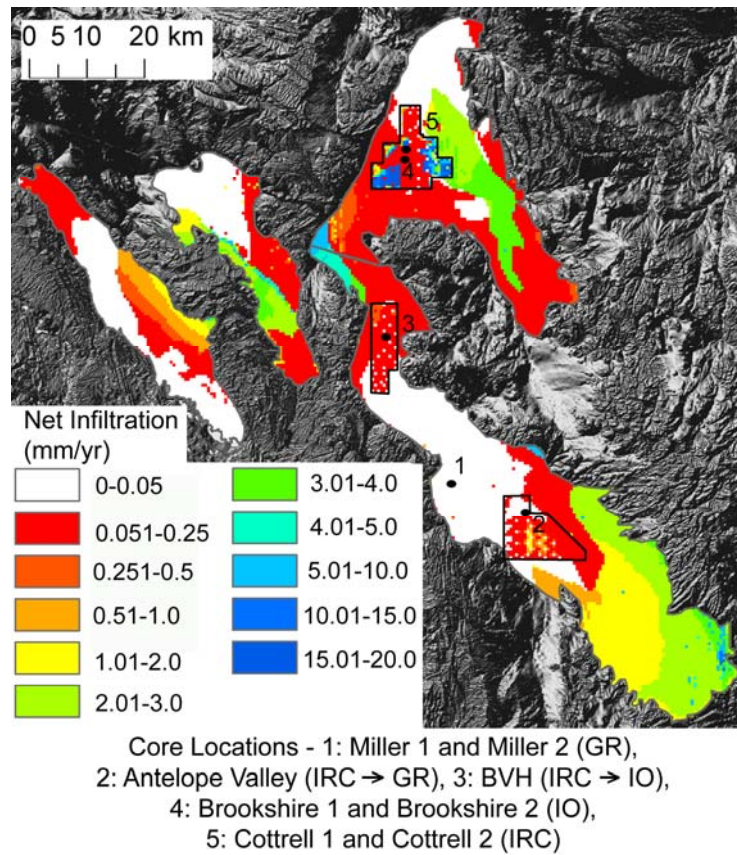


**Fig. 5.2** Map of the spatial distribution of potential recharge within the Trans-Pecos basins resulting from both natural (i.e., precipitation) and anthropogenic (i.e., irrigation return flow) sources. Irrigation districts in Wild Horse/Michigan Flats and Lobo/Ryan Flats are outlined in black.

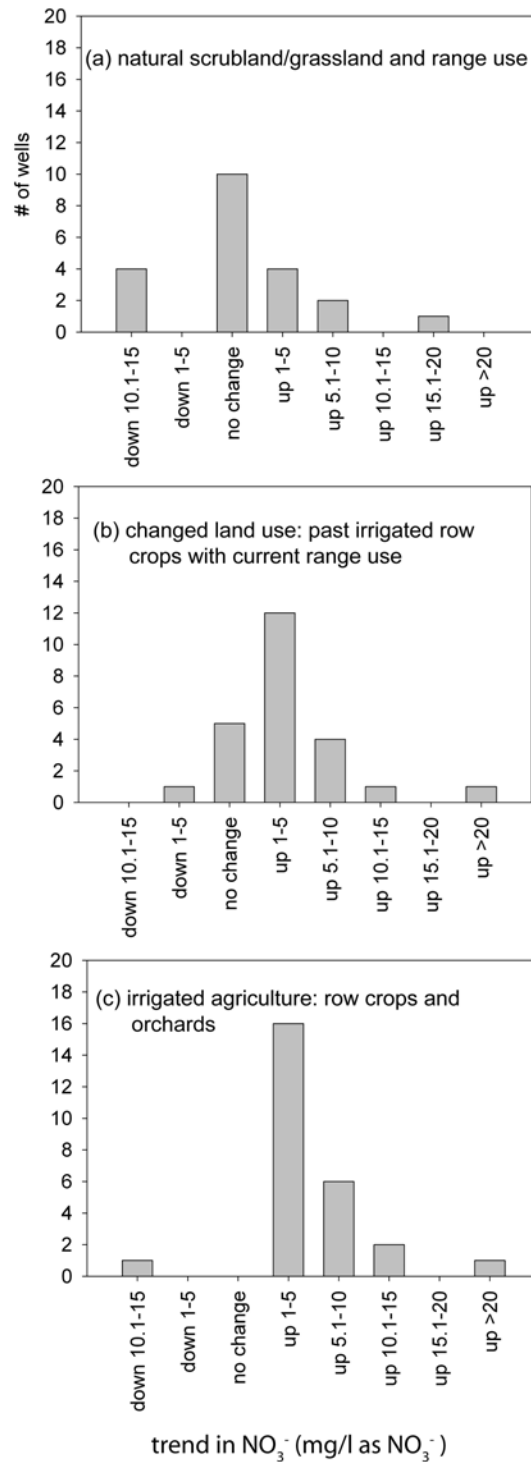


**Fig. 5.3** Distribution of groundwater  $\text{NO}_3^-$  trends (in mg/l as  $\text{NO}_3^-$ ) in the Trans-Pecos basins by overlying land-use type. Land use for each well was identified using DEM based contributing area surrounding each well head (up to 200 m radius).

## 5.4 Methods

### *Groundwater Sampling*

During a 2011 synoptic groundwater survey (Robertson and Sharp 2012) groundwater samples were collected for N and O isotopic analysis of dissolved  $\text{NO}_3^-$ . All samples (N: 83) but one were collected from continuously pumping wells. Samples were filtered into HDPE bottles and kept chilled for a maximum of 4 days before freezing. Water temperature, conductivity, and pH were measured in the field for all samples; select wells (n: 15) were also measured for dissolved oxygen in the field.

### *Vadose Zone Core Collection*

Vadose zone core samples were collected in October 2012 using a GeoProbe™. A total of 8 cores were collected; 2 from beneath land used exclusively for grazing (GR), 1 from beneath changed land use with a combination of irrigated row crops and grazing (IRC → GR), 1 from changed land use with a combination of irrigated row crops and irrigated orchard (IRC → IO), 2 from beneath land used since the 1960's for irrigated orchards (IO), and 2 from beneath land used since the 1960's for irrigated row crops (IRC) (Table 5.1). Cores were collected to depths between 3.7 and 13.1 m; presence of a hardpan caliche layer at ~3-5 m depth beneath the grazed land prevented collection of a full (10+ m) core. All cores were kept chilled for 1-4 days in the field before being frozen upon return to the laboratory.

### *Laboratory Analyses*

Cores were kept frozen (-8°C) until sample preparation and analysis. Core sections (0.15 m intervals in the top 1.2 m, 0.3 m intervals for the rest of the core) were weighed, oven dried for 24 hrs at (125-150 °C) and re-weighed to measure water content. A 60 g sub-section of oven-dried material from each core interval in the top 2 m was analyzed for organic matter (OM) content using the loss on ignition method (LOI); samples were heated at 550 °C for 4 hours. Another sub-selection of sediment from each interval of core (0.15 m in the upper 1m, 0.3 for the remainder) was collected for  $\delta^{15}\text{N}$  analysis of the bulk sediment/soil including organic matter (when present). Pore water leachates were collected by combining 25g of oven dried sediment with 40g of de-



ionized water, shaking for 4 hours, centrifuging and filtering the supernatant. These samples were analyzed for major anions and isotopic composition of N and O in  $\text{NO}_3^-$ . The sample remaining from each core section (after sub-sample collection) was sieved to determine grain size distribution using ASTM standard sieve sizes 4, 10, 20, 40, 100, 120, and 200. Major anion concentrations of pore water leachates were analyzed using ion chromatography at The University of Texas Bureau of Economic Geology.

Minimum detection limits for all analytes was 0.01 mg/l. Total N concentration and isotopic analyses of N in sediment and N and O in  $\text{NO}_3^-$  (groundwater and pore water leachate samples) were conducted by the University of California, Davis Stable Isotope Facility. N isotope analysis in sediments was carried out using a Micro Cube elemental analyzer and PDZ Europa 20-20 isotope ratio mass spectrometer (IRMS). Details for the full procedure are available at the Stable Isotope Facility's website:

<http://stableisotopefacility.ucdavis.edu/13cand15n.html>. The *Pseudomonas aureofaciens* denitrifier method was used to convert dissolved  $\text{NO}_3^-$  into  $\text{N}_2\text{O}$  gas (Casciotti et al. 2002). Isotope ratios of  $^{15}\text{N}$  and  $^{18}\text{O}$  from the resultant  $\text{N}_2\text{O}$  were measured using a ThermoFinnigan GasBench + PreCon trace gas concentration system and a ThermoScientific Delta V Plus IRMS. Details on analytical procedure are available at <http://stableisotopefacility.ucdavis.edu/no3.html>.

## 5.5 Results and Discussion

### *Vadose zone core profiles and salt inventories*

Water content in the vadose cores of the Trans-Pecos basins ranged from ~2 to 18%. Overall, water content tended to increase with both increased period of irrigation (# of seasons of irrigated agriculture) and with decreased rooting depth of overlying vegetation (Fig. 5.4). A notable exception is the drop in water content below the root zone in the well established pecan orchard (IO); this coincided with a gravelly-coarse sand layer within the soils which may have led to more rapid drainage in this zone. Similar, less significant, changes in water content occur between 5-7 m depth in both the IRC → GR and IRC cores; these are also coincident with layers of coarse sand and gravel. LOI content ranged from 5.5 to 12.1%; in all samples (Table 5.1), it is highest in

the first meter of vadose zone, decreasing gradually through meter 2. Based on this sample set, there is no observable correlation of LOI content and land use type. A hardpan caliche layer was present in the GR cores between ~3 and 5 meters depth; a caliche layer was noticeably absent from all cores with either ongoing or past irrigation. This physical difference in vadose composition has potentially significant implications. Studies of the Trans-Pecos region document widespread presence of caliche in basin soils and sub-soils (Darling et al. 1995; Walvoord 2002); its absence in irrigated (and historically irrigated) cores may indicate dissolution and mobilization of the caliche material by irrigation water. Caliche dissolution and degradation in the presence of increased moisture has been observed in the context of playa lakes and shifts in paleo-climate (semi-arid to humid shifts) in the southern High Plains (Reeves 1970; Osterkamp and Wood 1987). The absence of a caliche layer also has significant hydrologic implications; caliche often behaves as a barrier to downward flow, allowing moisture to remain available for evapo-transpiration. An increase in net infiltration and potentially recharge would be anticipated when the caliche layer is absent.

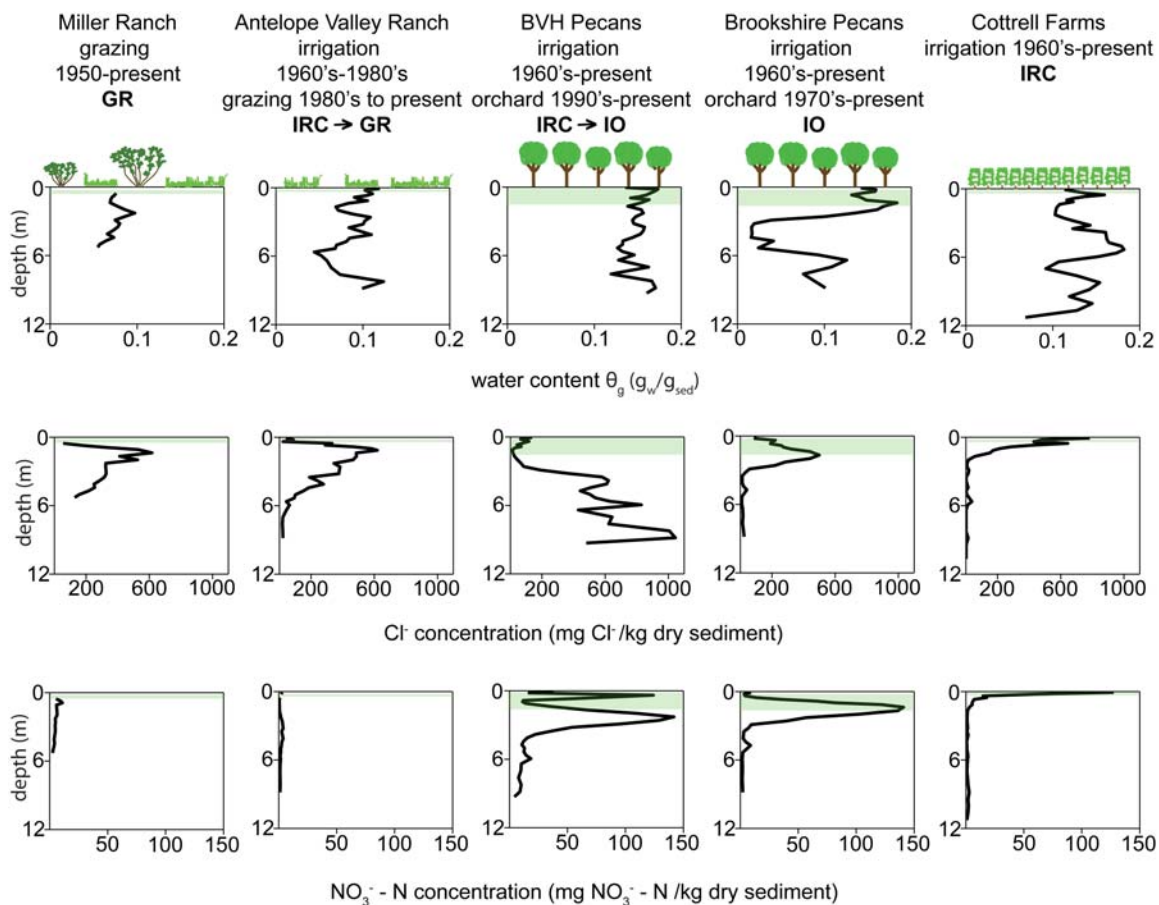


**Fig. 5.4** Profiles of water content,  $\text{Cl}^-$ , and  $\text{NO}_3^-$  concentration beneath representative core samples from grazed land (GR), land with historic irrigated row crops and current grazing (IRC  $\rightarrow$  GR), land with historic irrigated row crops and current irrigated orchard (IRC  $\rightarrow$  IO), an irrigated orchard (IO), and irrigated row crops (IRC). The green shaded zones show typical rooting depth for each vegetation type (Spalding 1904; Woodroof and Woodroof 1934; Schuster 1964; Ares 1976; Stone and Kalisz 1991; Briones et al. 1996; Goins and Russelle 1996; Stewart et al. 2010).

A  $\text{Cl}^-$  bulge is observed in vadose pore water beneath the root zone in both the grazed and IRC  $\rightarrow$  GR land; a corresponding  $\text{NO}_3^-$  bulge is absent in both cores.  $\text{NO}_3^-$  bulges have been observed in some arid and semi-arid rangeland (Walvoord et al. 2003) and are absent in others (Jackson et al. 2004; Scanlon et al. 2010); presence of  $\text{NO}_3^-$  accumulation beneath the root zone is spatially variable and its absence may be indicative of efficient N uptake by native vegetation during the time period of salt buildup (10,000-20,000 yrs) or of sufficient infiltration such that salt build up does not occur.

A  $\text{Cl}^-$  and  $\text{NO}_3^-$  bulge is observed near the maximum rooting depth in the established orchard (IO); the  $\text{Cl}^-$  bulge is similar in magnitude to the GR and IRC  $\rightarrow$  GR bulges that may result from the high ET demand of the pecan trees. However, the high  $\text{NO}_3^-$  bulge observed may be the result of added N fertilizer based on its size and isotopic composition (Figs. 5.4 and 5.6). It is of interest that the high  $\text{Cl}^-$  and  $\text{NO}_3^-$  pore water in the IO coincides with the highest water content; the presence of high clay content in the near surface at the IO location may result in an increase in un-extractable water at this depth. It is also unknown if this  $\text{Cl}^-$  bulge is solely long-term (10,000 + year) accumulation. The groundwater used to irrigate the IO orchard is high in  $\text{Cl}^-$  content (173 mg/l); the observed bulge may be (at least partially) the result of evaporated irrigation water and it is possible that some of the  $\text{Cl}^-$  from the long-term build up has already been flushed. Decadal scale accumulation of  $\text{Cl}^-$  and  $\text{NO}_3^-$  beneath irrigated agriculture in arid and semi-arid regions has been documented as the result of conservative irrigation techniques (Scanlon et al. 2010); this recent accumulation can mimic the patterns of long-term build-up.

Beneath the IRC  $\rightarrow$  IO land use, a displacement of the  $\text{Cl}^-$  bulge is observable (5-11 m as opposed to 1-5 m); the  $\text{Cl}^-$  bulge is also much larger than observed in the GR, IRC  $\rightarrow$  GR, and IO cores and is located below the zone of high  $\text{NO}_3^-$  concentration. The position, size, and isotopic composition of the pore water  $\text{NO}_3^-$  in the IRC  $\rightarrow$  IO core indicate a possible contribution of N fertilizer (Figs. 5.4 and 5.6). The location of the  $\text{Cl}^-$  bulge may be the result of partial flushing of  $\text{Cl}^-$  with irrigation water (relic of the  $\sim$ 30 years of IRC land use). Based on the accumulation of  $\text{NO}_3^-$  and  $\text{Cl}^-$  in the vadose zone, the pecan orchards in the Trans-Pecos behave more like a barrier to downward flux of moisture and solute than other orchards in semi-arid and arid regions. Almond orchards studied in the Merced River basin of California demonstrated episodic variability of vadose pore water  $\text{NO}_3^-$  concentrations based on timing of irrigation and storms (Hancock et al. 2008; Nolan et al. 2002) with flushing of labile N species and pesticides to the shallow ( $\sim$ 7 m) underlying groundwater. The differences between these sites may

be attributable to differences in water demand, irrigation type and timing, soil type, and thickness of the underlying vadose zone.

At the IRC location, complete flushing of vadose zone salts is observed. Below the zone (<1 m) affected by surface evaporation, minimal accumulation of either  $\text{Cl}^-$  or  $\text{NO}_3^-$  occurs and the zone of expected accumulation (present in the GR core) is absent, indicating flushing by irrigation water. This process has been documented in other arid and semi-arid regions (Scanlon et al. 2005), raising concern for the ultimate fate of mobilized salts and providing a potential source of labile N to basin groundwater. Unlike in some arid and semi-arid irrigated settings, re-accumulation of vadose salts (due to a combination of ET demand from vegetation and conservative irrigation practices) has not occurred; the amount of irrigation water applied to these irrigated row crops exceeds ET demand and continued flushing of the vadose zone occurs.

core	depth (m)	average water content (g/g)	range of NO <sub>3</sub> <sup>-</sup> /Cl <sup>-</sup> (mol/mol)	range of Cl <sup>-</sup> (mg/kg sediment )	range of NO <sub>3</sub> <sup>-</sup> -N (mg/kg sediment) <i>range land only</i>	peak Cl <sup>-</sup> (mg/kg sediment )	peak Cl <sup>-</sup> depth (m)	peak NO <sub>3</sub> <sup>-</sup> -N (mg/kg sediment)	peak NO <sub>3</sub> <sup>-</sup> depth (m)	organic matter (%)	peak organic matter depth (m)
milller 1*	5.4	0.08	0.02-2.67	54.8-617.4	2.5-11.0	617.4	1.37	11.0	0.2	8.6-12.1	0.7
milller 2*	3.6	0.08	0.13-1.53	4.1-57.4	1.4-4.0 <i>irrigated row crop to range land</i>	57.4	0.08	4.0	2.3	5.3-9.0	0.7
AV	9.2	0.09	0.002-0.19	18.4-619.3	0.5-3.8 <i>irrigated row crop to range land</i>	619.3	1.68	3.8	3.2	3.6-7.5	0.5
BVH	9.5	0.15	0.02-6.6	13.8-1044.0	4.2-141.8 <i>irrigated orchard</i>	1044.0	8.8	141.8	2.3	6-8.5	0.7
Brookshair 1	9.2	0.1	0.05-0.96	9.1-499.0	1.7-140.8 <i>irrigated row crop</i>	499.0	1.7	140.8	1.7	6-8	0.08
Cottrell 1	11.6	0.13	0.03-4.01	5.4-6906.5	2.6-716.7	6906.5	0.08	716.7	0.08	8-10.1	0.84

**Table 5.1** Summary of vadose zone core samples collected in fall 2012 from the Trans-Pecos basins. \*Range land cores had limited depth profiles.

Salt inventories of the vadose zone cores in the Trans-Pecos demonstrate noteworthy patterns (Fig. 5.5). The IRC core is consistent with literature values for irrigated agricultural land use (row crops) in the High Plains (humid-continental to semi-arid). No data are available for vadose salt inventories beneath orchards in semi-arid and arid regions; however, the IO core inventory is near the range of irrigated agriculture. It is higher in  $\text{NO}_3^-$  than typically found in irrigated row crops which may be a result of higher fertilizer application rates to pecan orchards than to cotton fields (97-132 lbs/acre vs 82 lbs/acre (USDA NASS, accessed 2013)). The IRC  $\rightarrow$  IO core is higher both in  $\text{NO}_3^-$  and in  $\text{Cl}^-$  than reported values for this climate range. Similar ranges in  $\text{Cl}^-$  have been documented in more arid regions including Utah and Nevada (Flint et al. 2002; Heilweil et al. 2006), but  $\text{NO}_3^-$  concentrations were not reported in these studies. The GR and IRC  $\rightarrow$  GR cores have very similar salt inventories and, notably, have smaller inventories (at least 10,000 kg less  $\text{Cl}^-$ ) than the reported range of cores in this region of the Chihuahan Desert (Walvoord 2002). Several factors may be contributing to this apparent 'deficit' of vadose zone salt; 1) the GR core did not go a full 10 m (salt inventories in literature were calculated for the first 10 m of core in the Chihuahan Desert cores (Walvoord 2002) or were normalized to core interval in the case of Southern High Plains and irrigated High Plains cores (McMahon et al. 2006; Scanlon et al. 2008; Scanlon et al. 2010)), therefore some of the salt inventory may have been missed, 2) the range of Chihuahan desert values is based on a sample size of 5, and 3) changes in vegetation regime driven both by intensive grazing (on both GR and IRC  $\rightarrow$  GR cores) and irrigated agriculture (on the IRC  $\rightarrow$  GR core) may have resulted in increased recharge and partial mobilization. Based on the available data, it is not possible to conclude which of these factors is responsible for the observed difference between the Trans-Pecos cores and literature data. Assuming that the 1) the literature values are inclusive of vadose salt inventories beneath un-irrigated grass and shrub land in this section of the Chihuahan desert, and 2) the GR core is an incomplete salt inventory, then there may be some evidence of partial flushing due to the short-term irrigation of the IRC  $\rightarrow$  GR as it does differ from the literature values for rangeland in the Chihuahan desert. It is also important to consider that  $\text{Cl}^-$  and

$\text{NO}_3^-$  vadose zone build up is spatially variable; the presence of a high concentration zone is in itself an indication of slow and diffuse infiltration. In areas where more rapid infiltration can occur (i.e., conduit flow through desiccation cracks, presence of highly permeable layers, etc.), salt build up will not be present either because flux rates were high enough to prevent formation of build up or because flushing of the built up salts has already occurred. It is documented that in the Trans-Pecos (and similar systems), recharge is both spatially and temporally variable (Harrington et al. 2002; Robertson and Sharp 2013, Robertson and Sharp, *in review*); therefore, flux of  $\text{NO}_3^-$  (and  $\text{Cl}^-$ ) to basin groundwater will likely also be spatially and temporally variable.

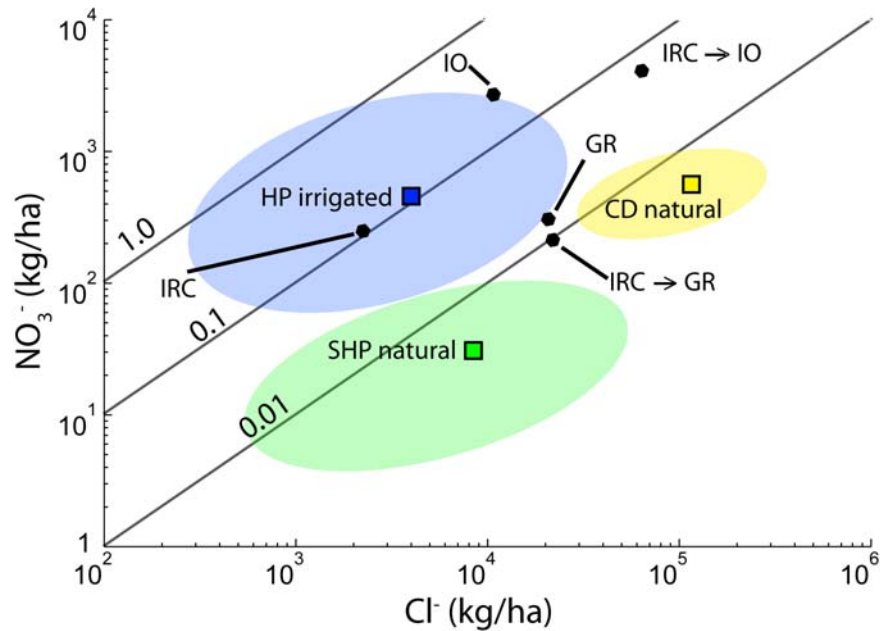


**Fig. 5.5** Vadose zone  $\text{NO}_3^-$  and  $\text{Cl}^-$  inventories from this study (black dots) and literature values. HP irrigated (blue) are the range of values observed in cores beneath irrigated row crops from the High Plains aquifer ( $n = 21$ ) (McMahon et al. 2006; Scanlon et al. 2010), SHP natural (green) are the range of values observed in cores beneath rangeland in the Southern High Plains aquifer ( $n = 15$ ) (Scanlon et al. 2008; Scanlon et al. 2010), and CD natural (yellow) are the range of values observed in cores beneath range/scrubland in the Chihuahan Desert ( $n = 5$ ) (Walvoord 2002).



*N and O isotopic composition of NO<sub>3</sub><sup>-</sup> in groundwater and pore water samples*

The isotopic composition of NO<sub>3</sub><sup>-</sup> dissolved in groundwater in the Trans-Pecos basins is consistent with 1) literature values for soil N derived NO<sub>3</sub><sup>-</sup> (Fig. 5.6a) and 2) the bulk sediment <sup>15</sup>N data collected from the vadose zone cores (Fig. 5.6b), both of which are consistent with a natural soil N derived NO<sub>3</sub><sup>-</sup> source to the basin groundwater. Soil derived NO<sub>3</sub><sup>-</sup> has been observed in groundwater beneath natural and irrigated agricultural land in arid and semi-arid regions. McMahon et al. (2006) and McMahon and Böhlke (2006) linked irrigated agriculture to mobilization of soil N derived NO<sub>3</sub><sup>-</sup> and increases in groundwater NO<sub>3</sub><sup>-</sup> concentrations in the High Plains aquifer, soil N derived NO<sub>3</sub><sup>-</sup> in groundwater has been associated with paleo-recharge in the Middle Rio Grande Basin (Plummer et al. 2006), and Stonestrom et al. (2003) examined deep percolation of irrigation water mobilizing Cl<sup>-</sup> and NO<sub>3</sub><sup>-</sup> in the vadose zone within the Amargosa desert; this study links soil N derived groundwater NO<sub>3</sub><sup>-</sup> to modern recharge (both from precipitation and irrigation return flow) and land use change in an environment. The NO<sub>3</sub><sup>-</sup> dissolved in Trans-Pecos groundwater is not consistent with either a direct atmospheric source or with synthetic fertilizers. Either these sources are not evident because the labile N is cycled through the soils prior to recharge or the contribution of soil N derived NO<sub>3</sub><sup>-</sup> is so much larger than labile N that had not been cycled through soils and plants (as could be the case in the mobilization of a large reservoir of labile N from beneath arid and semi arid root zones) that the signal of an additional source is overwhelmed. The vegetation may also be very efficient at N uptake, leaving no un-cycled labile N in the vadose zone, which is consistent with most of the observed vadose pore water NO<sub>3</sub><sup>-</sup> isotopic compositions. Even directly beneath agricultural land, the isotopic composition of NO<sub>3</sub><sup>-</sup> in the groundwater is not consistent with an unassimilated synthetic fertilizer source; either the addition of synthetic fertilizer is not in excess of crop demand, there is not a downward flux of unassimilated labile N in the vadose zone, or vadose zone transit times (from >15 m down to the water table) are long enough that unassimilated labile N from synthetic fertilizers has not yet reached the water table.

Based on the trend in some of the groundwater samples, it is possible that some

denitrification is occurring in some areas of the basins; enrichment of both  $^{15}\text{N}$  and  $^{18}\text{O}$  occur during the denitrification process (e.g. Bottcher et al. 1990; Aravena and Robertson 1998; Fukada et al. 2003). Dissolved oxygen (DO) (from 2011 and previous studies) in basin groundwater ranged from 1.7 to 6.8 mg/l (Ward 2002). Studies of in-situ groundwater/riparian zone denitrification indicate that denitrification can occur in water with DO concentrations less than 2 mg/l (Hill et al. 2000; Böhlke et al. 2002; Green et al. 2008); what may be occurring in the Trans-Pecos basins is that some zones of suboxia/anoxia are present in which denitrification occurs. This water subsequently mixes with groundwater with higher levels of DO and  $\text{NO}_3^-$ . Denitrification in the soil horizon is another possibility (e.g. Aulakh et al. 1992; Hofstra and Bouwman 2005), though the expected enrichment pattern for the isotopic composition of  $\text{NO}_3^-$  is not observed in the collected cores (Fig. 5.10).

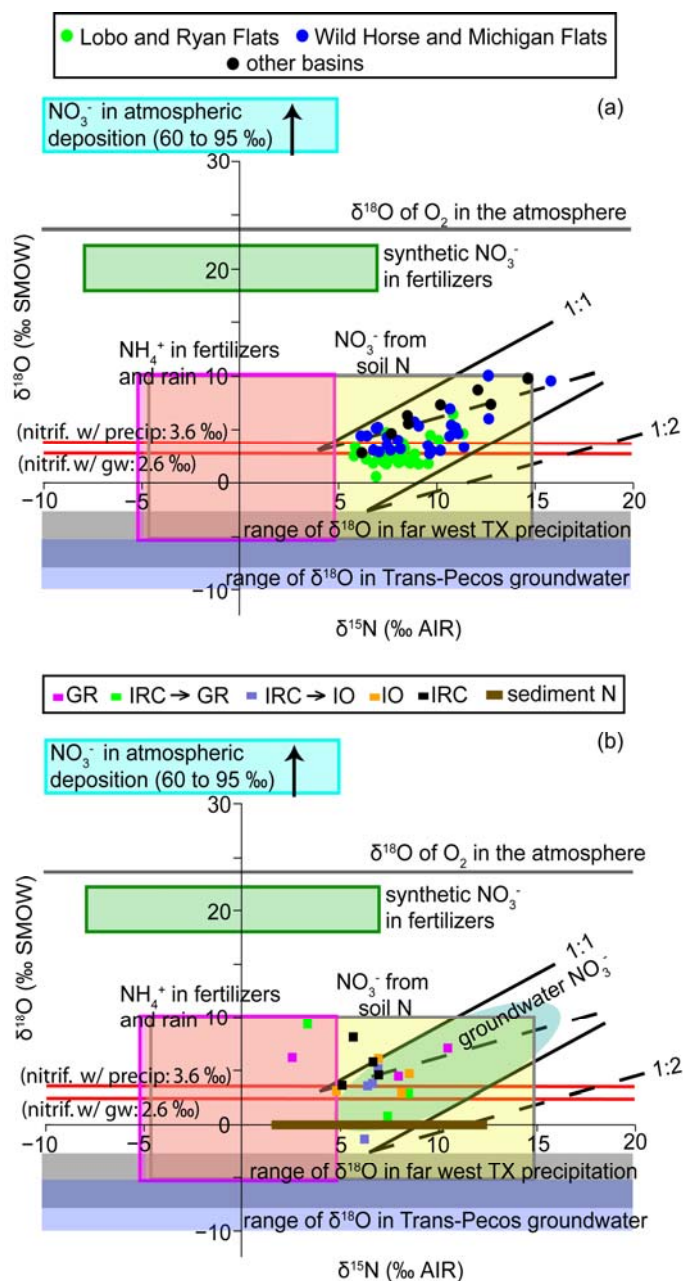


**Fig. 5.6** Plots of isotopic composition of <sup>15</sup>N and <sup>18</sup>O of NO<sub>3</sub><sup>-</sup> in groundwater (top) and pore water leachates (bottom), with ranges of literature values from various labile N sources (modified from Kendall 1998), <sup>15</sup>N from bulk soil/sediment in the Trans-Pecos cores, values for <sup>18</sup>O in precipitation and groundwater from previous studies (Dr. Barry J. Hibbs (personal correspondence); Nativ and Riggio 1990; Darling 1997), and lines for predicted values of <sup>18</sup>O for nitrified NO<sub>3</sub><sup>-</sup> using 1 part O from the atmosphere and 2 parts O from available water (average values of far west TX precipitation and Trans-Pecos groundwater used).

Also of note is the 2-4 ‰ difference between the minimum  $^{18}\text{O}$  values of  $\text{NO}_3^-$  in basin groundwater of hydrologically connected basins (Lobo/Ryan Flats and Wild Horse/Michigan Flats). The observed difference is compelling; for there to be a difference in the isotopic composition of  $\text{NO}_3^-$  in the groundwater indicates both that there are slight differences in the source/process of formation and that the perturbation of the system is on a time scale shorter than that of the regional mixing. The difference in  $^{18}\text{O}$  indicates a localized rather than regional  $\text{NO}_3^-$  source. As mentioned in the site description, the regional flow in this system is from south to north (Lobo/Ryan to Wild Horse/Michigan) on the scale of 100's to 1,000's of years (Uliana et al. 2007). The difference is also, at first glance, counterintuitive. Nitrification using a regional average  $^{18}\text{O}$  in precipitation combined with  $^{18}\text{O}$  of oxygen in the atmosphere (2:1) should create  $\text{NO}_3^-$  with an average  $^{18}\text{O}$  of  $\sim 3.6$  ‰, whereas nitrification using groundwater at the same ratio should create  $\text{NO}_3^-$  with an average  $^{18}\text{O}$  of  $\sim 2.6$  ‰. If the pore water in the vadose zone was isotopically consistent with groundwater (as could be expected in intensively irrigated areas), then the  $^{18}\text{O}$  of  $\text{NO}_3^-$  resulting from nitrification should be less enriched in the basin with more irrigated agriculture (i.e., Wild Horse and Michigan Flats). The data show the opposite effect;  $^{18}\text{O}$  in groundwater  $\text{NO}_3^-$  from Wild Horse and Michigan Flats is more enriched than in Lobo and Ryan Flats (a basin with less overall irrigated agricultural land use). Indeed, when isotopic composition of  $\text{NO}_3^-$  is plotted by land use, no difference in  $^{18}\text{O}$  is observed (Fig. 5.7). So while localized, it does not appear to be related to the use of groundwater for irrigation. Another localized process could be controlling variability of  $^{18}\text{O}$  values. Spatial variability of  $^{18}\text{O}$  in precipitation resulting from convective storm events has been documented in the Southwestern U.S. (Metcalf 1995); variations of  $\sim 1.5$  ‰ over short (less than 3 km) distances were documented. It is possible that the differences in  $^{18}\text{O}$  of  $\text{NO}_3^-$  from soil N result from local variability in the isotopic composition of  $^{18}\text{O}$  in precipitation.

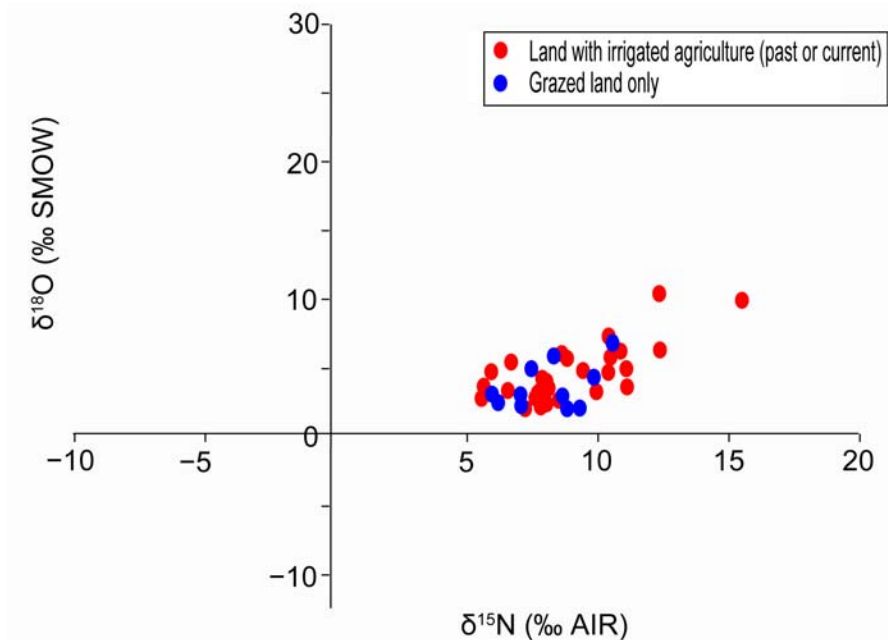


**Fig. 5.7** Plots of isotopic composition of  $^{15}\text{N}$  and  $^{18}\text{O}$  of  $\text{NO}_3^-$  in groundwater identified by land use. All wells beneath land formerly or currently used for irrigated agriculture are separated from wells beneath land used solely for grazing.

The isotopic composition of pore water  $\text{NO}_3^-$  in the vadose cores is, overall, consistent with literature values of soil N derived  $\text{NO}_3^-$  and with the  $\text{NO}_3^-$  dissolved in basin groundwater (Fig. 5.6b) (e.g. Kreitler 1979; Durka et al. 1994; Kendall 1998; Amundson et al. 2003). There is evidence of mixed sources of labile N in some near surface vadose samples. In the grazing land use only and the changed land use (IRC + GR) cores, the near surface pore water samples have  $\text{NO}_3^-$  with compositions that are noticeably different than most samples. The concentrations of  $\text{NO}_3^-$  in the pore water at the near surface are also very low. It may be that a small amount of unassimilated labile N from atmospheric deposition is mixing with the soil N derived  $\text{NO}_3^-$ ; its presence is only observable at very low concentrations of pore water  $\text{NO}_3^-$ . Conversely, some of the IO pore water samples have isotopic compositions observably different than other vadose pore samples and groundwater, and these occur at or near high concentrations of pore water  $\text{NO}_3^-$ . The orchards use a combination of  $\text{NH}_4^+$  /  $\text{NO}_3^-$  and urea fertilizers; some unassimilated fertilizer may be present in the pore water  $\text{NO}_3^-$ , creating a mix of fertilizer and soil N derived  $\text{NO}_3^-$ . At the near surface (0.07 m) in the IRC core, the isotopic

composition of pore water  $\text{NO}_3^-$  may also indicate a mix of synthetic fertilizer and soil N sources, but below the root zones of the shallow-rooted vegetation (IRC, IRC  $\rightarrow$  GR, and GR cores),  $\text{NO}_3^-$  is consistent with a soil N derived source, indicating that the vegetation is efficient at cycling the amount of labile N available. Several of the cores also display slight increases in  $\delta^{15}\text{N}$  and  $\delta^{18}\text{O}$  with depth (Fig. 5.9); increased soil moisture can lead to increased microbial activity and N cycling, leading to a slight fractionation of the residual labile N. This pattern has been observed in other systems (Densmore and Böhlke 1998; Handley et al. 1999; Amundson et al. 2003; McMahon et al. 2006) and may be occurring here, though the potential for a mix of sources of labile N and data scarcity at depth limit quantification of changes in N cycling through the profile.

#### *Cl<sup>-</sup>/Br<sup>-</sup> in groundwater and pore water*

The  $\text{Cl}^-/\text{Br}^-$  ratios of groundwater in the Trans-Pecos basins (specifically Lobo/Ryan Flats and Wild Horse Michigan Flats) largely differ from typical ratios of  $\text{Cl}^-/\text{Br}^-$  in far west Texas precipitation (24-167 (Scanlon et al. 2003)) (Fig. 5.8a). In Lobo/Ryan Flats the majority of groundwater samples have low  $\text{Cl}^-$  concentrations (less than 75 mg/l) and  $\text{Cl}^-/\text{Br}^-$  ratios between 175 and 300. In Wild Horse and Michigan Flats,  $\text{Cl}^-$  concentrations range from  $\sim 30$  to  $\sim 550$  mg/l with  $\text{Cl}^-/\text{Br}^-$  ratios of 275-3000. The high  $\text{Cl}^-/\text{Br}^-$  ratios and low  $\text{Cl}^-$  concentrations observed in Lobo/Ryan Flats may be a result of a combination of 1)  $\text{Br}^-$  concentrations near detection limits causing anomalously high ratios, and 2) cross-formational flow between the unconfined basin aquifer and the underlying Igneous aquifer (see green dashed box in Fig. 5.8a for ranges of reported groundwater values (Texas Water Development Board GWDB, accessed 2013)). High  $\text{Cl}^-/\text{Br}^-$  ratios ( $\sim 200$ -500) have been documented in volcanic rocks, including in the rock types of the Igneous aquifer (predominantly welded pyroclastics and basalts) (Yoshida et al. 1971; Becker and Manuel 1972) and in groundwater in these types of formations (Davis et al. 1998); groundwater upwelling from the Igneous fm may be contributing water of high  $\text{Cl}^-/\text{Br}^-$  ratio and low  $\text{Cl}^-$  concentration to the basin. In Wild Horse/Michigan Flats, the high  $\text{Cl}^-/\text{Br}^-$  ratios are consistent with halite and playa deposit dissolution or mixing with brines resulting from halite dissolution (Davis et al. 1998).

Both of these possible sources in Wild Horse/Michigan Flats; playa deposits are present north of the flats (it is also likely that there are buried playa deposits within the basin sediments) and cross-formational flow from the underlying Capitan Reef formation may contribute some brine-impacted groundwater to the system (Fig. 5.8a, yellow box).

The vadose pore waters have  $\text{Cl}^-/\text{Br}^-$  ratios that range from typical precipitation values to those of Trans-Pecos groundwater (Fig. 5.8b) and generally increase with depth (Fig. 5.8c). In the exclusively grazed land use areas,  $\text{Cl}^-/\text{Br}^-$  ratio increased sharply up to 1 m depth, then remained steady. Typical rooting depth of the grazed land vegetation is 30 to 80 cm (Schuster, 1964; Ares 1976); this increase in  $\text{Cl}^-/\text{Br}^-$  ratios beneath grazed land may be a result of preferential uptake of  $\text{Br}^-$  by vegetation (Kung 1990), though the  $\text{Cl}^-/\text{Br}^-$  ratios in the GR core all remain in the range of observed precipitation values. A sharp increase in  $\text{Cl}^-/\text{Br}^-$  ratios at/near rooting depths is observed in all cores except beneath irrigated row crops, and in all cores with past or current irrigation history, the  $\text{Cl}^-/\text{Br}^-$  ratios increase beyond the range of precipitation ratios. The increase between 0 and 1 m depth is also larger than that observed beneath exclusively grazed land use. In the IRC  $\rightarrow$  GR, IRC  $\rightarrow$  IO, and IO cores a combination of processes may be occurring. The preferential uptake of Br by vegetation and the addition of irrigation water (basin groundwater) could both be contributing to the increase in  $\text{Cl}^-/\text{Br}^-$  ratios. The addition of groundwater with high  $\text{Cl}^-/\text{Br}^-$  ratios is especially apparent in the IRC  $\rightarrow$  IO core where high Cl/Br ratios coincide with high pore water  $\text{Cl}^-$  concentrations (~1m and 7+ m depths (Figs. 5.4 and 5.8c) and in the IRC core where  $\text{Cl}^-/\text{Br}^-$  ratios of pore water are consistent with groundwater ratios at all depths (note:  $\text{Cl}^-/\text{Br}^-$  ratios are not available in the IRC core beneath 1 m due to low concentrations in pore water; this is consistent with the flushing of vadose zone salts due to irrigation (Fig. 5.4 (Scanlon et al. 2005; McMahon et al. 2006))).

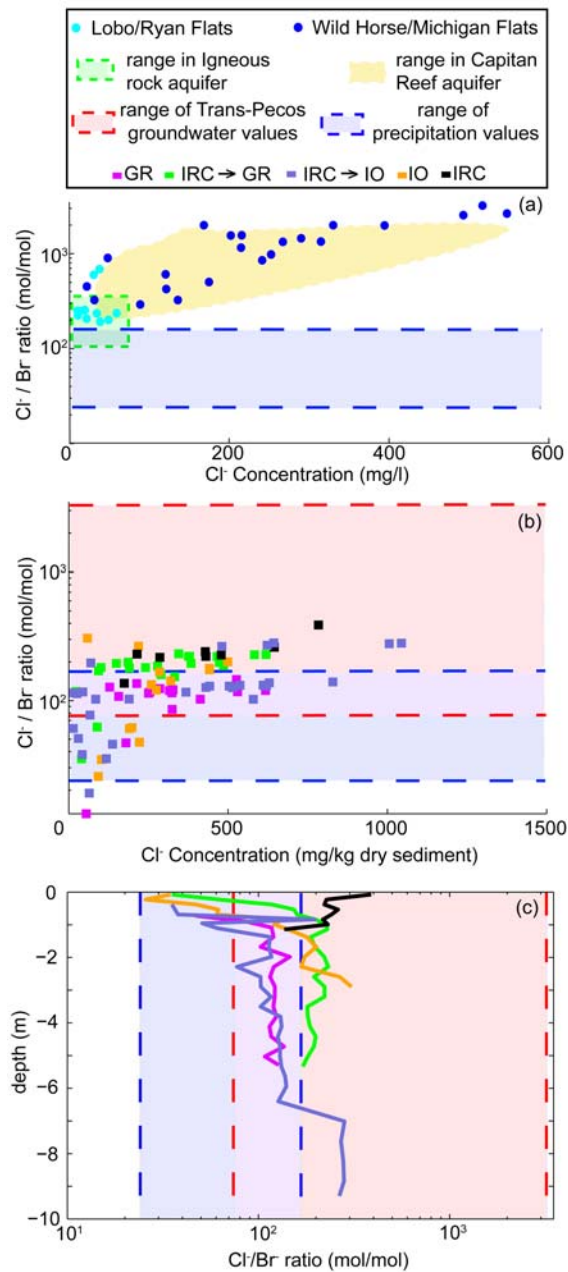


**Fig. 5.8** Plots of (a) Cl<sup>-</sup> concentration vs Cl<sup>-</sup>/Br<sup>-</sup> ratio in Trans-Pecos groundwater samples with ranges of precipitation values from the Trans-Pecos region (Scanlon et al. 2003) and ranges of values from underlying aquifer systems (TWDB GWDB, accessed 2013), (b) Cl<sup>-</sup> concentration versus Cl<sup>-</sup>/Br<sup>-</sup> ratio in vadose zone pore water leachates with ranges of precipitation and Trans-Pecos groundwater values, and (c) profiles of Cl<sup>-</sup>/Br<sup>-</sup> ratio in vadose zone pore water leachates with depth.

*NO<sub>3</sub><sup>-</sup> and Cl<sup>-</sup> in pore water*



Plots of  $\text{NO}_3^-$  vs  $\text{Cl}^-$  concentration can indicate the potential for N uptake or loss within a system. Assuming there are no additional sources of labile N (e.g., biotic fixation, manure, etc.) and the available labile N is not cycled (e.g., plant or microbial uptake) or lost (e.g., denitrification), then the  $\text{NO}_3^-$  and  $\text{Cl}^-$  concentrations of a water should fall along the atmospheric deposition line (Fig. 5.9a). Water falling off of this line indicates some perturbation of  $\text{NO}_3^-/\text{Cl}^-$  ratio in the resultant water; either labile N addition or loss in the system (addition of  $\text{Cl}^-$  will also cause water fall off this line and resemble a labile N loss in the system).

The GR core vadose pore waters plot in a range depleted in  $\text{NO}_3^-$  with respect to the modern atmospheric deposition line (Fig. 5.9a). This is indicative of efficient uptake of labile N by vegetation (vadose pore water shows no evidence of denitrification (Fig. 5.9b)). The pore water from the IRC  $\rightarrow$  GR core also plots depleted in  $\text{NO}_3^-$ , which may be indicative of efficient uptake of N by vegetation and may also be partially the result of added  $\text{Cl}^-$  from basin groundwater; addition of past irrigation water with elevated  $\text{Cl}/\text{Br}$  ratios (Fig. 5.8a) may lead to misleading estimates of vegetation uptake of labile N. Also plotted in Fig. 5.9a are the ranges of groundwater  $\text{NO}_3^-$  vs  $\text{Cl}^-$  and the  $\text{NO}_3^-$  vs  $\text{Cl}^-$  in irrigation water amended with fertilizer loads (based on the USDA agricultural census data for cotton and pecan orchard applications in TX (USDA NASS, accessed 2013)). Neither the  $\text{NO}_3^-$  nor  $\text{Cl}^-$  application in the irrigated areas is consistent with an atmospheric source. When compared to the ranges of amended groundwater, some of the IRC  $\rightarrow$  IO and IO core pore water ratios show significantly less N uptake/loss; this indicates that application rates in the orchards may exceed uptake and is consistent with both the high  $\text{NO}_3^-$  concentrations observed in pore water and with the isotopic composition of pore water  $\text{NO}_3^-$  (a mix of fertilizer and soil N source at points of higher  $\text{NO}_3^-$  concentrations). A few of the (near-surface) IRC pore water values also show less N uptake/loss than other pore water values (though they indicate more loss than the cores beneath the orchards); this, too, may be reflective of fertilizer amendment in excess of vegetation uptake.

The vadose zone pore waters (and most groundwater samples) have  $\text{NO}_3^-$  concentrations in excess of the concentrations found in modern atmospheric deposition (Fig. 5.9b); this is due to a combination of 1) evaporative concentration prior to recharge and 2) addition of N in the form of fertilizers to agricultural lands. When plotted against  $\text{NO}_3^-/\text{Cl}^-$  ratios (Fig. 5.9c), all samples plot below the modern atmospheric deposition line. Again, this is due to a combination of N loss and  $\text{Cl}^-$  addition. Vadose pore waters from irrigated lands overall plot higher than those from grazed and changed land use with grazing use lands which is consistent with fertilizer application at rates higher than vegetation uptake of N.

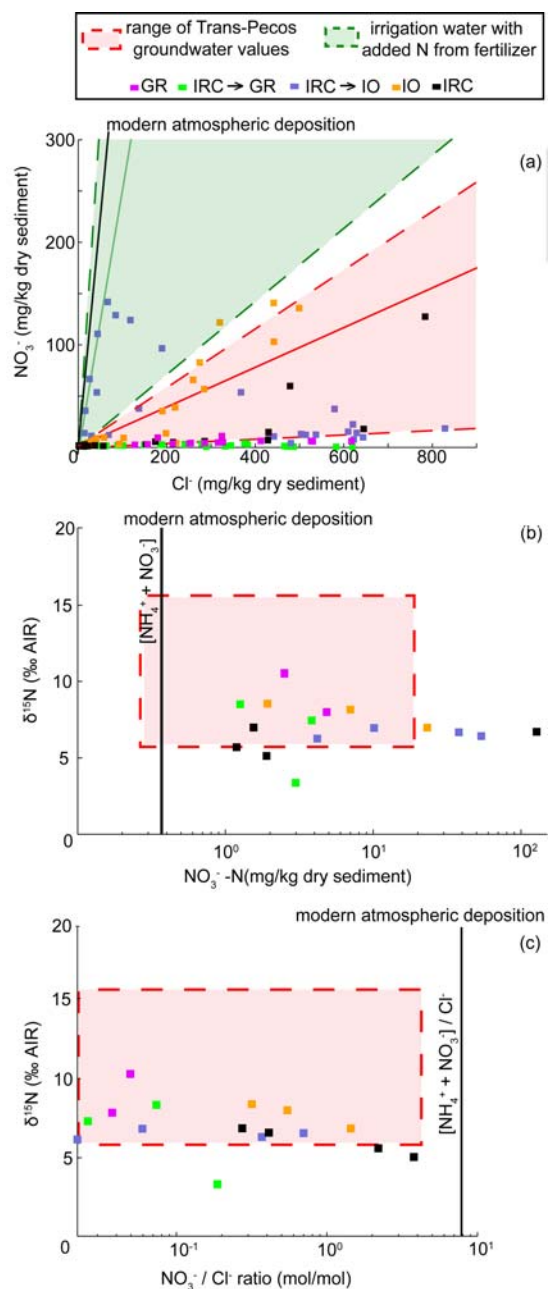


**Fig. 5.9** Plots of (a)  $\text{Cl}^-$  vs  $\text{NO}_3^-$  in pore water leachates with the ratio in modern atmospheric deposition (black line- NADP NTN sites at TX04 and TX22, accessed 2012), Trans-Pecos groundwater (red), and irrigation water with added fertilizer based on USDA agricultural census data of fertilizer application rates for cotton and pecans in Texas (USDA NASS accessed 2013) (green), (b)  $\text{NO}_3^-$  concentrations vs  $^{15}\text{N}$  in pore water leachates (dots) and Trans-Pecos groundwater (red), and (c)  $\text{NO}_3^- / \text{Cl}^-$  ratios vs  $^{15}\text{N}$  in pore water leachates (dots) and Trans-Pecos groundwater (red). Solid lines represent average values; dashed lines represent the range of the data.

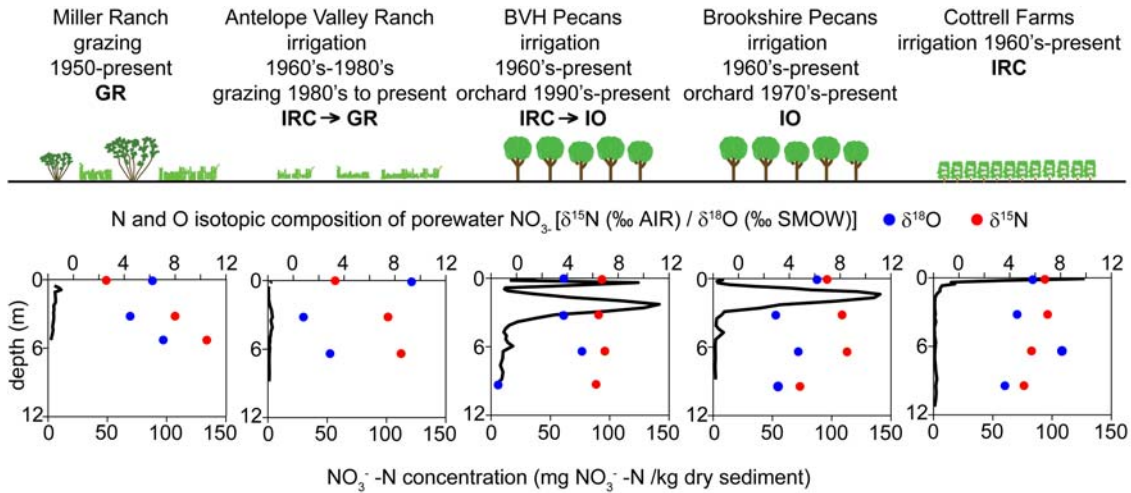


**Fig. 5.10** Profiles of  $\text{NO}_3^-$  concentration and isotopic composition ( $^{15}\text{N}$  and  $^{18}\text{O}$ ) of pore water  $\text{NO}_3^-$  beneath representative core samples from grazed land (GR), land with historic irrigated row crops and current grazing ( $\text{IRC} \rightarrow \text{GR}$ ), land with historic irrigated row crops and current irrigated orchard ( $\text{IRC} \rightarrow \text{IO}$ ), an irrigated orchard (IO), and irrigated row crops (IRC).

*Regional trends in vegetation cover and land use and the implications for the vadose zone and basin groundwater*

As mentioned in the site description, the Trans-Pecos basins have undergone substantial changes in land use and vegetation cover since the settlement of the area. First, human activities (in the form of intensive grazing, fire suppression and climate change) have shifted woody-herbaceous vegetation balances and allowed for shrub encroachment, increases in bare ground cover, and decreases in grass density; second, the rise (and subsequent fall) of irrigated agriculture has altered both vegetation type and density. Shifts such as those observed in the Trans-Pecos have the potential to alter ET demand, infiltration distribution and rates, and N input and uptake; based on analyses of vadose zone properties and long-term groundwater quality, these changes have measurable impacts on hydrological processes in the basins. Increases in groundwater  $\text{NO}_3^-$  concentrations are not evenly distributed in the basins (Robertson and Sharp 2012), neither is basin floor recharge (Robertson and Sharp 2013; Robertson and Sharp *in review*) (Fig. 5.2); the observed spatial distribution of net infiltration (and likely mobilization of  $\text{NO}_3^-$  and  $\text{Cl}^-$  accumulation) is highly dependent on the hydraulic

conductivity of the soils and unsaturated basin sediments and it is likely that the presence of sub-root zone  $\text{Cl}^-$  and  $\text{NO}_3^-$  accumulation is also spatially variable (Walvoord et al. 2003; Jackson et al. 2004; Scanlon et al. 2005). Acknowledging that intrinsic basin properties are driving some of the variability, the impacts of anthropogenic processes can still be examined:

- 1) On-going irrigated agriculture. Irrigation of row crops and orchards for the past 5 decades has replaced natural vegetation cover with plants and trees of non-native types; altering vegetation density, ET demand, and labile N demand. The addition of irrigation water and fertilizers compound these effects.
- 2) Historic irrigated agriculture and current intensive grazing. Past irrigation of row crops initially replaced natural vegetation cover and added water and N to system. Subsequent vegetation re-growth is distinct from both the historical accounts of natural vegetation (it is now less dense and shorter with an increase in bare ground) and the vegetation from grazed-only land. IRC  $\rightarrow$  GR land has less woody vegetation encroachment and less bare ground.
- 3) Ongoing intensive grazing. In combination with fire suppression activities and climatic shifts in the desert southwest, intensive cattle grazing has led to woody vegetation encroachment, decreases in grass density, and increases in bare ground cover.

Irrigated agriculture is generating significant recharge through irrigation return flow in impacted basins (Robertson and Sharp, *in review*). Beneath land with historic or ongoing irrigation, there is evidence for alteration of vadose zone properties including the absence of a hardpan caliche layer, partial or total flushing of long-term sub-root zone  $\text{NO}_3^-$  and  $\text{Cl}^-$  accumulation, increased moisture content, and (in some areas) presence of unassimilated fertilizer. However, not all of the increases in  $\text{NO}_3^-$  concentration can be attributed solely to irrigation return flow. At its greatest extent, irrigated agriculture covered ~20% of the basin floor in Wild Horse/Michigan Flats and Lobo/Ryan Flats; significant irrigated agriculture did not occur in either Eagle Flats or Red Light Draw

basins. Despite this,  $\text{NO}_3^-$  concentrations have increased in these basins and the isotopic composition of the  $\text{NO}_3^-$  in the basin groundwater is consistent with a soil N source. In grazed areas the decrease in grass density and increase in bare ground cover may lead to increased infiltration of water beneath the root zone, where it can mobilize salt and potentially become recharge. Estimates of net infiltration based on two vegetation scenarios (scenario 1 is reflective of the current vegetation regime, scenario 2 increases density of grasses to 50% cover and replaces scrubland (encroached areas) with grassland) show a marked difference in net infiltration on the basin floor (Fig. 5.11). Net infiltration (and potential recharge) decreases by as much as 48% (Robertson and Sharp, Chapter 4 of this document) when the vegetation regime on the basin floors is one of thick dense grasslands (e.g., Humphrey 1958) rather than of the current scrub/rangeland (McMahon et al. 1984; NASA Landsat program, accessed June 2012).

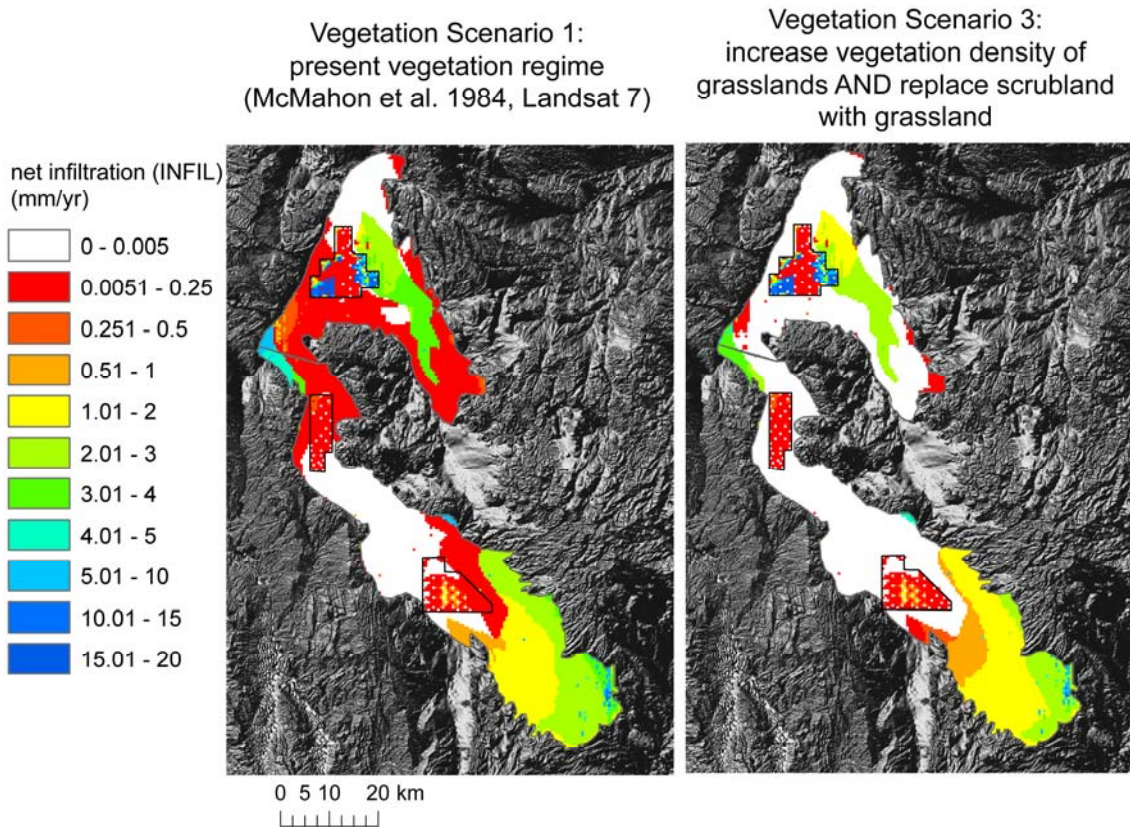


**Fig. 5.11** Comparison of net infiltration in the Wild Horse/Michigan Flats and Lobo/Ryan Flats basins with 2 vegetation regime scenarios.

While it is deemed unlikely that irrigated agricultural land use in the Trans-Pecos basins will again reach the levels observed in the 1960's and 70's, continued irrigation and fertilizer application will still contribute to increases in recharge (and possibly labile N in the form of un-cycled fertilizer) to basin groundwater. As native vegetation continues to respond to climatic shifts and grazing practices, it is likely that continued woody vegetation encroachment will lead to an increase in bare ground cover and result in increases in downward moisture and solute flux as well. The presence of thick unsaturated zones in the basins also complicates the observed changes and prediction of future conditions. Long travel times through the vadose zone make it unclear if increases to groundwater  $\text{NO}_3^-$  concentrations have peaked or will continue to increase for years to come in response to the land use changes that occurred in the past. Because of the spatial

and temporal variability of net infiltration (potential recharge) in this system, prediction of future groundwater quality is extremely difficult and even immediate changes to land use practices may not prevent continued deterioration of basin groundwater quality because the response time of the system is dependent on vadose zone travel times.

That land use changes can be linked to regional groundwater quality in arid systems with thick unsaturated zones is noteworthy for its implications on water quality and sustainability in these types of systems. Irrigated agriculture and, potentially, grazing practices (and other anthropogenic processes linked to woody vegetation encroachment) could be contributing to deterioration of groundwater quality. Increasing human populations in arid and semi-arid regions highlight the need to understand how land use changes impact groundwater quality before the impacts of anthropogenic processes are irreversible; long lag times between land use changes and observed effects mean that sustainable management of groundwater resources must consider processes on multi-decadal time scales.

#### **5.4 Conclusions**

In the Trans-Pecos basin aquifer system, changes to land use and vegetation on the basin floors has resulted in alterations of the vadose zone and regional groundwater quality. Irrigation for row crops and orchards has altered water content and salt inventories; partial to full flushing of  $\text{NO}_3^-$  and  $\text{Cl}^-$  from the vadose zone has occurred. The size of  $\text{NO}_3^-$  and  $\text{Cl}^-$  bulges in the vadose zone is spatially variable under natural conditions and the influence of human induced land use and vegetation changes will likely increase the heterogeneity of vadose zone salt inventories by altering moisture flux, labile N input, and demand for both water and nutrients. The source of  $\text{NO}_3^-$  to the basin aquifer system is likely the mobilization of soil N derived  $\text{NO}_3^-$  from the vadose zone;  $\text{NO}_3^-$  in the basin groundwater has an isotopic composition consistent with a soil N derived source and flushing of salts from the sub-root zone is evident in vadose zone core samples. The regional trends in  $\text{NO}_3^-$  concentration, combined with historic land use data and estimates of changes to net infiltration during pre-impact versus current vegetation regimes, indicate that both irrigated agriculture and over-grazing (combined with fire



suppression and climate change) have contributed to an increase in recharge and flux of labile N to the aquifer system.

This study has linked anthropogenic land use and vegetation shifts to changes in the vadose zone and in regional groundwater quality in arid environments with thick unsaturated zones. A combination of over-grazing, fire suppression, climate change, and irrigated agriculture has resulted in increases in both solute and moisture flux from the basin floors to the underlying unconfined aquifer system. Over-grazing, fire suppression, and climate change have led to woody vegetation encroachment and increases in bare-ground cover which has altered the amount and spatial distribution of infiltration, potentially mobilizing  $\text{NO}_3^-$  and  $\text{Cl}^-$  previously sequestered beneath the root zone of native vegetation. Irrigated agricultural practices have drastically changed the system by replacing native vegetation with cultivated crops, adding fertilizer amendments, and using basin groundwater for irrigation. This has enhanced infiltration beneath impacted lands, mobilized  $\text{NO}_3^-$  and  $\text{Cl}^-$ , and added labile N to the system. As a result of thick unsaturated zones and long transit times, the impacts of land use changes from several decades ago on the underlying groundwater may still be forthcoming; it is unclear if increases in groundwater  $\text{NO}_3^-$  concentration will continue or if they may stabilize in the coming years. This poses significant challenges for groundwater sustainability and for the development and implementation of management policies. The processes that have been documented in Trans-Pecos TX may be impacting groundwater in arid and semi-arid regions worldwide; further research is needed in order to predict how these systems will respond to increased stressors from population growth and climate change.

## Chapter 6: Summary

This dissertation utilized field observations and computational modeling simulations to examine recharge processes and solute flux in arid basin aquifer systems of the Trans-Pecos region of Texas, U.S.A. Both natural processes and the impacts of anthropogenic land use and vegetation change were studied. Links were made from surface processes on the basin floors to widespread changes in groundwater quality. Trends in basin groundwater  $\text{NO}_3^-$  over time were linked to land use and vegetation changes in the basins and to physical processes on the basin floors allowing recharge to occur where it had previously been assumed to be negligible. Model simulations of net infiltration were used to estimate the magnitude and spatial distribution of recharge within the basins, to estimate the impact of irrigation return flow, and to examine the impact of vegetation change on net infiltration between pre-western settlement and current vegetation regimes. A study of vadose zone properties provided insight into the impacts of land use and vegetation changes on moisture content,  $\text{Cl}^-$  and  $\text{NO}_3^-$  accumulation, and nitrogen cycling as well as providing additional evidence for the linkages between basin floor land use/vegetation changes and the underlying groundwater system. Conclusions from the research are as follows:

- 1) There is modern recharge to the arid basins.
- 2) Natural recharge mechanisms include mountain front/mountain block sources, discrete basin floor sources (i.e., dry washes), and widespread recharge on the basin floors from direct precipitation.
- 3) Recharge to the basins is temporally and spatially variable.
- 4) Anthropogenic recharge is occurring in the form of irrigation return flow in basins with irrigated agricultural land use.
- 5) One possible cause of increased modern recharge beneath non-irrigated land is changes in vegetation type and density; grazing and climate change are leading to woody vegetation encroachment into the basins and decreasing grass cover. Bare ground between shrubs is now able to transport water (and solute) to the water table.

- 6) Anthropogenic driven land use and vegetation change has resulted in changes to the physical and chemical properties of the basin floor vadose zone in impacted areas. Prolonged irrigation has lead to solute displacement (and in some cases flushing) and increased moisture flux beneath the root zone which translates to increased potential recharge. Grazing *may* have also resulted in solute displacement; in comparison to previous studies the salt inventories beneath grazed land are less than un-impacted land. The hardpan caliche layer present in un-irrigated basin soils is absent in the cores collected beneath land with any history of irrigation. This indicates that human-induced changes to the basin floors extend beyond water quality; it is potentially changing the hydrologic properties of the vadose zone in some areas.
- 7) The isotopic composition of pore water  $\text{NO}_3^-$  in the vadose zone is consistent with a soil N source.
- 8) The isotopic composition of groundwater  $\text{NO}_3^-$  is also consistent with a soil N source. This consistency indicates that mobilization of soil N from the basin floor vadose zone is the source of  $\text{Nr}$  in the groundwater (because of the limited development of soil horizons in the mountains, there is not sufficient soil  $\text{Nr}$  to be the main contributor).
- 9) Basin groundwater quality may continue to be at risk in the future; due to the thick unsaturated zones in the basins, it is not clear if the trend of increasing  $\text{NO}_3^-$  concentrations has peaked or if the bulk of mobilized  $\text{Nr}$  from the vadose zone has yet to reach the groundwater.

When combined, the observations of groundwater chemistry, vadose zone properties, and computational models of net infiltration draw a picture of surface processes on the basin floors connected to groundwater quantity and quality, despite the presence of thick unsaturated zones within the basins. This statement has significant and broad-reaching implications. For the Trans-Pecos basin aquifers, it means that sustainability planning for this resource must take into consideration both the additional

water input and the added risk to long-term water quality. Looking beyond this case study, it means that the governing assumptions behind the ‘classic’ model of recharge in arid basin systems must be re-examined in light of this research. The processes occurring in the Trans-Pecos basins are not unique to this system; they are likely to occur in similar settings around the world (including in the Western U.S., Australia, China, and others). In order to improve scientific understanding and sustainable management of groundwater resources in arid and semi-arid regions, anthropogenic impacts and the potential for modern recharge should not be discounted in studies moving forward.

**Appendix A:** Additional figures on groundwater  $\text{NO}_3^-$  concentrations and land use in the Trans-Pecos region not included in the publications (chapters 2-5)

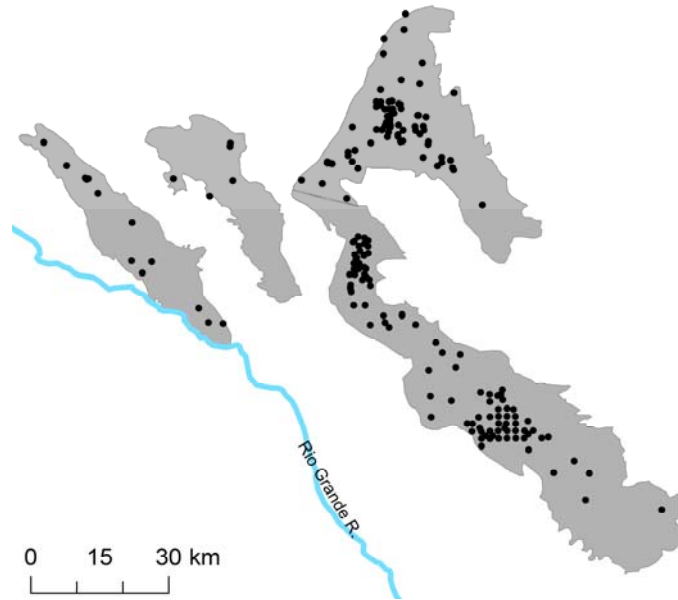


**Fig. A.1** Locations of TWDB wells with historical water quality data (including  $\text{NO}_3^-$ ) in the four basins of interest, Trans-Pecos, Texas, U.S.A.

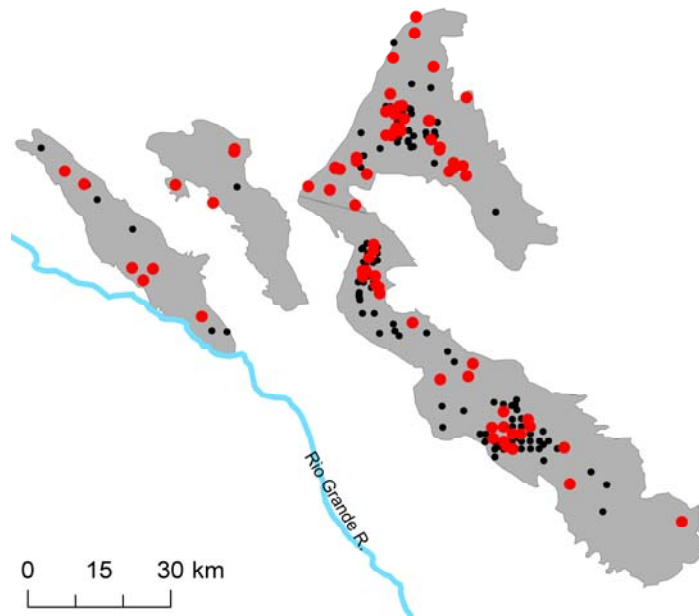


**Fig. A.2** Wells in the Trans-Pecos basin aquifers with 'elevated' (>140  $\mu\text{mol/l}$ )  $\text{NO}_3^-$  concentrations in red (based on TWDB historic water quality data). 'Elevated'  $\text{NO}_3^-$  concentrations are in comparison to U.S. average groundwater concentrations (Mueller and Helsel 2002).

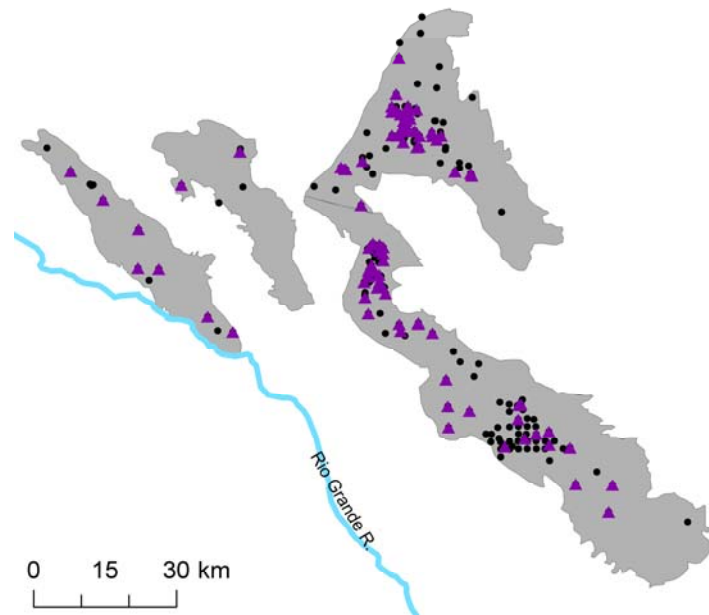


**Fig. A.3** Wells in the Trans-Pecos basin aquifers that demonstrated a trend in  $\text{NO}_3^-$  concentration over time in purple (based on TWDB historic water quality data). Trend is defined as having a change of greater than 1 mg/l (as  $\text{NO}_3^-$ ) between one or more sampling dates (from 1940's to 2001). Wells in black either showed no trend in  $\text{NO}_3^-$  or only had one water quality value reported between 1940 and 2000.

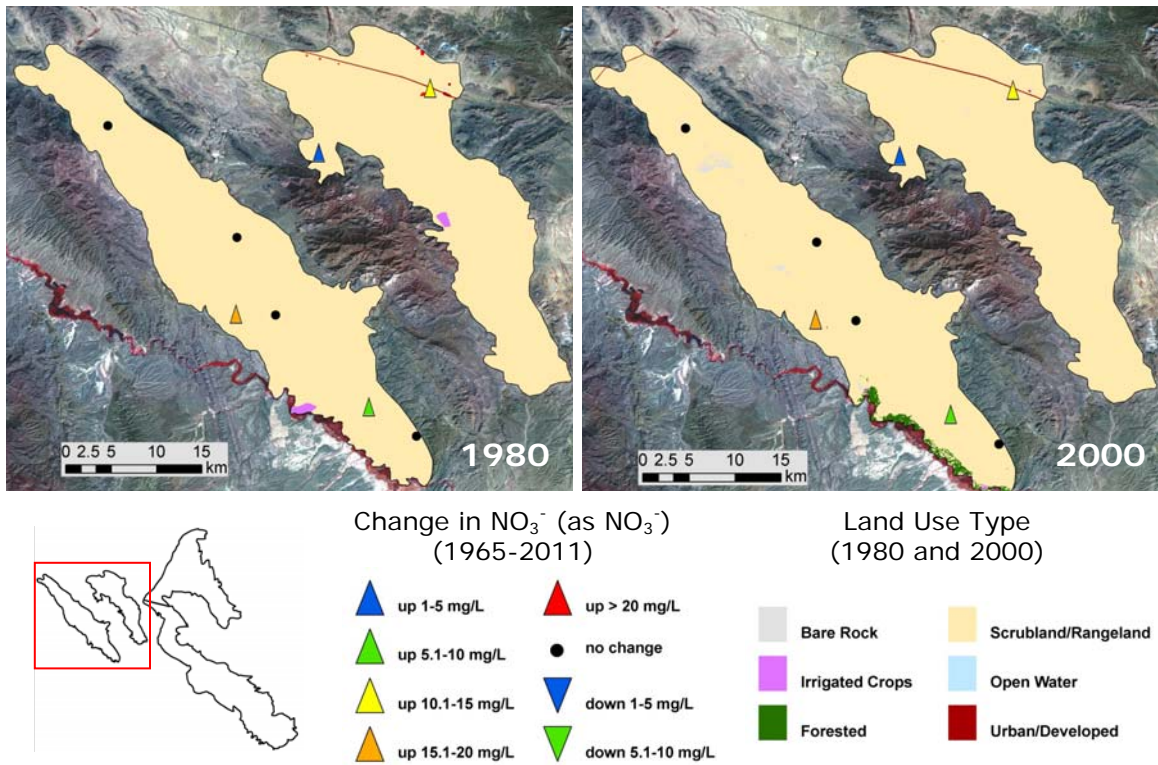


**Fig. A.4** Patterns of land use change from 1980-2000 (based on the International Satellite Land Surface Climatology (ISLSCP) Initiative (1980's) and the National Land Cover Dataset (2001)) and trends in groundwater  $\text{NO}_3^-$  concentration (1965-2011) in wells of the Red Light Draw and Eagle Flats basins.

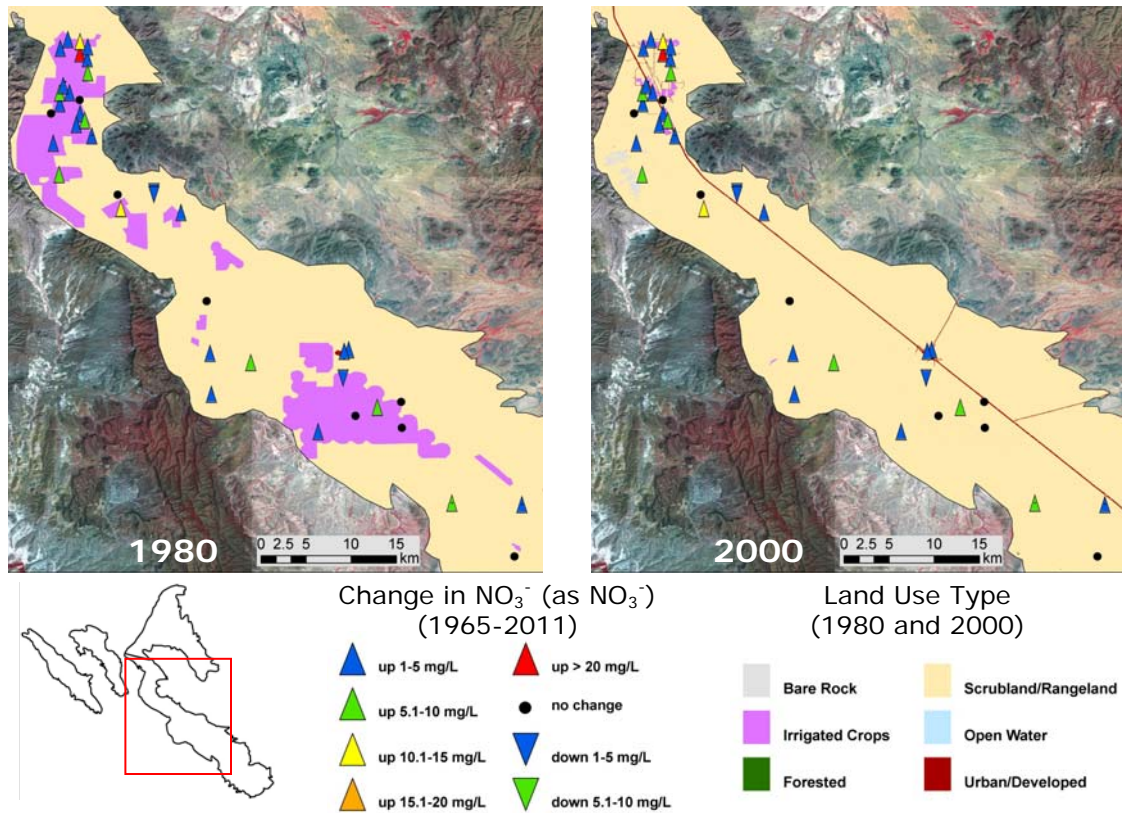


**Fig. A.5** Patterns of land use change from 1980-2000 (based on the International Satellite Land Surface Climatology (ISLSCP) Initiative (1980's) and the National Land Cover Dataset (2001)) and trends in groundwater  $\text{NO}_3^-$  concentration (1965-2011) in wells of Lobo and Ryan Flats.



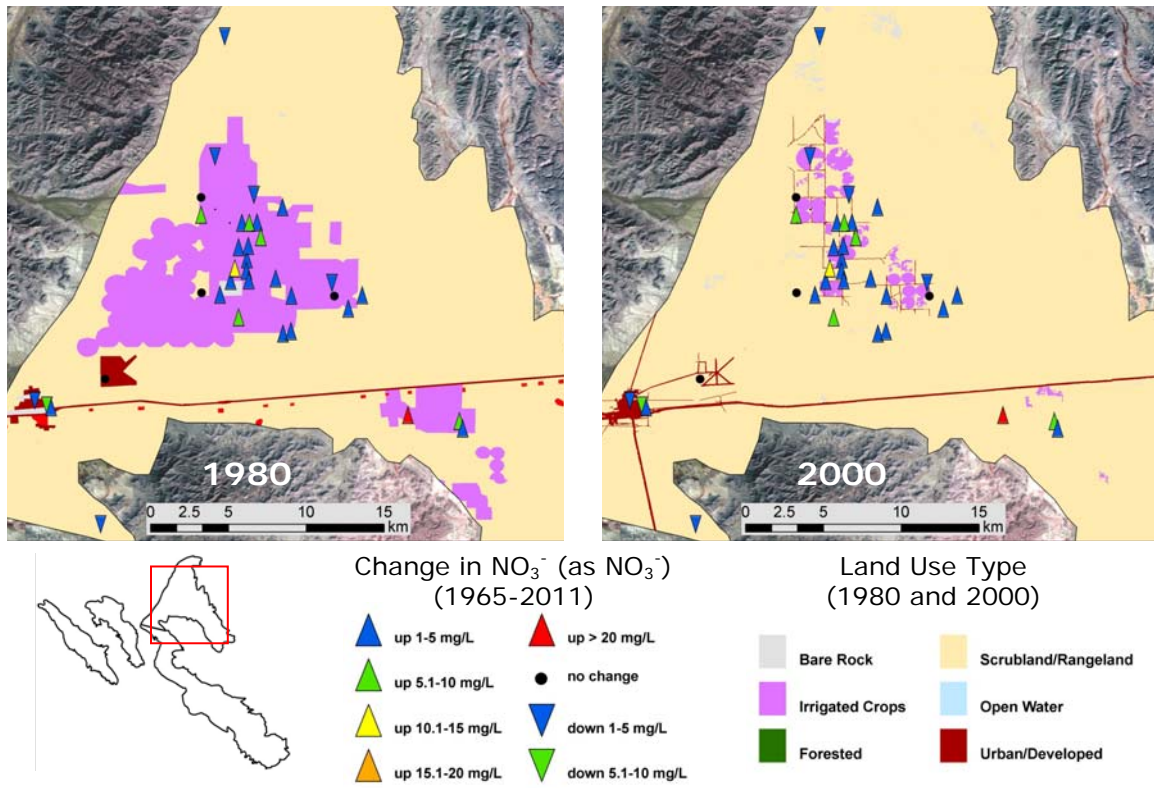


**Fig. A.6** Patterns of land use change from 1980-2000 (based on the International Satellite Land Surface Climatology (ISLSCP) Initiative (1980's) and the National Land Cover Dataset (2001)) and trends in groundwater NO<sub>3</sub><sup>-</sup> concentration (1965-2011) in wells of Wild Horse and Michigan Flats.

## Appendix B: Raw CFC data and modeled CFC values

Sample ID	Basin name	TX Well ID	total well depth (m)	depth to water (m)	screened interval (m)	Water Concentration (pmol/kg)				
						CFC-11	CFC-12	CFC-113		
Easley A	Lobo/Ryan	5110326	122	60.9	91 m of slotted casing- interval unknown	0.277	0.285	0.016	error	0.010
Easley B						0.248	0.280	0.016		0.010
Easley C						0.168	0.286	0.014		0.010
Miller A	Lobo/Ryan	5119902	43.25	33.6	screened interval unknown	1.867	1.101	0.000	error	0.010
Miller C						1.665	1.089	0.000		0.010
Miller E						1.759	1.078	0.141		0.010
Brookshier A	Wild Horse	4759104	201.2	67.1	140.2 to 201.2	0.063	0.008	0.002	error	0.010
Brookshier B						0.054	0.005	0.002		0.010
Brookshier C						0.062	0.100	0.003		0.010
Cottrell A	Wild Horse	4751701	289.5	61.2	92.0 to 289.5	0.051	0.005	0.002	error	0.010
Cottrell B						0.081	0.009	0.001		0.010
Booth A	Eagle Flats	4864604	67	49.9	screened interval unknown	0.813	0.889	0.069	error	0.010
Booth C						0.912	0.943	0.076		0.010

**Table B.1** Well information, raw CFC concentrations (in water), modeled atmospheric CFC concentrations, and apparent groundwater ages based on CFC data.

Sample ID	Equivalent Atmospheric Concentration (pmol/mol)			Apparent Recharge Age (years before sampling date)		
	CFC-11 error	CFC-12 error	CFC-113 error	CFC-11 error	CFC-12 error	CFC-113 error
Easley A	26.8	100.1	5.2	46	43	40
Easley B	24.0	98.4	5.2	47	43	40
Easley C	16.2	100.4	4.8	49	43	41
Miller A	180.5	386.8	46.5	30	27	26
Miller C	160.9	382.5	47.2	33	27	25
Miller E	170.0	378.8	46.7	32	28	26
Brookshier A	6.1	2.7	0.5	55	65	48
Brookshier B	5.2	1.9	0.5	55	66	48
Brookshier C	6.0	3.4	1.1	55	64	46
Cottrell A	4.9	1.9	0.7	53	66	47
Cottrell B	7.8	3.1	0.3	53	64	49
Booth A	78.6	312.4	23.0	40	32	31
Booth C	89.8	337.4	25.6	38	30	30

**Table B.1** continued.

**Appendix C:** Estimates of labile N (from soil N, atmospheric deposition, and synthetic fertilizer application) and the resultant groundwater NO<sub>3</sub><sup>-</sup> concentrations based on 130 years (1880-2010) of INFIL modeled potential recharge in Wild Horse / Michigan Flats and Lobo / Ryan Flats basins. These estimates do not account for any potential loss of labile N (either from uptake/assimilation or from denitrification processes).

	<b>Soil N reservoir</b> (NO <sub>3</sub> <sup>-</sup> as N (kg/ha)) (Walvoord 2002)	<b>Atmospheric deposition per year</b> (NH <sub>4</sub> <sup>+</sup> + NO <sub>3</sub> <sup>-</sup> as N (kg/ha)) (NADP NTN accessed 2012)	<b>Synthetic fertilizer application per year</b> (as N (kg/ha)) (USDA NASS, accessed 2013)
min	120	1.046	91.9
max	910	1.706	147.9
		<i>Sum of atmospheric deposition (1880-2010)</i>	<i>Sum of synthetic fertilizer application (1950-2010)</i>
	min	136	5514
	max	222	8874

**Table C.1** Three major sources of labile N in the Trans-Pecos basins.

Basin	Soil N (kg as N)	Atmospheric deposition (kg as N)	Irrigated agricultural land use on basin floor (%)	Synthetic fertilizer (kg as N)
Lobo / Ryan Flats basin floor area: ( $1.46 \times 10^5$ ha)	min	$1.98 \times 10^7$	5% of basin floor used for irrigated agriculture	min
	max	$3.24 \times 10^7$		max
Wild Horse / Michigan Flats basin floor area: ( $9.2 \times 10^4$ ha)	min	$1.25 \times 10^7$	20% of basin floor used for irrigated agriculture	min
	max	$2.04 \times 10^7$		max

**Table C.2** Mass of labile N (from the sources outlined in Table C.1) within Wild Horse / Michigan Flats and Lobo/Ryan Flats basins.

Basin	Total mass of N (kg) with synthetic fertilizer included	Total mass of N (kg) with no synthetic fertilizer application
Lobo / Ryan Flats	min	$3.73 \times 10^7$
	max	$1.65 \times 10^8$
Wild Horse / Michigan Flats	min	$2.35 \times 10^7$
	max	$1.04 \times 10^8$

**Table C.3** Total mass of labile N in Wild Horse / Michigan Flats and Lobo / Ryan Flats basins (sum of labile N from Table C.2).

<b>Estimated recharge (based on INFIL simulations (1880-2010))</b>			
<b>Basin</b>	<b>Vegetation regime</b>	<b>m<sup>3</sup></b>	<b>liters</b>
Lobo / Ryan Flats	natural vegetation (pre-western settlement)	$1.09 \times 10^9$	$1.09 \times 10^{12}$
	natural vegetation (current)	$1.64 \times 10^9$	$1.64 \times 10^{12}$
	natural vegetation (current) + 25 years of irrigation return flow	$1.67 \times 10^9$	$1.67 \times 10^{12}$
	natural vegetation (current) + 40 years of irrigation return flow	$1.71 \times 10^9$	$1.71 \times 10^{12}$
Wild Horse / Michigan Flats	natural vegetation (pre-western settlement)	$9.58 \times 10^8$	$9.58 \times 10^{11}$
	natural vegetation (current)	$1.34 \times 10^9$	$1.34 \times 10^{12}$
	natural vegetation (current) + 25 years of irrigation return flow	$1.37 \times 10^9$	$1.37 \times 10^{12}$
	natural vegetation (current) + 40 years of irrigation return flow	$1.40 \times 10^9$	$1.40 \times 10^{12}$

**Table C.4** Estimates of total volume of recharge to Lobo / Ryan Flats and Wild Horse / Michigan Flats basins from 1880-2010 under different modeled vegetation regimes.

Basin	Vegetation regime	min mg/l (as NO <sub>3</sub> <sup>-</sup> ) including fertilizer	max mg/l (as NO <sub>3</sub> <sup>-</sup> ) including fertilizer	min mg/l (as NO <sub>3</sub> <sup>-</sup> ) no fertilizer	max mg/l (as NO <sub>3</sub> <sup>-</sup> ) no fertilizer
Lobo / Ryan Flats	natural vegetation (pre-western settlement)	361.7	2136.3	95.6	670.2
	natural vegetation (current)	240.4	1419.7	63.3	445.3
	natural vegetation (current) + 25 years of irrigation return flow	236.4	1394.4	62.4	437.4
	natural vegetation (current) + 40 years of irrigation return flow	230.6	1361.7	60.6	427.2
Wild Horse / Michigan Flats	natural vegetation (pre-western settlement)	411.7	2430.7	108.5	762.3
	natural vegetation (current)	294.4	1737.5	77.5	544.9
	natural vegetation (current) + 25 years of irrigation return flow	288.2	1699.4	76.1	533.0
	natural vegetation (current) + 40 years of irrigation return flow	281.5	1663.1	74.4	521.9

**Table C.5** Estimates for basin groundwater NO<sub>3</sub><sup>-</sup> concentrations (assuming no loss/assimilation) based on labile N sources listed in Table C.1 and recharge rates based on INFIL model simulations (Table C.4). Median NO<sub>3</sub><sup>-</sup> concentration of groundwater in Lobo / Ryan Flats and Wild Horse / Michigan Flats basins are 7.8 mg/l and 8.8 mg/l (as NO<sub>3</sub><sup>-</sup>), respectively based on the summer 2011 synoptic survey results (Robertson and Sharp 2012).

## References

- Adams, H.D., Luce, C.H., Breshears, D.D., Allen, C.D., Weiler, M., Hale, V.C., Smith, A.M.S., and Huxman, T.E., 2012, Ecohydrological consequences of drought- and infestation- triggered tree die-off: insights and hypotheses: *Ecohydrology*, v. 5, p. 145–159, doi: 10.1002/eco.233.
- Adar, E.M., and Neuman, S.P., 1988, Estimation of spatial recharge distribution using environmental isotopes and hydrochemical data, II. Application to Aravaipa Valley in Southern Arizona, U.S.A.: *Journal of Hydrology*, v. 97, p. 279–302, doi: 10.1016/0022-1694(88)90120-5.
- Alcalá, F.J., and Custodio, E., 2008, Using the Cl/Br ratio as a tracer to identify the origin of salinity in aquifers in Spain and Portugal: *Journal of Hydrology*, v. 359, p. 189–207, doi: 10.1016/j.jhydrol.2008.06.028.
- Amundson, R., Austin, A.T., Schuur, E. a. G., Yoo, K., Matzek, V., Kendall, C., Uebersax, A., Brenner, D., and Baisden, W.T., 2003, Global patterns of the isotopic composition of soil and plant nitrogen: *Global Biogeochemical Cycles*, v. 17, p. n/a–n/a, doi: 10.1029/2002GB001903.
- Aravena, R., and Robertson, W.D., 1998, Use of Multiple Isotope Tracers to Evaluate Denitrification in Ground Water: Study of Nitrate from a Large-Flux Septic System Plume: *Ground Water*, v. 36, p. 975–982, doi: 10.1111/j.1745-6584.1998.tb02104.x.
- Archer, S., 1994, Woody plant encroachment into southwestern grasslands and savannas: rates, patterns and proximate causes., *in* *Society for Range Management.*, p. 13–68.
- Ares, J., 1976, Dynamics of the Root System of Blue Grama: *Journal of Range Management*, v. 29, p. 208–213, doi: 10.2307/3897277.
- Aulakh, M.S., Doran, J.W., and Mosier, A.R., 1992, Soil Denitrification—Significance, Measurement, and Effects of Management, *in* Stewart, B.A. ed., *Advances in Soil Science*, *Advances in Soil Science* 18, Springer New York, p. 1–57.
- Barnes, V.E., 1983, *Geologic Atlas of Texas- Van Horn/El Paso Sheet*: Bureau of Economic Geology.
- Barnes, V.E., 1979, *Geologic Atlas of Texas-Marfa Sheet*: Bureau of Economic Geology.



- Beach, J.A., Ashworth, J.B., Finch, S.T., Chastain-Howley, A., Calhoun, K., Urbanczyk, K.M., Sharp Jr., J.M., and Olson, J., 2004, Groundwater availability model for the igneous aquifer and parts of the West Texas Bolsons (Wild Horse Flat, Michigan Flat, Ryan Flat, and Lobo Flat) aquifer: Texas Water Development Board, 407 p.
- Beach, J.A., Symank, L., Huang, Y., Ashworth, J.B., Davidson, T., Collins, E.W., Hibbs, B.J., Darling, B.K., Urbanczyk, K.M., Calhoun, K., and Finch, S.T., 2008, Groundwater availability model for the West Texas Bolsons (Red Light Draw, Green River Valley, and Eagle Flat) aquifer in Texas: Texas Water Development Board, 320 p.
- Beare, S., and Heaney, A., 2001, Irrigation, water quality, and water rights in the Murray Darling Basin, Australia, *in* Girona, Spain, Australia Bureau of Agricultural and Resource Economics, p. Conference paper 2001.15 17 pgs.
- Becker, V.J., and Manuel, O.K., 1972, Chlorine, bromine, iodine, and uranium in tektites, obsidians, and impact glasses: *Journal of Geophysical Research*, v. 77, p. 6353–6359, doi: 10.1029/JB077i032p06353.
- Bellot, J., Sanchez, J.R., Chirino, E., Hernandez, N., Abdelli, F., and Martinez, J.M., 1999, Effect of different vegetation type cover on the soil water balance in semi-arid areas of South Eastern Spain: *Physics and Chemistry of the Earth, Part B: Hydrology, Oceans and Atmosphere*, v. 24, p. 353–357, doi: 10.1016/S1464-1909(99)00013-1.
- Belnap, J., 2002, Nitrogen fixation in biological soil crusts from southeast Utah, USA: *Biology and Fertility of Soils*, v. 35, p. 128–135, doi: 10.1007/s00374-002-0452-x.
- Bennett, J., 2006, Salinity and source of nutrients in the Rio Grande/Rio Bravo between Presidio and Amistad Reservoir. Report for the International Boundary and Water Commission.
- Böhlke, J.K., Wanty, R., Tuttle, M., Delin, G., and Landon, M., 2002, Denitrification in the recharge area and discharge area of a transient agricultural nitrate plume in a glacial outwash sand aquifer, Minnesota: *Water Resources Research*, v. 38, p. 10–1–10–26, doi: 10.1029/2001WR000663.
- Böttcher, J., Strebel, O., Voerkelius, S., and Schmidt, H.-L., 1990, Using isotope fractionation of nitrate-nitrogen and nitrate-oxygen for evaluation of microbial denitrification in a sandy aquifer: *Journal of Hydrology*, v. 114, p. 413–424, doi: 10.1016/0022-1694(90)90068-9.

- Breshears, D.D., Cobb, N.S., Rich, P.M., Price, K.P., Allen, C.D., Balice, R.G., Romme, W.H., Kastens, J.H., Floyd, M.L., Belnap, J., Anderson, J.J., Myers, O.B., and Meyer, C.W., 2005, Regional vegetation die-off in response to global-change-type drought: *Proceedings of the National Academy of Sciences of the United States of America*, v. 102, p. 15144–15148, doi: 10.1073/pnas.0505734102.
- Briones, O., Montaña, C., and Ezcurra, E., 1996, Competition between three Chihuahuan desert species: evidence from plant size-distance relations and root distribution: *Journal of Vegetation Science*, v. 7, p. 453–460, doi: 10.2307/3236289.
- Brown, A.E., Zhang, L., McMahon, T.A., Western, A.W., and Vertessy, R.A., 2005, A review of paired catchment studies for determining changes in water yield resulting from alterations in vegetation: *Journal of Hydrology*, v. 310, p. 28–61, doi: 10.1016/j.jhydrol.2004.12.010.
- De Bruin, H.A.R., 1988, Evaporation in Arid and Semi-Arid Regions, *in* Simmers, I. ed., *Estimation of Natural Groundwater Recharge*, Dordrecht, Springer Netherlands, p. 73–88.
- Bu, X., and Warner, M.J., 1995, Solubility of chlorofluorocarbon 113 in water and seawater: *Deep Sea Research Part I: Oceanographic Research Papers*, v. 42, p. 1151–1161, doi: 10.1016/0967-0637(95)00052-8.
- Buffington, L.C., and Herbel, C.H., 1965, Vegetation changes on a semidesert grassland range from 1858 to 1963., *in* *Ecological Monographs*, 35, p. 139–164.
- Bullister, J.L., Wisegarver, D.P., and Menzia, F.A., 2002, The solubility of sulfur hexafluoride in water and seawater: *Deep Sea Research Part I: Oceanographic Research Papers*, v. 49, p. 175–187, doi: 10.1016/S0967-0637(01)00051-6.
- Casciotti, K.L., Sigman, D.M., Hastings, M.G., Böhlke, J.K., and Hilkert, A., 2002, Measurement of the Oxygen Isotopic Composition of Nitrate in Seawater and Freshwater Using the Denitrifier Method: *Analytical Chemistry*, v. 74, p. 4905–4912, doi: 10.1021/ac020113w.
- Causapé, J., Quílez, D., and Aragüés, R., 2004, Assessment of irrigation and environmental quality at the hydrological basin level: II. Salt and nitrate loads in irrigation return flows: *Agricultural Water Management*, v. 70, p. 211–228, doi: 10.1016/j.agwat.2004.06.006.

- Christensen, A.H., Rewis, D.L., Hevesi, J.A., Matti, J., Martin, P., and Nishikawa, T., 2006, *Geology, Ground-Water Hydrology, Geochemistry, and Ground-Water Simulation of the Beaumont and Banning Storage Units, San Geronio Pass Area, Riverside County, California*: U.S. Geological Survey Scientific Investigations Report 2006-5026, 191 p.
- Cleveland, C.C., Townsend, A.R., Schimel, D.S., Fisher, H., Howarth, R.W., Hedin, L.O., Perakis, S.S., Latty, E.F., Von Fischer, J.C., Elseroad, A., and Wasson, M.F., 1999, Global patterns of terrestrial biological nitrogen (N<sub>2</sub>) fixation in natural ecosystems: *Global Biogeochemical Cycles*, v. 13, p. 623–645, doi: 10.1029/1999GB900014.
- Covington, W.W., and Sackett, S.S., 1986, Effect of Periodic Burning on Soil Nitrogen Concentrations in Ponderosa Pine: *Soil Science Society of America Journal*, v. 50, p. 452–457, doi: 10.2136/sssaj1986.03615995005000020040x.
- Custodio, E., 2007, Groundwater in volcanic hard rocks, *in* Krasny, J. and Sharp Jr., J.M. eds., *Selected Papers from the Groundwater in Fractured Rocks International Conference*, International Association of Hydrogeologists Selected Papers, Prague, 2003, Taylor and Francis, London.
- Darling, B.K., 1997, Delineation of the ground-water flow systems of the Eagle Flat and Red Light Basins of the Trans-Pecos Texas: The University of Texas at Austin, 179 p.
- Darling, B.K., Hibbs, B.J., and Dutton, A.R., 1994, Ground-water hydrology and hydrochemistry of Eagle Flat and surrounding area. Contract report prepared for Texas Low-Level Radioactive Waste Disposal Authority under Interagency Contract IAC(92-93)-0910: The University of Texas at Austin, Bureau of Economic Geology, 137 p.
- Darling, B.K., Hibbs, B.J., Dutton, A.R., and Sharp Jr., J.M., 1995, Isotope hydrology of the Eagle Mountains area, Hudspeth County, Texas: implications for development of ground-water resources, *in* Denver, CO, American Institute of Hydrology, p. SL-12 to SL-23.
- Darling, B.K., Hibbs, B.J., and Sharp Jr., J.M., 1998, Environmental isotopes as indicators of the residence time of ground waters in the Eagle Flat and Red Light Draw Basins of Trans-Pecos, Texas, *in* 98-15, West Texas Geological Society, p. 259–270.
- Davis, S.N., Whittemore, D.O., and Fabryka-Martin, J., 1998, Uses of Chloride/Bromide Ratios in Studies of Potable Water: *Ground Water*, v. 36, p. 338–350, doi: 10.1111/j.1745-6584.1998.tb01099.x.

- Densmore, J.N., and Böhlke, J.K., 1998, Use of nitrogen isotopes to determine sources of nitrate contamination in two desert basins in California, *in* IAHS-AISH publication, International Association of Hydrological Sciences, p. 63–73.
- Derby, N.E., Casey, F.X.M., and Knighton, R.E., 2009, Long-Term Observations of Vadose Zone and Groundwater Nitrate Concentrations under Irrigated Agriculture: *Vadose Zone Journal*, v. 8, p. 290–300, doi: 10.2136/vzj2007.0162.
- Dingman, S.L., 2008, *Physical hydrology*: Long Grove, IL, Waveland Press Inc.
- Domenico, P.A., and Schwartz, F.W., 1998, *Physical and chemical hydrogeology*: New York, Wiley.
- Durka, W., Schulze, E.-D., Gebauer, G., and Voerkeliust, S., 1994, Effects of forest decline on uptake and leaching of deposited nitrate determined from  $^{15}\text{N}$  and  $^{18}\text{O}$  measurements: *Nature*, v. 372, p. 765–767, doi: 10.1038/372765a0.
- Ellis, S.R., Levings, G.W., Carter, L.F., Richey, S.F., and Radell, M.J., 1993, Rio Grande Valley, Colorado, New Mexico, and Texas1: *JAWRA Journal of the American Water Resources Association*, v. 29, p. 617–646, doi: 10.1111/j.1752-1688.1993.tb03230.x.
- Evans, R.D., and Belnap, J., 1999, Long-term consequences of disturbance on nitrogen dynamics in an arid ecosystem: *Ecology*, v. 80, p. 150–160, doi: 10.1890/0012-9658(1999)080[0150:LTCODO]2.0.CO;2.
- Finch, S.T., and Armour, J., 2001, *Hydrogeologic analysis and groundwater flow model of the Wild Horse Flat Area, Culberson County, Texas*. Consultant's report prepared by Shomaker and Associates, for Beldon Foundation and Culberson County Groundwater Conservation District:, 37 p.
- Fitzgerald, P.D., and Rickard, D.S., 1960, A comparison of penman's and thornwaite's method of determining soil moisture deficits: *New Zealand Journal of Agricultural Research*, v. 3, p. 106–112, doi: 10.1080/00288233.1960.10419864.
- Flint, A.L., and Childs, S.W., 1987, Calculation of solar radiation in mountainous terrain: *Agricultural and Forest Meteorology*, v. 40, p. 233–249, doi: 10.1016/0168-1923(87)90061-X.
- Flint, A.L., Flint, L.E., Hevesi, J.A., and Blainey, J.B., 2004, Fundamental concepts of recharge in the desert southwest: A regional modeling perspective, *in* Hogan, J.F., Phillips, F.M., and Scanlon, B.R. eds., *Water Science and Application*, Washington, D. C., American Geophysical Union, p. 159–184.

- Flint, A.L., Flint, L.E., Hevesi, J.A., D'Agnese, F., and Faunt, C., 2000, Estimation of Regional Recharge and Travel Time Through the Unsaturated Zone in Arid Climates, *in* Faybishenko, B., Witherspoon, P.A., and Benson, S.M. eds., *Dynamics of Fluids in Fractured Rock*, American Geophysical Union, p. 115–128.
- Flint, A.L., Flint, L.E., Kwicklis, E.M., Fabryka-Martin, J.T., and Bodvarsson, G.S., 2002, Estimating recharge at Yucca Mountain, Nevada, USA: comparison of methods: *Hydrogeology Journal*, v. 10, p. 180–204, doi: 10.1007/s10040-001-0169-1.
- Frankl, R., and Schmeidl, H., 2000, Vegetation change in a south German raised bog: ecosystem engineering by plant species, vegetation switch or ecosystem level feedback mechanisms?: *Flora (Jena)*, v. 195, p. 267–276.
- Freeze, R.A., and Cherry, J.A., 1979, *Groundwater*: Englewood Cliffs, N.J., Prentice-Hall.
- Fry, J.A., Xian, G., Jin, S., Dewitz, J., Homer, C., Yang, L., Barnes, C., Herold, N., and Wickham, J., 2011, Completion of the 2006 National Land Cover Database for the Conterminous United States: *Photogrammetric Engineering and Remote Sensing*, v. 77, p. 858–866.
- Fukada, T., Hiscock, K.M., Dennis, P.F., and Grischek, T., 2003, A dual isotope approach to identify denitrification in groundwater at a river-bank infiltration site: *Water Research*, v. 37, p. 3070–3078, doi: 10.1016/S0043-1354(03)00176-3.
- Galloway, J.N., Dentener, F.J., Capone, D.G., Boyer, E.W., Howarth, R.W., Seitzinger, S.P., Asner, G.P., Cleveland, C.C., Green, P.A., Holland, E.A., Karl, D.M., Michaels, A.F., Porter, J.H., Townsend, A.R., et al., 2004, Nitrogen Cycles: Past, Present, and Future: *Biogeochemistry*, v. 70, p. 153–226, doi: 10.1007/s10533-004-0370-0.
- Gates, J.S., 1980, Availability of fresh and slightly saline ground water in the basins of westernmost Texas: TDWR Texas Department of Water Resources Report 256, 108 p.
- Gehler, J., Cantz, M., O'Brien, J.F., Tolksdorf, M., and Spranger, J., 1975, Mannosidosis: clinical and biochemical findings: *Birth defects original article series*, v. 11, p. 269–272.

- Gesch, D.B., 2007,, *in* Maune, D.F. ed., Digital elevation model technologies and applications: the DEM user manual, 2nd. edition, Bethesda, ASPRS.
- Gesch, D.B., Oimoen, M., Greenlee, S., Nelson, C., Steuck, M., and Tyler, D., 2002, The national elevation dataset: Photogrammetric Engineering and Remote Sensing, v. 68.
- Goetz, L., 1985, Giant polygonal desiccation cracks in Wildhorse Flat, Culberson County, West Texas; revisited, *in* Structure and tectonics of Trans-Pecos Texas, 85-81, West Texas Geological Society, p. 235–238.
- Goins, G.D., and Russelle, M.P., 1996, Fine root demography in alfalfa (*Medicago sativa* L.): Plant and Soil, v. 185, p. 281–291, doi: 10.1007/BF02257534.
- Green, C.T., Fisher, L.H., and Bekins, B.A., 2008, Nitrogen Fluxes through Unsaturated Zones in Five Agricultural Settings across the United States: Journal of Environment Quality, v. 37, p. 1073, doi: 10.2134/jeq2007.0010.
- Grover, H.D., and Musick, H.B., 1990, Shrubland encroachment in southern New Mexico, U.S.A.: An analysis of desertification processes in the American Southwest: Climate Change, v. 17, p. 305–330.
- Gurdak, J.J., and Qi, S.L., 2006, Vulnerability of recently recharge ground water in the high plains aquifer to nitrate contamination: U.S. Geological Survey USGS Scientific Investigations Report 2006-5050, 50 p.
- Gustafson, J.R., Brooks, P.D., Molotch, N.P., and Veatch, W.C., 2010, Estimating snow sublimation using natural chemical and isotopic tracers across a gradient of solar radiation: Water Resources Research, v. 46, p. n/a–n/a, doi: 10.1029/2009WR009060.
- Hadas, A., Hadas, A., Sagiv, B., and Haruvy, N., 1999, Agricultural practices, soil fertility management modes and resultant nitrogen leaching rates under semi-arid conditions: Agricultural Water Management, v. 42, p. 81–95, doi: 10.1016/S0378-3774(99)00026-8.
- Hancock, T.C., Sandstrom, M.W., Vogel, J.R., Webb, R.M.T., Bayless, E.R., and Barbash, J.E., 2008, Pesticide Fate and Transport throughout Unsaturated Zones in Five Agricultural Settings, USA: Journal of Environment Quality, v. 37, p. 1086, doi: 10.2134/jeq2007.0024.

- Handley, L.L., Austin, A.T., Stewart, G.R., Robinson, D., Scrimgeour, C.M., Raven, J.A., Heaton, T.H.E., and Schmidt, S., 1999, The  $^{15}\text{N}$  natural abundance ( $\delta^{15}\text{N}$ ) of ecosystem samples reflects measures of water availability: *Functional Plant Biology*, v. 26, p. 185–199.
- Hanson, R.T., Anderson, S.R., and Pool, D.R., 1990, Simulation of ground-water flow and potential land subsidence, Avra Valley, Arizona: United States Geological Survey WRI - 90-4178.
- Harrington, G.A., Cook, P.G., and Herczeg, A.L., 2002, Spatial and Temporal Variability of Ground Water Recharge in Central Australia: A Tracer Approach: *Ground Water*, v. 40, p. 518–527, doi: 10.1111/j.1745-6584.2002.tb02536.x.
- Heilweil, V.M., Solomon, D.K., and Gardner, P.M., 2006, Borehole Environmental Tracers for Evaluating Net Infiltration and Recharge through Desert Bedrock: *Vadose Zone Journal*, v. 5, p. 98–120, doi: 10.2136/vzj2005.0002.
- Herczeg, A.L., and Leaney, F.W., 2011, Review: Environmental tracers in arid-zone hydrology: *Hydrogeology Journal*, v. 19, p. 17–29, doi: 10.1007/s10040-010-0652-7.
- Hevesi, J.A., Flint, A.L., and Flint, L.E., 2002, Preliminary estimates of spatially distributed net infiltration and recharge for the Death Valley region, Nevada-California: United States Geological Survey WRI - 2002-4010.
- Hevesi, J.A., Flint, A.L., and Flint, L.E. Simulation of Net Infiltration and Potential Recharge Using a Distributed-Parameter Watershed Model of the Death Valley Region, Nevada and California: Water Resource Investigations Report 03-4090, 171 p.
- Hill, A.R., Devito, K.J., Campagnolo, S., and Sanmugadas, K., 2000, Subsurface Denitrification in a Forest Riparian Zone: Interactions between Hydrology and Supplies of Nitrate and Organic Carbon: *Biogeochemistry*, v. 51, p. 193–223.
- Hofstra, N., and Bouwman, A.F., 2005, Denitrification in Agricultural Soils: Summarizing Published Data and Estimating Global Annual Rates: *Nutrient Cycling in Agroecosystems*, v. 72, p. 267–278, doi: 10.1007/s10705-005-3109-y.
- Holloway, J.M., and Dahlgren, R.A., 2002, Nitrogen in rock: Occurrences and biogeochemical implications: *Global Biogeochemical Cycles*, v. 16, p. 65–1–65–17, doi: 10.1029/2002GB001862.
- Hornberger, G.M., 1998, *Elements of physical hydrology*: Baltimore; London, The Johns Hopkins University Press.

- Humphrey, R.R., 1958, The desert grassland: a history of vegetational change and an analysis of causes: *Botanical Review*, v. 24, p. 193–252.
- J. Causapé, D.Q. Assessment of irrigation and environmental quality at the hydrological basin level: II. Salt and nitrate loads in irrigation return flows: *Agricultural Water Management*,, p. 211–228, doi: 10.1016/j.agwat.2004.06.006.
- Jackson, R.B., Berthrong, S.T., Cook, C.W., Jobbágy, E.G., and McCulley, R.L., 2004, Comment on “A Reservoir of Nitrate Beneath Desert Soils:” *Science*, v. 304, p. 51–51, doi: 10.1126/science.1094294.
- Johnston, M.C., 1963, Past and Present Grasslands of Southern Texas and Northeastern Mexico: *Ecology*, v. 44, p. 456–466, doi: 10.2307/1932524.
- Jury, W.A., and Horton, 2004, *Soil physics*: Hoboken, NJ, J. Wiley.
- Kendall, C., 1998, Tracing nitrogen sources and cycling in catchments, *in* Kendall, C. and McDonnell, J.J. eds., *Isotope Tracers in Catchment Hydrology*, Amsterdam, Elsevier, p. 519–576.
- Kreitler, C.W., 1979, Nitrogen-isotope ratio studies of soils and groundwater nitrate from alluvial fan aquifers in Texas: *Journal of Hydrology*, v. 42, p. 147–170, doi: 10.1016/0022-1694(79)90011-8.
- Kung, K.-J.S., 1990, Influence of Plant Uptake on the Performance of Bromide Tracer: *Soil Science Society of America Journal*, v. 54, p. 975, doi: 10.2136/sssaj1990.03615995005400040006x.
- LBG-Guyton Associates, Freese and Nicholes, Inc., Moreno Cardenas, Inc., and M3H Consulting, Inc., 2001, Far West Texas Regional Water Plan. Consultatn’s Report: Texas Water Development Board.
- Levang-Brilz, N., and Biondini, M.E., 2003, Growth rate, root development and nutrient uptake of 55 plant species from the Great Plains Grasslands, USA: *Plant Ecology*, v. 165, p. 117–144, doi: 10.1023/A:1021469210691.
- Levings, G.W., Healy, D.F., Richey, S.F., and Carter, L.F. Water Quality in the Rio Grande Valley, Colorado, New Mexico, and Texas, 1992-95: U.S. Geological Survey USGS NAWQA Circular 1162.
- Lewis, F.M., and Walker, G.R., 2002, Assessing the potential for significant and episodic recharge in southwestern Australia using rainfall data: *Hydrogeology Journal*, v. 10, p. 229–237, doi: 10.1007/s10040-001-0172-6.



- Llamas, M., and Martínez-Santos, P., 2005, Intensive Groundwater Use: Silent Revolution and Potential Source of Social Conflicts: *Journal of Water Resources Planning and Management*, v. 131, p. 337–341, doi: 10.1061/(ASCE)0733-9496(2005)131:5(337).
- Luckey, R.R., Gutentag, E.D., and Weeks, J.B., 1981, Water-level and saturated-thickness changes, predevelopment to 1980, in the High Plains aquifer in parts of Colorado, Kansas, Nebraska, New Mexico, Oklahoma, South Dakota, Texas, and Wyoming: *US Geological Survey Hydrologic Investigations Atlas*.
- Mahlknecht, J., Horst, A., Hernández-Limón, G., and Aravena, R., 2008, Groundwater geochemistry of the Chihuahua City region in the Rio Conchos Basin (northern Mexico) and implications for water resources management: *Hydrological Processes*, v. 22, p. 4736–4751, doi: 10.1002/hyp.7084.
- Maxey, G.B., 1968, Hydrogeology of Desert Basins: *Ground Water*, v. 6, p. 10–22, doi: 10.1111/j.1745-6584.1968.tb01660.x.
- Mayer, J.R., 1995, The role of fractures in regional groundwater flow: field evidence and model results from the basin-and-range of Texas and New Mexico [Ph.D Dissertation]: The University of Texas at Austin, 218 p.
- Mayer, J.R., and Sharp, J.M., 1998, Fracture control of regional ground-water flow in a carbonate aquifer in a semi-arid region: *Geological Society of America Bulletin*, v. 110, p. 269–283.
- McMahon, C.A., Frye, R.G., and Brown, K.L., 1984, The vegetation types of Texas including cropland: *Texas Parks and Wildlife Department Bulletin 700-120*, 40 p.
- McMahon, P.B., and Böhlke, J.K., 2006, Regional Patterns in the Isotopic Composition of Natural and Anthropogenic Nitrate in Groundwater, High Plains, U.S.A.: *Environmental Science & Technology*, v. 40, p. 2965–2970, doi: 10.1021/es052229q.
- McMahon, P.B., Böhlke, J.K., and Christenson, S.C., 2004, Geochemistry, radiocarbon ages, and paleorecharge conditions along a transect in the central High Plains aquifer, southwestern Kansas, USA: *Applied Geochemistry*, v. 19, p. 1655–1686, doi: 10.1016/j.apgeochem.2004.05.003.
- McMahon, P.B., Dennehy, K.F., Bruce, B.W., Böhlke, J.K., Michel, R.L., Gurdak, J.J., and Hurlbut, D.B., 2006a, Storage and transit time of chemicals in thick unsaturated zones under rangeland and irrigated cropland, High Plains, United States: *Water Resources Research*, v. 42, p. n/a–n/a, doi: 10.1029/2005WR004417.

- Metcalf, L., 1995, Ground water- surface water interactions in the Lower Virgin River area Arizona and Nevada [M.S. Thesis]: University of Nevada, Las Vegas, 186 p.
- Millennium Ecosystem Assessment, 2005, Ecosystems and Human Well-Being - Desertification Synthesis: A Report of the Millennium Ecosystem Assessment: World Resources Institute, 36 p.
- Miyamoto, S., Fenn, L.B., and Swietlik, D., 1995, Flow, salts, and trace elements in the Rio Grande: a review: Texas Water Resources Institute.
- NADP Program Office, Illinois State Water Survey, 2007, National Atmospheric Deposition Program (NRSP-3): Illinois State Water Survey Dataset.
- Naito, A.T., and Cairns, D.M., 2011, Patterns and processes of global shrub expansion: *Progress in Physical Geography*, v. 35, p. 423–442, doi: 10.1177/0309133311403538.
- NASA Landsat Program Landsat ETM+scene LE703 103820001 64EDC00, SLC-On: U.S. Geological Survey Dataset.
- NASA Landsat Program, 2000, Landsat ETM+scene LE703 20392000171EDC00: U.S. Geological Survey Dataset.
- Nativ, R., and Riggio, R., 1990, Precipitation in the southern High Plains: Meteorologic and isotopic features: *Journal of Geophysical Research: Atmospheres*, v. 95, p. 22559–22564, doi: 10.1029/JD095iD13p22559.
- Newman, B.D., Wilcox, B.P., Archer, S.R., Breshears, D.D., Dahm, C.D., Duffy, C.J., McDowell, N.G., Phillips, F.M., Scanlon, B.R., and Vivoni, E.R., 2006, Ecohydrology of water-limited environments: A scientific vision: *Water Resources Research*, v. 42, p. 15, doi: 10.1029/2005WR004141.
- Nielson, P.D., and Sharp Jr., J.M., 1985, Tectonic controls on the hydrogeology of the salt basin Trans-Pecos, Texas, *in* Structure and tectonics of Trans-Pecos Texas, 85-81, West Texas Geological Society, p. 231–234.
- Nishikawa, T., Izbicki, J., Hevesi, J.A., Stamos, C.L., and Martin, P., 2004, Evaluation of Geohydrologic Framework, Recharge Estimates and Ground-Water Flow of the Joshua Tree Area, San Bernardino County, California: U.S. Geological Survey Scientific Investigations Report 2004-5267, 127 p.
- NOAA National Climatic Data Center, 2010, The statewide long term precipitation map: 1969 to Present: NOAA NCDC.

- Nolan, B.T., Puckett, L.J., Ma, L., Green, C.T., Bayless, E.R., and Malone, R.W., 2010, Predicting Unsaturated Zone Nitrogen Mass Balances in Agricultural Settings of the United States: *Journal of Environment Quality*, v. 39, p. 1051, doi: 10.2134/jeq2009.0310.
- Oren, O., Yechieli, Y., Böhlke, J., and Dody, A., 2004, Contamination of groundwater under cultivated fields in an arid environment, central Arava Valley, Israel: *Journal of Hydrology*, v. 290, p. 312–328, doi: 10.1016/j.jhydrol.2003.12.016.
- Osterkamp, W.R., and Wood, W.W., 1987, Playa-lake basins on the Southern High Plains of Texas and New Mexico: Part I. Hydrologic, geomorphic, and geologic evidence for their development: *Geological Society of America Bulletin*, v. 99, p. 215–223, doi: 10.1130/0016-7606(1987)99<215:PBOTSH>2.0.CO;2.
- Pereira, A.R., and Paes De Camargo, Â., 1989, An analysis of the criticism of Thornthwaite's equation for estimating potential evapotranspiration: *Agricultural and Forest Meteorology*, v. 46, p. 149–157, doi: 10.1016/0168-1923(89)90118-4.
- Peterjohn, W.T., and Schlesinger, W.H., 1990, Nitrogen loss from deserts in the southwestern United States: *Biogeochemistry*, v. 10, p. 67–79, doi: 10.1007/BF00000893.
- Plummer, L.N., Böhlke, J.K., and Doughten, M.W., 2006, Perchlorate in Pleistocene and Holocene Groundwater in North-Central New Mexico: *Environmental Science & Technology*, v. 40, p. 1757–1763, doi: 10.1021/es051739h.
- Pool, D.R., and Dickinson, J.E., 2006, Ground-water flow model of the Sierra Vista Subwatershed and Sonoran portions of the Upper San Pedro Basin, Southeastern Arizona, United States, and Northern Sonora, Mexico: *USGS Scientific Investigations Report 2006-5228*, 60 p.
- Prinn, R.G., Weiss, R.F., Fraser, P.J., Simmonds, P.G., Cunnold, D.M., Alyea, F.N., O'Doherty, S., Salameh, P., Miller, B.R., Huang, J., Wang, R.H.J., Hartley, D.E., Harth, C., Steele, L.P., et al., 2000, A history of chemically and radiatively important gases in air deduced from ALE/GAGE/AGAGE: *Journal of Geophysical Research: Atmospheres*, v. 105, p. 17751–17792, doi: 10.1029/2000JD900141.
- PRISM Climate Group at Oregon State University, 2012, United States average monthly or annual precipitation, 1981-2010 dataset: Data.
- Reeves Jr., C.C., 1970, Origin, Classification, and Geologic History of Caliche on the Southern High Plains, Texas and Eastern New Mexico: *The Journal of Geology*, v. 78, p. 352–362.

- Rewis, D.L., Christensen, A.H., Matti, J., Hevesi, J.A., Nishikawa, T., and Martin, P., 2006, *Geology, Ground-Water Hydrology, Geochemistry, and Ground-Water Simulation of the Beaumont and Banning Storage Units, San Gorgonio Pass Area, Riverside County, California*: USGS Scientific Investigations Report 2006-5026.
- Robertson, W.M., Böhlke, J.K., and Sharp Jr., J.M., 2012, Changing nitrate concentrations in arid basin aquifers: how anthropogenic and natural processes affect water quality and availability in Trans-Pecos, TX. H24B-05, *in* San Francisco, AGU Fall Meeting.
- Robertson, W.M., and Sharp Jr., J.M., 2013, Estimates of recharge in two arid basin aquifers: a model of spatially variable net infiltration and its implications (Red Light Draw and Eagle Flats, Texas, USA) - Springer: , doi: 10.1007/s10040-013-1018-8.
- Robertson, W.M., and Sharp Jr., J.M., *in review*, Estimates of spatially distributed potential recharge to arid basin aquifers resulting from natural and anthropogenic sources
- Robertson, W.M., and Sharp Jr., J.M., 2012, Variability of groundwater nitrate concentrations over time in arid basin aquifers: sources, mechanisms of transport, and implications for conceptual models: *Environmental Earth Sciences*, p. 1–12, doi: 10.1007/s12665-012-2069-1.
- Rodell, M., and Famiglietti, J.S., 2002, The potential for satellite-based monitoring of groundwater storage changes using GRACE: the High Plains aquifer, Central US: *Journal of Hydrology*, v. 263, p. 245–256, doi: 10.1016/S0022-1694(02)00060-4.
- Royer, P.D., Cobb, N.S., Clifford, M.J., Huang, C.-Y., Breshears, D.D., Adams, H.D., and Villegas, J.C., 2011, Extreme climatic event-triggered overstorey vegetation loss increases understorey solar input regionally: primary and secondary ecological implications: *Journal of Ecology*, v. 99, p. 714–723, doi: 10.1111/j.1365-2745.2011.01804.x.
- Sami, K., 1992, Recharge mechanisms and geochemical processes in a semi-arid sedimentary basin, Eastern Cape, South Africa: *Journal of Hydrology*, v. 139, p. 27–48, doi: 10.1016/0022-1694(92)90193-Y.
- Scanlon, B.R., 1991, Evaluation of moisture flux from chloride data in desert soils: *Journal of Hydrology*, v. 128, p. 137–156, doi: 10.1016/0022-1694(91)90135-5.

- Scanlon, B.R., Darling, B.K., and Mullican, W.F., 2001, Evaluation of groundwater recharge in basins in Trans-Pecos, Texas, *in* Aquifers of West Texas, Texas Water Development Board Report 356, Austin, TX U.S.A, Texas Water Development Board, p. 26–40.
- Scanlon, B.R., Gates, J.B., Reedy, R.C., Jackson, W.A., and Bordovsky, J.P., 2010, Effects of irrigated agroecosystems: 2. Quality of soil water and groundwater in the southern High Plains, Texas: *Water Resources Research*, v. 46, p. n/a–n/a, doi: 10.1029/2009WR008428.
- Scanlon, B.R., Keese, K.E., Flint, A.L., Flint, L.E., Gaye, C.B., Edmunds, W.M., and Simmers, I., 2006a, Global synthesis of groundwater recharge in semiarid and arid regions: *Hydrological Processes*, v. 20, p. 3335–3370, doi: 10.1002/hyp.6335.
- Scanlon, B.R., Keese, K.E., Flint, A.L., Flint, L.E., Gaye, C.B., Edmunds, W.M., and Simmers, I., 2006b, Global synthesis of groundwater recharge in semiarid and arid regions: *Hydrological Processes*, v. 20, p. 3335–3370, doi: 10.1002/hyp.6335.
- Scanlon, B.R., Keese, K., Reedy, R.C., Simunek, J., and Andraski, B.J., 2003, Variations in flow and transport in thick desert vadose zones in response to paleoclimatic forcing (0–90 kyr): Field measurements, modeling, and uncertainties: *Water Resources Research*, v. 39, p. n/a–n/a, doi: 10.1029/2002WR001604.
- Scanlon, B.R., Reedy, R.C., and Bronson, K.F., 2008, Impacts of Land Use Change on Nitrogen Cycling Archived in Semiarid Unsaturated Zone Nitrate Profiles, Southern High Plains, Texas: *Environmental Science & Technology*, v. 42, p. 7566–7572, doi: 10.1021/es800792w.
- Scanlon, B.R., Reedy, R.C., Stonestrom, D.A., Prudic, D.E., and Dennehy, K.F., 2005, Impact of land use and land cover change on groundwater recharge and quality in the southwestern US: *Global Change Biology*, v. 11, p. 1577–1593, doi: 10.1111/j.1365-2486.2005.01026.x.
- Scanlon, B.R., Tyler, S.W., and Wierenga, P.J., 1997, Hydrologic issues in arid, unsaturated systems and implications for contaminant transport: *Reviews of Geophysics*, v. 35, p. 461–490, doi: 10.1029/97RG01172.
- Schmidt, R.H., 1995, The climate of Trans-Pecos Texas, *in* Norwine, J., Giardino, J.R., North, G.R., and Valdés, J.B. eds., *The Changing Climate of Texas Predictability And Implications For The Future*,

- Schmidt, K., and Sherman, I., 1987, Effect of Irrigation on Groundwater Quality in California: *Journal of Irrigation and Drainage Engineering*, v. 113, p. 16–29, doi: 10.1061/(ASCE)0733-9437(1987)113:1(16).
- Schuster, J.L., 1964, Root Development of Native Plants Under Three Grazing Intensities: *Ecology*, v. 45, p. 63–70, doi: 10.2307/1937107.
- Seyfried, M.S., Schwinning, S., Walvoord, M.A., Pockman, W.T., Newman, B.D., Jackson, R.B., and Phillips, F.M., 2005, Ecohydrological Control of Deep Drainage in Arid and Semiarid Regions: *Ecology*, v. 86, p. 277–287, doi: 10.2307/3450946.
- Sharp Jr., J.M., 2001, Regional groundwater flow systems in Trans-Pecos, Texas, *in* Mace, R.E., Mullican, W.F.I., and Angle, E.S. eds., *Texas Water Development Board Report 356*, 356, Austin, TX U.S.A., Texas Water Development Board, p. 41–55.
- Sharp Jr., J.M., 1989, Regional ground-water systems in northern Trans-Pecos Texas, *in* *Structure and Stratigraphy of Trans-Pecos Texas*, American Geophysical Union field trip Guidebook T317, American Geophysical Union.
- Simpson, H.J., and Herczeg, A.L., 1991, Salinity and evaporation in the River Murray Basin, Australia: *Journal of Hydrology*, v. 124, p. 1–27, doi: 10.1016/0022-1694(91)90003-Z.
- Smedema, L.K., and Shiati, K., 2002, Irrigation and Salinity: a Perspective Review of the Salinity Hazards of Irrigation Development in the Arid Zone: *Irrigation and Drainage Systems*, v. 16, p. 161–174, doi: 10.1023/A:1016008417327.
- Soil Survey Staff Web Soil Survey: U.S. Department of Agriculture Dataset.
- Spalding, V.M., 1904, Biological Relations of Certain Desert Shrubs. I. The Creosote Bush (*Covillea Tridentata*) in Its Relation to Water Supply: *Botanical Gazette*, v. 38, p. 122–138, doi: 10.2307/2465942.
- Stannard, D.I., 1993, Comparison of Penman-Monteith, Shuttleworth-Wallace, and Modified Priestley-Taylor Evapotranspiration Models for wildland vegetation in semiarid rangeland: *Water Resources Research*, v. 29, p. 1379–1392, doi: 10.1029/93WR00333.
- Stewart, J.M., Oosterhuis, D.M., Heitholt, J.J., and Mauney, J.R. (Eds.), 2010, *Physiology of Cotton*.

- Stoesser, D.B., Green, G.N., Morath, L.C., Heran, W.D., Wilson, A.B., Moore, D.W., and Van Gosen, B.S., 2007, Preliminary Integrated Geologic Map Databases of the United States: Central States: Montana, Wyoming, Colorado, New Mexico, North Dakota, South Dakota, Nebraska, Kansas, Oklahoma, Texas, Iowa, Missouri, Arkansas, and Louisiana: Open File Report 2005-1351.
- Stone, E.L., and Kalisz, P.J., 1991, On the maximum extent of tree roots: *Forest Ecology and Management*, v. 46, p. 59–102.
- Stonestrom, D.A., Prudic, D.E., Lacznia, R.J., Akstin, K.C., Boyd, R.A., and Henkelman, K.K., 2003, Estimates of deep percolation beneath native vegetation, irrigated fields, and the Amargosa-River Channel, Amargosa Desert, Nye County, Nevada: U.S. Geological Survey Open File Report OFR 03-104, 88 p.
- Texas Water Development Board Groundwater Data: Texas Water Development Board, available online at <http://www.twdb.state.tx.us/groundwater/data/>.
- Thornthwaite, C.W., 1948, An Approach toward a Rational Classification of Climate: *Geographical Review*, v. 38, p. 55–94, doi: 10.2307/210739.
- Trajkovic, S., 2005, Temperature-Based Approaches for Estimating Reference Evapotranspiration: *Journal of Irrigation and Drainage Engineering*, v. 131, p. 316–323, doi: 10.1061/(ASCE)0733-9437(2005)131:4(316).
- U.S. Department of Agriculture: USDA/NASS QuickStats Ad-hoc Query Tool, available online at [http://www.nass.usda.gov/Quick\\_Stats/](http://www.nass.usda.gov/Quick_Stats/).
- U.S. Geological Survey Staff, 2008, Documentation of computer program INFIL 3.0: a distributed-parameter watershed model to estimate net infiltration below the root zone: U.S. Geological Survey USGS Scientific Investigations Report 2008-5006.
- Uliana, M.M., 2000, Delineation of regional groundwater flow paths and their relation to structural features in the Salt and Toyah basins, Trans-Pecos Texas [Ph.D Dissertation]: The University of Texas at Austin, 215 p.
- Uliana, M.M., Banner, J.L., and Sharp Jr., J.M., 2007, Regional groundwater flow paths in Trans-Pecos, Texas inferred from oxygen, hydrogen, and strontium isotopes: *Journal of Hydrology*, v. 334, p. 334–346, doi: 10.1016/j.jhydrol.2006.10.015.
- Uliana, M.M., and Sharp Jr., J.M., 2001, Tracing regional flow paths to major springs in Trans-Pecos Texas using geochemical data and geochemical models: *Chemical Geology*, v. 179, p. 53–72, doi: 10.1016/S0009-2541(01)00315-1.

- USGS Landsat Mosaic Orthoimagery Database, 2000, Dataset, available online at <http://nationalmap.gov/ortho.html>.
- Van Auken, O.W., 2000, Shrub Invasions of North American Semiarid Grasslands: Annual Review of Ecology and Systematics, v. 31, p. 197–215, doi: 10.2307/221730.
- Van Broekhoven, N.G., 2002, Recharge in a semi-arid basin aquifer: Ryan Flat and Lobo Flat, Trans-Pecos, Texas [M.S. Thesis]: The University of Texas at Austin, 257 p.
- Veatch, W., Brooks, P.D., Gustafson, J.R., and Molotch, N.P., 2009, “Quantifying the effects of forest canopy cover on net snow accumulation at a continental, mid-latitude site.” *Ecohydrology*, v. 2, p. 115–128, doi: 10.1002/eco.45.
- Wade, S.C., 2012, Groundwater flow model of the Presidio-Redford Bolson aquifer, *in* Geological Society of America abstracts with programs (South-Central Section), Alpine, TX U.S.A., Geological Society of America, p. 32.
- Walker, S.J., Weiss, R.F., and Salameh, P.K., 2000, Reconstructed histories of the annual mean atmospheric mole fractions for the halocarbons CFC-11 CFC-12, CFC-113, and carbon tetrachloride: *Journal of Geophysical Research: Oceans*, v. 105, p. 14285–14296, doi: 10.1029/1999JC900273.
- Walvoord, M.A., 2002, A unifying conceptual model to describe water, vapor, and solute transport in deep arid vadose zones [Ph.D Dissertation]: New Mexico Institute of Mining and Technology, 319 p.
- Walvoord, M.A., and Phillips, F.M., 2004, Identifying areas of basin-floor recharge in the Trans-Pecos region and the link to vegetation: *Journal of Hydrology*, v. 292, p. 59–74, doi: 10.1016/j.jhydrol.2003.12.029.
- Walvoord, M.A., Phillips, F.M., Stonestrom, D.A., Evans, R.D., Hartsough, P.C., Newman, B.D., and Striegl, R.G., 2003, A Reservoir of Nitrate Beneath Desert Soils: *Science*, v. 302, p. 1021–1024, doi: 10.1126/science.1086435.
- Walvoord, M.A., Phillips, F.M., Tyler, S.W., and Hartsough, P.C., 2002, Deep arid system hydrodynamics 2. Application to paleohydrologic reconstruction using vadose zone profiles from the northern Mojave Desert: *Water Resources Research*, v. 38, p. 27–1 to 27–12, doi: 10.1029/2001WR000825.
- Walvoord, M.A., Plummer, M.A., Phillips, F.M., and Wolfsberg, A.V., 2002, Deep arid system hydrodynamics 1. Equilibrium states and response times in thick desert vadose zones: *Water Resources Research*, v. 38, p. 44–1–44–15, doi: 10.1029/2001WR000824.



- Ward, J.W., 2002, Report of data gathered on 8-7-02 for CCGWCD:, 6 p.
- Warner, M.J., and Weiss, R.F., 1985, Solubilities of chlorofluorocarbons 11 and 12 in water and seawater: Deep Sea Research Part A. Oceanographic Research Papers, v. 32, p. 1485–1497, doi: 10.1016/0198-0149(85)90099-8.
- West, N.E., 1978, Physical inputs of nitrogen to desert ecosystems, *in* Nitrogen in desert ecosystems, Dowden, Hutchison, and Ross, p. 165–170.
- Wilcox, B.P., Wood, M.K., and Tromble, J.M., 2006, Factors influencing infiltrability of semiarid mountain slopes: Journal of Range Management Archives, v. 41, p. 197–206.
- Wilson, J.L., and Guan, H., 2004, Mountain-Block Hydrology and Mountain-Front Recharge, *in* Hogan, J.F., Phillips, F.M., and Scanlon, B.R. eds., Groundwater Recharge in a Desert Environment: The Southwestern United States, American Geophysical Union, p. 113–137.
- Winograd, I.J., 1981, Radioactive Waste Disposal in Thick Unsaturated Zones: Science, v. 212, p. 1457–1464, doi: 10.1126/science.212.4502.1457.
- Woodroof, J.G., and Woodroof, N.C., 1934, Pecan root growth and development: Journal of Agricultural Research, v. 49, p. 511–530.
- Yoshida, M., Takahashi, K., Yonehara, N., Ozawa, T., and Iwasaki, I., 1971, The Fluorine, Chlorine, Bromine, and Iodine Contents of Volcanic Rocks in Japan: Bulletin of the Chemical Society of Japan, v. 44, p. 1844–1850.